XXXII INTERNATIONAL SCIENTIFIC SYMPOSIUM

METROLOGY AND METROLOGY ASSURANCE 2022

PROCEEDINGS

September 7-11, 2022, Sozopol, Bulgaria

http://metrology-bg.org/

TECHNICAL UNIVERSITY OF SOFIA

8 Blvd Kl. Ohridski, 1797, Sofia, Bulgaria

MFACULTY OF MECHANICAL ENGINEERING

Department of
PRECISION ENGINEERING AND MEASURING INSTRUMENTS

Prof. Dimitar Diakov, PhD

Phone: (+359) 2 965 3056

Mobile: (+359) 889 531 258

E-mail: diakov@tu-sofia.bg

metrology@tu-sofia.bg

FACULTY OF AUTOMATICS

Department of
ELECTRICAL MEASUREMENTS

assoc. prof. Ivan Kodjabashev

Phone: (+359) 2 965 2896

Mobile: (+359) 887 516 765

E-mail: kodjabashev@tu-sofia.bg

assoc. prof. Georgi Milushev

Phone: (+359) 2 965 2380

Mobile: (+359) 888 501 235

E-mail: gm@tu-sofia.bg

metrology@tu-sofia.bg

Technical University of Sofia

Bulgarian Institute of Metrology

Union of Metrologists in Bulgaria

Bulgarian Academical Association of Metrology

Kozloduy Nuclear Power Plant

32ND INTERNATIONAL SCIENTIFIC SYMPOSIUM

METROLOGY AND METROLOGY ASSURANCE 2022

PROCEEDINGS

7-11 September 2022

Sozopol, Bulgaria

ORGANISED BY

Technical University of Sofia

- ***Department of Electrical Measurements***
- ***Department of Precision Engineering and Measuring Instruments***

Institute of Electrical and Electronics Engineers, Bulgaria Section

WITH THE ATTENDANCE OF

Bulgarian Institute of Metrology

Union of Metrologists in Bulgaria

Bulgarian Academical Association of Metrology

Kozloduy Nuclear Power Plant

WITH THE SUPPORT OF

RESEARCH AND DEVELOPMENT SECTOR BY THE TU-SOFIA

SOFTTRADE **NIK 47 Ltd** **R&DL “CMME”**

NATIONAL ORGANIZING COMMITTEE

Co-Chairmen

Assoc. Prof. Ivan Kodjabashev, PhD	*TU-Sofia*
Prof. Dimitar Diakov, DSc	*TU-Sofia*

Vice Chairmen

Snejana Spasova, MEng	*BIM*
Vessela Konstantinova, PhD	*UMB*
Prof. Branko Sotirov, PhD	*BAAM*
Emilyan Edrev, MEng	*NPP*

Scientific Secretary

Prof. Georgi Djukendjiev, PhD	*TU-Sofia*

Members

Kiril Banev, MEng	*Kozloduy NPP*
Assoc. Prof. Vassil Bogev, PhD	*TU-Sofia*
Milko Djambazov, PhD	*TU-Sofia*
Assist. Prof. Krasimir Galabov, PhD	*TU-Sofia*
Assoc. Prof. Ivanka Kalimanova, PhD	*TU-Sofia*
Assoc. Prof. Valentina Markova, PhD	*IEEE Bulgarian Section*
Nikola Panchev, MEng	*NIK 47*
Assoc. Prof. Nikolay Stoyanov, PhD	*TU-Sofia*
Prof. Plamen Tzvetkov, PhD	*NBU*
Assoc. Prof. Velizar Vassilev, PhD	*TU-Sofia*
Antoaneta Yovcheva, PhD	*BIM NCM*

Secretariat

Assist. Prof. Ivailo Blagov, PhD	*TU-Sofia*
Assist. Prof. Bozhidar Dzhudzhev, PhD	*TU-Sofia*
Nikolay Gurov, MEng	*TU-Sofia*
Sen. Res. Fel. Momchil Hardalov, PhD	*TU-Sofia*
Assoc. Prof. Hristiana Nikolova, PhD	*TU-Sofia*
Assoc. Prof. Rositza Miteva, PhD	*TU-Sofia*
Assist. Prof. Antonia Pandelova, PhD	*TU-Sofia*

INTERNATIONAL PROGRAMME COMMITTEE

Chairman

Assoc. Prof. George Milushev, PhD	*TU-Sofia*

Members

Assoc. Prof. Kiril Aleksiev, PhD	*BAS, IEEE, Bulgaria*
Prof. Konstantionos Athanasiadis	*EMI, Greece*
Anna Chunovkina, DSc	*VNIIM, Russia*
Prof. Dimitar Dichev, DSc	*TU-Gabrovo, Bulgaria*
Prof. Vladimir Dmitriev, DSc	*TsAGI, Russia*
Dr. Manus Henry	*University of Oxford, England*
Prof. Dietrich Hofmann, PhD	*ICC Spectronet, Germany*
Assoc. Prof. Kiril Kirov, PhD	*TU-Varna, Bulgaria*
Assoc. Prof. Ivan Kodjabashev, PhD	*TU-Sofia, Bulgaria*
Prof. Ivan Kralov, DSc	*TU-Sofia, Bulgaria*
Prof. Peter Lauda, DSc	*TU-Liberec, Czech Republic*
Prof. Ignacio Lira, DSc	*PUCC, Chile*
Prof. Valeri Mladenov, DSc	*TU-Sofia, Bulgaria*
Prof. Zvezditza Nenova, PhD	*TU-Gabrovo, Bulgaria*
Assoc. Prof. Elmo Pettai, PhD	*TUT, Estonia*
Prof. Georgii Rannev, DSc	*IIT, Russia*
Acad. Chavdar Rumenin, DSc	*BAS, Bulgaria*
Prof. Alexandru Salceanu, DSc	*TU Gheorghe Asachi, Romania*
Assoc. Prof. Nikolay Serov, PhD	*NRU MPEI, Russia*
Prof. Alexandr Shestakov, DSc	*SUSU NRU, Russia*
Prof. Branko Sotirov, PhD	*RU Angel Kanchev, Bulgaria*
Jiri Šurán	*CMI, Czech Republic*
Roald Taymanov, DSc	*VNIIM, Russia*
Assoc. Prof. Danko Tonev, PhD	*RU Angel Kanchev, Bulgaria*
Assoc. Prof. Stanimir Valchev, PhD	*NOVA, Portugal*
Prof. Evgeniy Volodarsky, DSc	*NTUU KPI, Ukraine*
Prof. Wiesław Winiecki, DSc	*WUT, Poland*
Prof. Ighor Zaharov, DSc	*NURE, Ukraine*
Prof. Ilia Zhelezarov, PhD	*TU-Gabrovo, Bulgaria*

All papers published in the Proceedings of the 32nd International Scientific Symposium "Metrology and Metrology Assurance 2022" are reviewed by the International Programme Committee.

METROLOGY AND METROLOGY ASSURANCE 2022

7-11 September 2022

Sozopol, Bulgaria

PROCEEDINGS

Technical University of Sofia

Technical University of Sofia Publishing House

ISSN 2603-3194

CONTENT

PLENARY SESSION

Section I GENERAL ASPECTS OF METROLOGY. MEASUREMENT METHODS. UNITY AND ACCURACY OF MEASUREMENTS

Section IV MEASUREMENTS IN THE INDUSTRY

Section V MEASUREMENTS IN THE ELECTRICAL POWER ENGINEERING

Section VII MEASUREMENTS IN THE ECOLOGY, BIOTECHNOLOGY, MEDICINE, AND SPORT

Section VIII METROLOGY PRACTICE

PLENARY SESSION

Creation of centralized automated systems in metrology

Tsvetomir Petkov
BIM, DG NCM
Mechanical Measurements Department
Sofia, Bulgaria
Ts.Petkov@ bim.government.bg

The computer is no longer just a machine that allows us to perform an activity faster. It has become a powerful tool for creating, storing, managing, transmitting and analyzing vast arrays of data. The task of experts is to find a way to use all this power, as rationally as possible, trying to save energy resources. The creation of centralized automated systems in the field of metrology, dealing with the processing and management of technical records, will provide experts with working conditions in an automated laboratory environment. It will reduce the risk of errors in processing and transmission of measurement results. This will increase the reliability of the measurements and reduce the processing time of the results while limiting the possibilities for manipulation. The unification of the systems of the separate laboratories in the country in one national metrological network would provide an opportunity for machine exchange of data between the different laboratories and their clients. This turns the electronic certificate into a real digital tool, not a digital mark in an analog system.

Keywords—automatic system, electronic sertificate, national metrology network

I. INTRODUCTION

One of the main tasks of the Bulgarian Institute of Metrology, as part of the State Administration and in particular the Main Directorate of the National Center of Metrology, is to take care of the National Standards and ensure the traceability of all standards in the country to SI units through calibration. The calibration process is carried out in the laboratory premises of the departments by means of the output and working standards in the individual departments, various auxiliary equipment, under strict measures of controlling the conditions of the surrounding environment. With this activity, BIM is one of the main pillars of the national economy. This, as well as the increasing demands from our customers and international partners, puts before BIM the responsibility to keep up with all modern trends in the field of metrology. Every BIM laboratory in itself has impressive capabilities, protected in international comparisons and recognized by all metrological institutes around the world. Combined, these capabilities open up new horizons for BIM experts, significantly ease their work and enable the organization as a whole to provide faster and better services to its customers, to all of us. This prompted a group of BIM experts to develop a project to build an electronic activity management system not only for BIM laboratories, but for accredited and non-accredited calibration and testing laboratories as well as large factory. In this way, BIM provides conditions for business to take a direct part in developments and implement in practice solutions related to a main direction in the development of metrology at the world level[2].

II. THE ACTIVITIES IN THE LABORATORIES AND THE CONNECTIONS BETWEEN THEM

One of the most important tasks that the team managed to specify during the work on the project was the unambiguous definition of the main activities in the laboratories and the connections between them (Fig. 1).

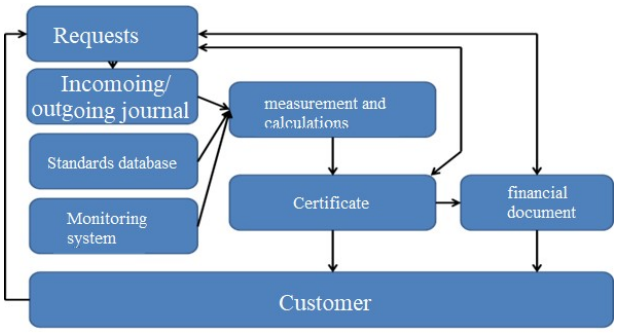

Fig. 1

As you can see, customers are at the heart of everything. This is all of us represented by various government and private organizations, laboratories, productions and industries, retail outlets and chains, individual private customers. After submitting a request to the laboratory and presenting the measurement object (measuring device, sample, etc.), it enters the laboratory. There it receives an incoming number, is measured using the laboratory standards and taking into account the parameters of the surrounding environment (temperature, atm. pressure, humidity, vibration, dustiness, electromagnetic interference and countless others) so that various side effects can be determined and reported factors, experts process the measurement results. A certificate/report is issued and the object is returned to the customer after the service fee is paid. The work algorithm thus presented can be used as a

basis for building an automated process management system in laboratories. Within the framework of a pilot project in one of the measurement areas of BIM, NCM, MI, IMOP, a CPMS system (Calibration Process Management System) was built. The aim of the project was to test the viability of the idea in practice and to gain the necessary experience for a future upgrade. Over time, SUPK has established itself as a powerful tool to assist IMOP experts during calibration. Of course, many compromises were made during development, both with the architecture of the system and with its functionalities. This made the system exclusive to the IMOP field and highly unsuitable for direct use in other measurement fields. This necessitated the development of a new unified system with greater scope to provide:

- Better working environment and reduction of errors in information transfer;
- Reduction of documentation stored on paper;
- Ensuring and guaranteeing the use of a single structure of the stored information;
- Flexibility of information management;
- Machine readable information;
- Creating conditions for automating the analysis of measurement results and assisting experts in making decisions when working in an environment with elements of artificial intelligence;
- Creation of conditions for future upgrading of the system in order to reach the level for issuing electronic certificates and the possibility for customers to make online inquiries about the level of completion of their requests.

The future system will be built on a modular basis. This will allow a gradual understanding and implementation of the system, making it flexible and adaptable in different conditions. The modules planned for development are:

- Environmental monitoring system;
- System for authorized access;
- Database of standards and auxiliary equipment;
- Incoming /outgoing journal ;
- Math server;
- System for creating and managing forms;
- Public register.

III. ENVIRONMENTAL MONITORING SYSTEM

The main requirement for the system is the need to work with many different sensors monitoring different parameters, making recordings from these sensors at a certain time interval, reviewing the recordings, as well as submitting the sensor readings to the respective customers in online mode. Having such a system will allow laboratories to:

- keep automated logs for monitoring in the room;
- carry out data exchange between sensors in different laboratories, which in turn will make it possible to reduce the number of active sensors in the laboratories for the measured parameters for which this is possible;
- reduced the operator's burden, allowing him to concentrate on the measurement itself without distracting his attention to follow the monitoring data;
- build an automated process of keeping primary records during the measurement.

IV. AUTHORIZED ACCESS SYSTEM

This system is necessary in order to enforce rules for creating, editing, accessing and authenticating the information managed and stored by the system. The following levels of access to documents are provided:

- creation;
- editing;
- signing;
- review,

as well as an opportunity for the laboratory to define 24 possible categories of documents by itself. In order to ensure security, access to the system will be done through a personal certificate and PIN code.

V. DATABASE OF STANDARDS AND ANCILLARY EQUIPMENT

The availability of machine-readable databases with reference and auxiliary equipment is a prerequisite for:

- reduction of errors from information transfer (automatic output);
- provision of an automated process of analysis of the condition of the equipment;

- provision of machine-readable input to the database (automatic input);
- use of the data for other needs and references needs for the quality system of the laboratory.

Taking into account the variety of standards and auxiliary equipment used by the various laboratories, the future database should provide maximum data flexibility without rigid limits in the quantities used and at the same time respecting the quantities. For this, it is necessary to enable the laboratory itself to create a register with the required and values, and the database of standards and auxiliary equipment to use references to this register.

VI. INCOMING /OUTGOING JOURNAL

The main standard on the basis of which every quality system of calibration and testing laboratories is built is ISO-17025[1]. This standard requires laboratories to keep an incoming /outgoing journal of measuring instruments received in the laboratory. The creation of a machine-readable incoming /outgoing journal will allow laboratories to create a journal of activities to control the fulfillment of requests, while providing machine input and output of customer data needed for both the certificate/report and the financial document , required to pay for the service.

VII. MATH SERVER

The variety of measurements faced by metrology today implies the use of a wide variety of personal and complex mathematical methods and functions. One of the most commonly used functions in metrology, these are the statistical analysis functions. There is virtually no measurement that goes without statistical analysis of the data. The mass use of the same mathematical tools in multiple fields of measurement is a prerequisite to create a mathematical server to process this data. This will allow to provide control over the mathematical functions used without having to personally validate their application in each separate area of measurement. This will significantly shorten the time to implement new methods and measurement areas, allowing us to use time-tested features. At the same time, the centrality of the math server will allow optimizations and improvements to be instantly applied to each of our protocols that take advantage of this server. Of course, it will be possible to add new functions or formulas related not only to statistics, but widely used in metrology, such as density of air, density of water and other liquids, uncertainty budget, etc., specific to the given laboratory.

VIII. SYSTEM FOR CREATING AND MANAGING FORMS

Having the aforementioned systems alone will not have a transformative effect on laboratories unless the individual systems work as a whole. The information stored and managed by them can be combined and used to generate multiple reports and reports. Creating a system that allows labs to model this data for their specific needs brings completeness to the system itself.

IX. PUBLIC REGISTER

Of course, all activities carried out in the laboratories are aimed at their customers. The public registry will provide machine-readable access to laboratory customers to the results of their funds.

X. ARCHITECTURE OF MODULES

The modular approach to building the system enables each module to be built according to a different architecture. However, choosing a unified architecture would make it possible to use the experience of building the previous ones when building each subsequent module. For this reason, a standardized module architecture was chosen.

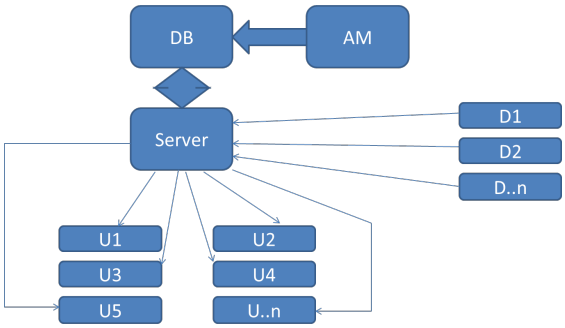

Fig. 2

Each module stores and accesses the data in a relational database (DB) (Fig 2). Database administration is done by an administrator module (AM). This allows the structure of the database to be manipulated only by a person in charge of administrative functions, and the access to the database by the clients is made through a two-layer WEB service (Server). The outer layer of which provides a connection with the customers, and the inner layer with the database. This separation ensures controlled access of clients to the database in order to avoid deliberate manipulations.

XI. NATIONAL METROLOGICAL NETWORK

"Partnership for Open Government" is an international initiative whose goal is to achieve concrete commitments from governments to promote transparency, empower citizens, fight corruption through the use of new technologies and strengthen governance. As part of the Fourth National Action Plan within the framework of the "Partnership for Open Government" initiative, BIM together with its partners in the form of[3]:

- Union of Metrologists in Bulgaria;

- Institute of Transport Construction and Infrastructure;
- Club 9000;
- Union of Construction Laboratory Specialists in Bulgaria,

managed to initiate a measure «Building a national metrological network». Joint activities between BIM experts and partners will allow to build unified elements of an automated system, as well as to select an optimal format of machine-readable data in the field of metrology. The construction of a national metrology network will provide the possibility of machine exchange of data between the various laboratories and their customers, and work in an automated laboratory environment will reduce the risk of errors in processing and transfer of measurement results. This will increase the reliability of the measurements, reduce the processing time and limit the possibilities of manipulation.

XII. CONCLUSION

One of the hallmarks of the digital age is its ubiquity. The existence of an analog society in the digital age is antithetical to its essence. Today, it is increasingly difficult to accept everyday life without the help of powerful computing systems to help process and store the ever-increasing amount of data that has to be handled. This comprehensiveness requires that the solutions to the problems are selected in such a way that they meet not just the needs, but rather satisfy the needs of the customers excluding self-serving solutions. In particular, the provision of an electronic certificate only makes sense if and only if the counterparty can use it as a digital instrument, rather than becoming a digital footprint in an analog system.

REFERENCES

[1] БДС EN ISO/IEC 17025:2018

[2] Цв. Петков, Изграждане на национална метрологична мрежа, XVII-та Национална научно-техническа конференция Метрология 2022

[3] Четвърти национален план за действие в рамките на инициативата „Партньорство за открито управление“

SECTION I
GENERAL ASPECTS OF METROLOGY. MEASUREMENT METHODS. UNITY AND ACCURACY OF MEASUREMENTS

Optimization and standardization of schemes for realisation of the mass scale

Tsvetomir Petkov
BIM, DG NCM
Mechanical Measurements Department
Sofia, Bulgaria
Ts.Petkov@ bim.government.bg

The introduction of the new definition of mass, related to the Planck constant, makes it possible to realize not only 1 kg, but also any other nominal value of the mass. In practice, these conversions are characterized by high uncertainties, while not being available to most NMIs. In the foreseeable future, our well-known weights will continue to be widely used as standards. Following the introduction of the new definition, the BIPM has significantly increased the uncertainties of national standards. The aim of the project "19RPT02- RealMass Improvement of the realization of the mass scale" is the project participants to optimize and standardize the schemes and methods of realisation of the mass scale.

Keywords—EMPIR, mass scale, 19RPT02

I. INTRODUCTION

From May 20, 2019, the new definition of the kilogram, based on Planck's constant, entered into force. This resulted in an additional contribution (Planck's constant) to the uncertainty given by the BIPM. All this led to a revision of NMI's SMS lines. In an effort to meet the high demands of their customers, NMIs from all over Europe have joined forces to optimize and standardize the schemes and methods of realisation of the mass scale

II. 19RPT02 REALMASS

Realisation of the mass scale is done using subdivision matrices. There are many different die designs as well as measurement processing methods. A design cannot be qualified as "good" in general since it is the subject of optimisation. Usually, more weighings provide smaller uncertainties, but more weighings require more efforts, time, money and even complex calculations. This is an important part of the investigation providing a possibility to some laboratories not to increase their uncertainties (CMCs). Additionally the robustness of the design is important. It should be eliminate or at least detect possible erroneous measurements[3].

Participants in the 19RPT02 RealMass Improvement of the realisation of the mass scale project are[1]:

- CMI, Czech Republic;
- BEV-PTP, Austria;
- BIM, Bulgaria;
- BRML, Romania;
- DMDM, Serbia;
- IMBiH, Bosnia and Herzegovina;
- INRIM, Italy;
- NSAI, Ireland;
- SMD, Belgium;
- ME-BoM, North Macedonia;
- NSC-IM, Ukraine.

Work on the project began with the sharing of information between the participants about the designs and methods used to process the measurements, as well as the available reference and auxiliary equipment. This information enabled a preliminary analysis of the designs used in practice, and also enabled individual participants to experiment with different designs from other institutes. This happened during the online training from Italy. This allowed the participants to independently optimize their matrices at a very early stage of the project. We also reviewed our designs and made changes to them. First, we will analyze the design used so far in BIM.

(1) –standard 134
(2) –Sum 134 (500+200+200*+100) [g]
(3) –standard 133
(4) –National standard

	(1) 1kg	(2) Suma 1kg	(3) 1kg	(4) 1kg
Y1	+	-		
Y2	+		-	
Y3	+			-
Y4		+	-	
Y5		+		-
Y6			+	-
Restraint				+

Fig. 1

(1) –standard 134 500 g
(2) - standard 134 200 g
(3) - standard 134 200 g
(4) – standard 134 100 g
(5) – standard 133 100 g
(6) – Sum 134 (50+20+20*+10) [g]

	(1)	(2)	(3)	(4)	(5)	(6)
	500g	200g	200*g	100g	100 g	Suma100g
Y1	+	-	-	-	-	+
Y2	+	-	-	-	+	-
Y3	+	-	-	+	-	-
Y4	+	-		-	-	-
Y5	+		-	-	-	-
Y6		+	-	+	-	
Y7		+	-	-		+
Y8		+	-		+	-
Restraint	+	+	+	+		

Fig. 2

The presented design demonstrates the realisation of the mass scale in the range 1kg – 100 g. First, I want to emphasize the presence of sum standards in both matrices. This is imperative in this model in order to transmit the unit in lower denominations. To realize the given range according to the considered model, 14 measurements are performed with the participation of 10 conditional ones representing 13 real standards. 2 control standards are also included in the design, with which the reliability of the measurements in the matrix itself is guaranteed. It should be noted here that the "subdivision" method is applicable not only for unit transmission of output standards to NMIs but can also be used to calibrate client standards. Despite the fact that the same design and the same mathematical model can be used in both applications of the method, one significant difference is noticeable - available archival data for the calibrated standards. When the method is used for its own purposes, then this data is available for all standards and then each standard can be considered as a control in terms of its history. When calibrating client standards, this information is not available or is not complete, necessitating the inclusion of control standards in the model. The use of standards helps with data analysis even in cases where you are using the model for your own needs. This is due to the fact that during the recalibration periods, you used your source standards to transfer the unit to your working standards, and it is also possible to use them when calibrating customer standards, in cases where you do not have suitable working standards. This is a prerequisite for the presence of a real drift of the output standard, which should be taken into account when analyzing the measurement data. Despite the accumulated experience and good results obtained by the considered model, this design is distinguished by one significant drawback - an excessively large number of simultaneously participating standards. Even a quick look at the matrix is enough to see that in some rows 9 real standards are involved in the measurements at the same time. This in turn leads to the following problems:

Unstable measurement process – The instability of the process is observed both when measuring automatic and when using manual comparators. In the case of automatic comparators, the reason for this is shifts in the positions of the standards during the change of plates, while in the case of manual comparators, the time between the measurement of the standard and calibrated weights is added and increased;

Danger of swapping standards - such a danger always exists when calibrating weights, especially high-end ones (there are no identification marks on the standards themselves, they are made of the same material, with the same shape and dimensions), but when you have 9 standards on the table in front of you, with which you work simultaneously, this problem becomes extremely dangerous;

Placement of standards on the dish – In order to reduce the eccentricity of their comparators, manufacturers try to make the plates of minimum dimensions. This improves the stability of the equipment, but at the same time presents the operator with a very serious challenge during the implementation of subdivision in his effort to evenly and stably distribute a large number of standards over a small area.

BIM's participation in the 19RPT02 project allowed NCM experts to learn about practices in other metrology institutes and to get first-hand information about the mass unit transmission models they use. This information allowed us to weigh the positives and negatives of each of the designs presented and develop a new design for our needs.

(1) –Standard 134
(2) – Standard 133
(3) –National standard

	(1)	(2)	(3)
	1kg	1kg	1kg
Y1	1	0	-1
Y2	0	1	-1
Y3	1	-1	0
Y4	-1	1	0
Y5		-1	1
Y6	-1		1
Restraint			+

(1) –Standard 134 1000 g
(2) – Standard 134 500 g
(3) - Standard 134 200 g
(4) - Standard 134 200 g*
(5) – Standard 134 100 g
(6) – Standard 133 100 g

	(1)	(2)	(3)	(4)	(5)	(6)
Y1	-	+	+	+	+	
Y2	-	+	+	+		+
Y3		-	+	+	+	
Y4		-	+	+		+
Y5			-	+	-	+
Y6			-	+	+	-
Y7			-		+	+
Y8				-	+	+
Restraint	+					

Fig. 3

A design is presented in the same range from 1 kg to 100 g. To realize the given range according to the considered model, 14 measurements are performed with the participation of 8 real standards. 2 control standards are also included in the design, with which the reliability of the measurements in the matrix itself is guaranteed. Impressive in this design is the fact that the very realization of the scale is possible only from the second matrix. This would reduce the number of measurements and the standards used. On the other hand, it would exclude the possibility of measured at the output and control standards for point 1 kg. This necessitated the creation of a separate design for only 1 kg. In practice, this design can be realized with only 3 measurements, but in order to increase the reliability of the results, mirror rows are included. As can be seen in this design the number of involved standards is greatly reduced. The maximum number of simultaneously participating standards in one measurement is 5, which is almost double the number of the old design.

		design_2019		design_2021				
standard	nominal	value [g]	uncertainty [mg]	value [g]	uncertainty [mg]	difference [mg]	CMC [mg]	1/3 MPE E1[mg]
133	1 kg	999,999995	0,042	999,999998	0,049	0,003	0,056	0,167
134	1 kg	999,999986	0,042	999,999983	0,049	0,003	0,056	0,167
134	500 g	499,999983	0,021	500,000012	0,033	0,029	0,035	0,083
134	200* g	199,999978	0,012	199,999991	0,020	0,013	0,03	0,033
134	200 g	200,00002	0,012	200,000011	0,020	0,009	0,03	0,033
134	100 g	99,999999	0,008	99,999999	0,018	0	0,025	0,017
133	100 g	99,999983	0,008	99,999992	0,018	0,009	0,025	0,017

Fig. 5

On fig. 5 you can see a comparison between actual measurements of the two designs. It is important to note that the recorded data for differences in prescribed values between the two models are within the calibration uncertainties. This fact gives us reason to believe that the results of the two calibrations are reliable and stable, without raising doubts about gross errors in the measurement process or damage in standards. At the same time, it is noticed that the deviation at 500 g is significant and comparable to the measurement uncertainty. Looking at the history of the standard, we see that the previous calibration registered a difference of 0.010 mg, in the positive direction. The registered difference is now significantly larger and requires further analysis regarding the standard itself, but at the same time it is not so high as to raise doubts about the unit transmission pre-assessment itself. It is impressive that the measurements obtained with the old design have a significantly lower uncertainty, despite our expectations for a more stable measurement process due to the smaller number of simultaneously participating standards. This initially disconcerting fact prompted us to further analyze the results. The first thing that should be noted is that the design in this range is implemented on an automatic comparator, with relatively large area standards, allowing easier and more stable positioning of the standards as a group. This significantly reduces the risk of possible instabilities due to displacement of standards in the calibration process. In addition, the new design uses national standard data after the redefinition of the kilogram. It is clearly seen that the values obtained as an uncertainty for 1 kg exceed the effective 2020 CMC of 0.044mg, which proves the need for the revision of the CMC lines of the NMIs. The way in which the uncertainty data of the standard is received for each matrix should also be taken into account. In the 2019 design, the sum of standards (500+200+200*+100) gets its uncertainty directly from the national standard, and in the second matrix this uncertainty is distributed among the single standards. In the 2021 design, this connection is indirect and goes through the 1 kg output standard. Of course, it is possible to implement a design that avoids this shortcoming by merging the two matrices, but taking such a move, we should use the same approach for the other decades as well. This results in a huge matrix which, apart from being a mathematical challenge, would cause additional problems in data analysis. However, some NMIs (e.g. NPLs) use exactly this approach. From the analysis presented above, it is clear that the expectations of the experts are that the 2021 design will reveal its potential in the smaller denominations. The design used is the same, so we will move directly to the data analysis.

		design_2019		design_2021				
standard	nominal	value [g]	uncertainty [mg]	value [g]	uncertainty [mg]	difference [mg]	CMC [mg]	1/3 MPE E1[mg]
134	1 g	1,000006	0,003	1,0000046	0,002	0,0014	0,006	0,0033
134	500 mg	0,499998	0,003	0,4999984	0,001	0,0004	0,005	0,0027
134	200 mg	0,200000	0,002	0,1999998	0,0006	0,0002	0,004	0,0020
134	200* mg	0,200001	0,002	0,2000001	0,0006	0,0009	0,004	0,0020
133	100 mg	0,100006	0,001	0,1000053	0,0004	0,0004	0,004	0,0017
134	100 mg	0,099999	0,001	0,0999987	0,0004	0,0003	0,004	0,0017

Fig. 6

As you can see, this decade is extremely important for BIM. The reason for this is the fact that the protected CMC rows do not allow the laboratory to cover the calibration requirements of class E1 standards[2]. It is clearly seen that the reason is not in the previously used design, but lies in the updated equipment after the protection of the CMC lines. The first thing we notice is the difference between the two calibrations. This difference for all standards is within the uncertainty, leading us to assume that the measurements are credible. As expected, the stability of the measurement process has been significantly improved, not only in this decade, but also in the previous decade, as evidenced by the lower uncertainty obtained for the 1 g weight as well.

The results obtained from the given comparison are not a basis to conclude which of the two designs is more suitable, due to the little experience we have with the new

design. It should also be noted that when comparing two measurements, there is no way to account for accidentally occurring errors, disturbances in the surrounding environment, as well as possible methodical errors from the smaller experience with the given model. The design itself demonstrates serious potential, especially in the milligram range, where the danger of simultaneous work with a large number of standards is much more serious. This gives us reason to continue work on the optimization of designs. Naturally, BIM will not go this way alone. Our partners within 19RPT02 – RealMass, have already shown their support. During the project meeting at BEV, our participants were shown software for preliminary analysis of designs. Within the framework of the project, it is expected to develop more:

- software to assist NMIs in processing measurement data;
- to prepare a guide for applying the method and choosing the most appropriate design;
- to conduct 2 comparisons to validate both the designs and the mathematical methods used to analyze the data.

III. CONCLUSION

The choice of die design when realisation of the mass scale can directly affect the measurements. Each design has its own strengths and weaknesses, and the choice of a particular design involves a trade-off between measurement time, necessary and available standards and equipment, and personnel experience. The designs themselves are suitable to varying degrees for one laboratory or another. Creating a universal design is practically impossible. Of course, in practice there are necessarily designs that to varying degrees suit one or another NMI. The research of these designs, their adaptation in the specific conditions and the creation of a mechanism for processing the data from the measurements is a goal that the partners of the project 19RPT02 RealMass Improvement of the realization of the mass scale have set themselves in response to the growing customer requirements.

REFERENCES

[1] EMPIR project 19RPT02 RealMass Improvement of the realisation of the mass scale

[2] OIML R 111-1(2004)

[3] Z. Zelenka, Why and how to improve the subdivision technique in mass metrology, XXIII IMEKO World Congress "Measurement: sparking tomorrow's smart revolution."August 30 - September 3, 2021, Yokohama, Japan

Optimization of the environment and equipment in the laboratories for measuring mass and related units

Tsvetomir Petkov
BIM, DG NCM
Mechanical Measurements Department
Sofia, Bulgaria
Ts.Petkov@ bim.government.bg

The rapidly evolving competitive environment in the field of mass and related measurement, as well as the growing demands of customers, fueled by equipment manufacturers, are the reason why many laboratories seek to improve the quality of their services. Purchasing new, modern and more precise equipment is a step towards more reliable results, but when embarking on this path, laboratories often miss or underestimate the impact of the environment in which they place and operate their equipment. This leads to the risk of self-purchase of new equipment, which is unable to reveal its potential. Poor balance between equipment and facilities can not only lead to unnecessary material costs for the laboratory but also risks compromising the measurement results.

Keywords—mass measuring, laboratory equipment, mass and related units

I. INTRODUCTION

In recent years there has been an increased interest in calibration of mass and related quantities on the part of laboratories. There are many reasons for this, but the following deserve attention:

- New laboratories in the region ;
- Expanding the activity and scope of the laboratories ;
- Increasing customer requirements ;
- An intensifying competitive environment from equipment suppliers offering increasingly high level equipment at competitive prices.

All of this presents laboratories with challenges that they are not always in a position to handle on their own. This leads to numerous questions for BIM experts regarding recommendations for what standards and what equipment to purchase from new or developing laboratories in the field. What is specific about these questions is that they mainly refer to the equipment, but not to the conditions in which it should work and the ways to control these conditions. First of all, I want to pay special attention to the strict compliance with the instructions for working with the equipment provided by its manufacturer and, in particular, those related to its setting and the heating time, which can vary from a few minutes (for III and IV class) up to 8 hours for class I scales and comparators.

The main environmental elements affecting measurements of mass and related quantities are:

- temperature;
- relative humidity;
- atmospheric pressure;
- vibrations;
- Air flow speed.

II. TEMPERATURE

The permissible temperature range in the laboratory premises for the calibration of mass and related quantities according to R-111 is from 15 °C to 27 °C[2]. Unlike other types of measurements, the temperature range is quite wide, while very strict restrictions are imposed on the temperature gradient.

Weight class	Temperature change during calibration (2)
E_1	± 0.3 °C per hour with a maximum of ± 0.5 °C per 12 hours
E_2	± 0.7 °C per hour with a maximum of ± 1 °C per 12 hours
F_1	± 1.5 °C per hour with a maximum of ± 2 °C per 12 hours
F_2	± 2 °C per hour with a maximum of ± 3.5 °C per 12 hours
M_1	± 3 °C per hour with a maximum of ± 5 °C per 12 hours

Fig.1

The reason for this is not only the fact that temperature has a direct effect on air density, but also the effect of natural air flow caused by this gradient, which

directly affects the measuring equipment. In an effort to maintain a constant temperature, many laboratories use air conditioning systems. Conventional air conditioning systems, on the other hand, create a very strong air flow, and the temperature of the air blown out by them in some cases differs by 10 or more degrees from the basic room temperature. This places the equipment in an extremely unfavorable environment, and despite the stable reading of the thermometer, obtaining a stable reading of the device is impossible. The situation worsens further if the room has poor thermal insulation and windows, which implies direct sunlight. Even the installation of blinds is not able to completely remove the heating effect of direct sunlight[3].

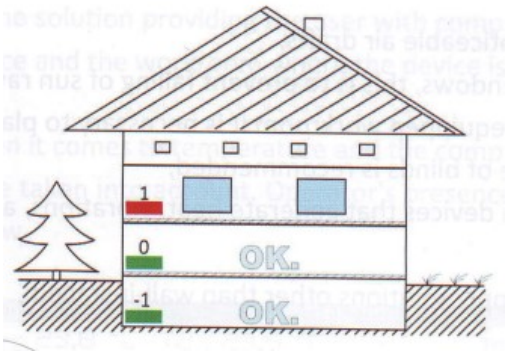

Fig.2

For this reason, laboratory rooms for measuring mass and related quantities are recommended to be built in underground floors or, if that is not possible, in rooms without windows. Unfortunately, even these dark rooms are not able to provide the necessary temperature comfort in cold winter or hot summer days. However, this necessitates the use of some type of air conditioning system. Ideally, this should be a room with double walls, and between them circulate air with a temperature of (20 - 22) °C.

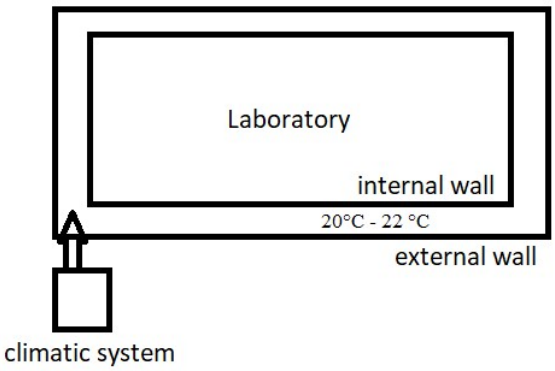

Fig.3

When it is not possible to build such a room, it is recommended to install climate walls or floor heating. The climate walls and floor heating are connected to a heat pump and the water temperature is maintained (20 -22) °C. This is done in order to limit the temperature gradient as much as possible while reducing the risk of condensation in cooling mode. The advantages of climate walls over floor heating are the following:

- Direct isolation of the room from external temperature impacts with an effect similar to double walls;
- Possibility to build a larger yielding area;
- More efficient operation in cooling mode;
- Limiting the air flow in the "under-ceiling" direction in heating mode, while reducing the probability of movement of fine dust particles in the same direction.

It should be noted that the role of double walls can also be played by neighboring rooms.

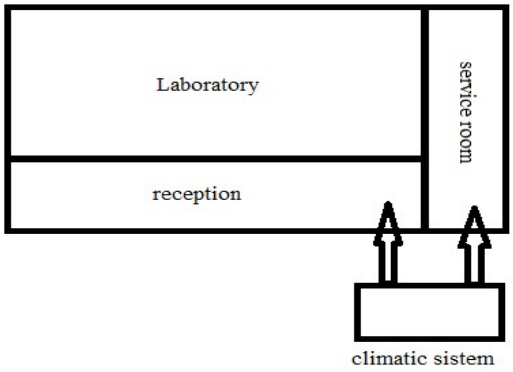

Fig.4

III. HUMIDITY

Ensuring humidity in the (40 - 60) %rh range during the winter months can be a particularly big problem for most laboratories[2].

Weight class	Range of relative humidity (*hr*) of the air [3]
E_1	40 % to 60 % with a maximum of ± 5 % per 4 hours
E_2	40 % to 60 % with a maximum of ± 10 % per 4 hours
F	40 % to 60 % with a maximum of ± 15 % per 4 hours

Fig.5

To maintain the necessary humidity, there are special devices - humidifiers, which work according to two main methods:

- Isothermal humidification. It is done by mixing the air flow with the water vapor released by the humidifier. The main task of a humidifier is to turn liquid (water) into steam. Isothermal humidifiers are connected to the electrical network and do not change the air temperature during operation[1];

- Adiabatic humidification. Based on the natural evaporation of water in the environment - the air. The principle of operation is based on the difference in pressure of the steam generated above the water surface and the pressure of the surrounding air. The air stream absorbs moisture, after which this moisture must be converted into water vapor. In this process, the air consumes a lot of energy, so it cools[1].

The main problem in this case is again ensuring homogeneity of humidity throughout the room without creating an air flow. A wide variety of industrial humidifiers are available on the market. Most of them practice turning water into steam and spreading this steam around the room. The main difference between them is the method by which water is turned into steam. As it is not the subject of the report, we will not dwell in detail at this time on the various methods of turning water into steam, but will concentrate on the means of delivering this steam into the room itself. In rooms where humidification is required, but the presence of air flow is not critical, concentrated humidifiers are usually used,

Fig.6

relying on the airflow created by the humidifier to distribute the steam throughout the room(Fig. 6) . To limit the strength of this flow and improve homogeneity, it is recommended to distribute this flow evenly throughout the room using multiple and large-section diffusers. Usually, these sprinklers are installed on the walls or ceiling of the room, and the steam itself reaches them through steam pipes. In these cases, there is a risk of condensation in the steam line and the formation of water droplets on the edges of the sprinkler, which, in the case of a ceiling installation, can fall on the equipment and cause critical damage. Another type of humidifiers is widely used in practice, in which water is delivered to the room through high-pressure nozzles, sprayed on microscopic particles (about 8 micrometers), and the steam itself is produced as a result of the contact of these particles with the air(Fig. 7).

Fig. 7

The advantage of this method is a reduced risk of condensation on the sprinklers, in this case the nozzles. Particular attention should also be paid to the fact that whichever of the air humidification methods you choose, the humidification itself should be done with clean water to ensure a healthy working environment for employees. For this purpose, it is necessary to provide for the construction of a water purification system for the air humidification system, trying to avoid buffer tanks in which water can stagnate.

IV. VIBRATIONS

Providing the necessary parameters of the surrounding environment for the operation of the equipment, we should not underestimate on what basis our equipment will be installed. In the official documents, there are no concrete requirements for the levels and frequency of permissible vibrations, but it is written that measures must be taken to limit them. There is a wide variety of different types and models of laboratory tables on the market, which, despite the assurances of their manufacturers, are not suitable for use in measuring mass and related quantities. Ideally, the equipment for measuring mass and related quantities should be mounted on a solid granite slab placed on air cushions. This construction really effectively dampens vibrations and provides a strong, deformable base.

This perfectionism unfortunately comes at a high price, which is not always within the capabilities of laboratories. For this reason, in practice, a significantly cheaper solution has become necessary - a granite slab on a sand base. The main condition for making a quality laboratory table is that the base of the table is located on a pedestal, separated from the main structure of the building[3].

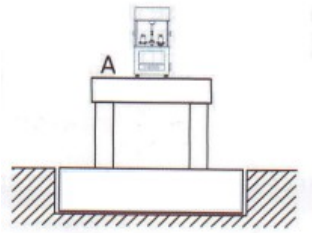

Fig.8

This is done in order to limit the transmission of vibrations from the main structure to the measuring table. The base of the table itself is made hollow, and its interior is filled with sand, which serves as a base for a granite slab with a minimum width of 30 mm. The structure built in this way provides a reliable foundation for our equipment and can serve us for tens of years without additional costs. Floor pedestals should also be made according to a similar scheme, in cases where the equipment is installed on the floor.

V. SENSORS

Special attention should be paid to the selection of the equipment itself. The best equipment on the market is not always the best for our particular tasks. By buying the best equipment, we should provide it with the best working environment. On the other hand, only by improving working conditions should we not expect miracles from our equipment. This applies not only to our scales, comparators and standards, but also to the auxiliary equipment that will be used to monitor the surrounding environment.

For example:

We wish to calibrate F1 class weights. The conditions for temperature drift are 1.5 °C /hour. In order to be able to guarantee the reliability of the measured parameters, our temperature sensor must have a scale division of 0.01 °C with a maximum uncertainty of 0.1 °C. Using a coarser sensor allows for the possibility of getting a larger drift during the measurement without being able to detect it, therefore compromising the measurement results, and using a more precise thermometer makes the investment in it pointless.

VI. CONCLUSION

In an effort to provide better services to their customers, laboratories for measuring mass and related quantities are resorting to the purchase of new, modern and more precise equipment. What they should pay attention to is the conditions under which they will put this equipment to work. The bad balance between equipment and material base can lead not only to unnecessary material costs for the laboratory, but also poses a risk of compromising the results of measurements.

REFERENCES

[1] https://desigusxpro.com/bg/
[2] OIML R 111-1(2004)
[3] Radwag, Automatic Comparison of Weights and Mass Standards

Uncertainty of Measurement of the Calibration Factor of the Dose Rate Unit

Yulia Verhusha
ATOMTEX SPE
Minsk, Republic of Belarus
verhusha_ya@atomtex.com

Sergey Lazarenko
ATOMTEX SPE
Minsk, Republic of Belarus
lazarenko_sv@atomtex.com

***Abstract*—The calculation of measurement uncertainty is carried out in accordance with the international standard ISO/IEC Guide 98-3:2008, national technical regulations, experience in the field of calibration. The report presents a variant of uncertainty calculation of the calibration factor when measuring dose rate.**

***Keywords*—dosimeter, calibration facility, dose rate, calibration factor, uncertainty.**

I. INTRODUCTION

Calibration of radiation monitoring instruments and universal clinical dosimeters: dosimeters, dosimeters-radiometers, dosimeters-spectrometers, dose rate meters, detection units (dosimeter) designed to determine the air kerma rate, ambient and directed dose equivalents rate of X-ray and gamma radiation is performed in calibration laboratories.

In order to recognize calibration results and calibration certificates provided at the international level, laboratories undergo the procedure of conformity assessment in the national accreditation body. When accrediting calibration laboratories they are assessed for compliance with the requirements of the standard ISO/IEC 17025-2019 “General requirements for the competence of testing and calibration laboratories”. The important requirements of the standard are the confirmation of the level of technical competence of the laboratory, the calibration method used, its validation (verification) and evaluation of measurement uncertainty.

The purpose of this work is to determine the contributions to the measurement uncertainty of the calibration factor when calibrating a dosimeter that measures the ambient dose equivalent rate, directional dose equivalent rate, exposure dose rate, and air kerma rate (dose rate).

II. MATERIALS AND METHODS OF RESEARCH

The calibration procedure consists in determining the calibration factor of the dosimeter at the calibration point in order to determine under given conditions the value of the corresponding physical and operational quantity reproduced by the reference facility and to calculate the uncertainty of the calibration factor measurements at the calibration points.

The reference dose rate is reproduced by the AT130 and AT110 gamma calibration facilities [1] designed to reproduce and transmit the air kerma, exposure dose, ambient, directed individual dose equivalents and their respective rates into working standards and measurement instruments during verification, calibration and test procedures “Fig. 1”,“Fig. 2”.

Fig.1. AT110 gamma calibration facility

Fig.2. AT130 gamma calibration facility

AT110 and AT130 facilities is based on the use of ^{137}Cs radionuclide sources. The facility implements an irradiation scheme with a stationary irradiator and a linearly positioned platform of the calibration bench. A range of gamma radiation dose rate values is achieved by using ^{137}Cs sources of different activity and varying the "source-detector" distance. The size of the radiation field is varied by the "source-detector" distance or the diameter of the collimator channel. Characteristics in "Table 1" and "Table 2".

TABLE 1. AT110 GAMMA CALIBRATION FACILITY SPECIFICATION

Gamma radiation sources: **Maximum activity**	^{137}Cs: 9.6·10^{13} Bq (2600 Ci) ^{60}Co: 7.2·10^{9} Bq (0.2 Ci) ^{241}Am: 1.6·10^{10} Bq (0.4 Ci)
Number of sources	Up to 6
Ranges: **- Air kerma rate** **- Exposure dose rate** **- Ambient and personal dose equivalent rates**	0.36 μGy/h – 48.6 Gy/h 40 μR/h – 5540 R/h 0.42 μSv/h – 58 Sv/h
Intrinsic relative error for certification as a working standard of 1-st category (2-nd category)	±2.5% (±5%) [air kerma rate and exposure dose rate] ±4.5% (±7%) [ambient and personal dose equivalent rates]
Collimator channel	Ø60 mm / Ø90 mm Length 150 mm
Diameter of uniform radistion field at R=1m **(Non-uniformity ±6%)** **- for Ø60 mm collimator** **- for Ø90 mm collimator**	 300 mm 450 mm
Working distances interval	0.3 – 7 m
Radiation background at 1 m distance from irradiator in storage position	≤0.5 μSv/h

TABLE 2. AT130 GAMMA CALIBRATION FACILITY SPECIFICATION

Gamma radiation sources: **Maximum activity**	^{137}Cs: 1.3·10^{12} Bq (35 Ci)
Number of sources	Up to 5
Ranges: **- Air kerma rate** **- Exposure dose rate** **- Ambient and personal dose equivalent rates**	0.25 μGy/h – 350 mGy/h 30 μR/h – 40 R/h 0.30 μSv/h – 420 mSv/h
Intrinsic relative error for certification as a working standard of 1-st category (2-nd category)	±2.5% (±5%) [air kerma rate and exposure dose rate] ±4.5% (±7%) [ambient and personal dose equivalent rates]
Collimator channel	Ø60 mm / Ø90 mm Length 150 mm
Diameter of uniform radistion field at R=1m **(Non-uniformity ±6%)** **- for Ø60 mm collimator** **- for Ø90 mm collimator**	 160 mm 260 mm
Working distances interval	0.3 – 7 m
Radiation background at 1 m distance from irradiator in storage position	≤0.6 μSv/h

Metrological traceability is ensured by calibration facility by the accredited laboratory of The D.I. Mendeleev All-Russian Institute for Metrology (VNIIM). The calibration facility is calibrated using the State Primary Standard by direct measurement using an ionization chamber at different distances. Extended uncertainty the certainty of the values of the air kerma rate is 1.8 % for AT130 and 1.9 % for AT110 with a coverage coefficient of k = 2.

The general model for determining the dose rate calibration factor will include the following components:

$$C_{\dot{D}} = \frac{\dot{D}}{\bar{M}_{\dot{D}_K} - \bar{M}_{\dot{D}_{bg}}} \cdot k_\tau \cdot k_{T_{1/2}} \cdot k_r \cdot k_\mu \cdot k_O \cdot k_h \quad (1)$$

where $\dot{D}$ – is the dose rate at the calibration point on the calibration date of the calibration facility;

$\bar{M}_{\dot{D}_K}$ – average reading of the dose rate at the calibration point on the date of dosimeter calibration;

$\bar{M}_{\dot{D}_{bg}}$ – average reading of the dose rate of the radiation background dosimeter at the calibration point;

k_τ – correction factor for the difference between the calibration date of the reference facility and the calibration date of the dosimeter;

$k_{T1/2}$ – correction factor for half-life of the radionuclide source used in calibration facility;

k_r – correction factor for the square of the distance if the dosimeter is calibrated at a point other than the calibration point of the facility;

k_μ – correction factor for the linear coefficient in air if the dosimeter is not calibrated at the facility calibration point;

k_O – correction factor for non-uniformity of the radiation field;

k_h – correction factor for transition from air kerma rate.

III. THE RESULTS

Based on formula 1 of the above mathematical model for determining the calibration factor of the dosimeter, an uncertainty budget can be made "Table 3".

The general formula for determining the expanded uncertainty of the dosimeter calibration factor measurement will be as follows according to the requirements of [2] - [6]:

$$U(C_{\dot{D}}) = 2 \cdot \sqrt{\begin{aligned} &u_A^2(\dot{D}_\Phi) + u_A^2(\dot{D}_K) + u_B^2(\dot{D}_0) + \\ &+c_\tau^2 \cdot u_B^2(\tau) + c_{T_{\frac{1}{2}}}^2 \cdot u_B^2\left(T_{\frac{1}{2}}\right) + \\ &+c_{r_1}^2 \cdot u_B^2(r_1) + c_{r_2}^2 \cdot u_B^2(r_2) + \\ &+c_\mu^2 \cdot u_B^2(\mu) + u_B^2(O) + u_B^2(h) \end{aligned}} \quad (2)$$

It is important to determine the sensitivity coefficients specified in formula (2) for each component of uncertainty of the calibration factor measurements "Table 3".

The "Table 3" shows the main components of uncertainty with sensitivity coefficients in relative units, but in some cases other contributions may appear, for example on temperature, pressure, humidity, etc.

TABLE 2. EVALUATION OF MEASUREMENT UNCERTAINTY

Value	Type and law of probability distribution	Uncertainty	Sensitivity coefficient c	Contribution to total uncertainty
$M_{\dot{D}_{bg}}$	A (normal)	$u_A(\dot{D}_{bg})$	1	$u_A(\dot{D}_{bg})$
$M_{\dot{D}_K}$	A (normal)	$u_A(\dot{D}_K)$	1	$u_A(\dot{D}_K)$
$\dot{D}_0$	B (normal)	$u_B(\dot{D}_0)$	1	$u_A(\dot{D}_0)$
τ	B (uniform)	$u_B(\tau)$	$-\frac{0{,}693\tau}{T_{1/2}}$	$-\frac{0{,}693\tau}{T_{1/2}} \cdot u_B(\tau)$
$T_{1/2}$	B (uniform)	$u_B(T_{1/2})$	$\frac{0{,}693\tau}{T_{1/2}}$	$\frac{0{,}693\tau}{T_{1/2}} \cdot u_B(T_{1/2})$
r_1	B (uniform)	$u_B(r_1)$	$-(\mu r_1 + 2)$	$-(\mu r_1 + 2) \cdot u_B(r_1)$
r_2	B (uniform)	$u_B(r_2)$	$\mu r_2 + 2$	$(\mu r_2 + 2) \cdot u_B(r_2)$
μ	B (uniform)	$u_B(\mu)$	$-\mu(r_1 - r_2)$	$-\mu(r_1 - r_2) \cdot u_B(\mu)$
O	B (uniform)	$u_B(O)$	1	$u_B(O)$
h	B (uniform)	$u_B(h)$	1	$u_B(h)$

This example of measurement uncertainty calculation is implemented in the calibration method MC.AT 05-2022/GVL, which has received a positive metrological certificate of suitability at the National Metrology Institute of the Republic of Belarus. Calibration laboratory of ATOMTEX SPE, which applies this methodology, took part in proficiency testing program CDG-210-06/01.2022 VNIIM "Calibration of gamma radiation dosimeters" on En scores [7] with satisfactory results. The results are in "Table 4".

TABLE 4 ESULTS OF PARTICIPATION IN PROFICIENCY TESTING

Object	**Dose rate, μSv/h**	**The assigned value**	**The expanded uncertainty of the assigned value (k=2)**	**The laboratory result**	**The expanded uncertainty of a laboratory result (k=2)**	**En[a] scores**
Dosimeter AT1123	20	1.04	0.03	1.045	0.059	0.1
	200	1.04	0.03	1.025	0.058	0.2
	6000	1.05	0.03	1.020	0.058	0.5

[a]The scores of En ≥ 1.0 or En ≤ -1.0 could indicate a need to review the uncertainty estimates, or to correct a measurement issue; similarly -1.0 < En < 1.0 should be taken as an indicator of successful performance

IV. CONCLUSION

It should be noted that in the practice of verification of dosimeters (not calibration) all additional components of measurement accuracy are defined in the technical regulations by a single number for different classes of measurement standards (primary standard, 1st class standard, 2nd class standard, working standard). For example, for a 1st grade reference set, the total additional component according to [8, 9] will be equal to 0.8. Such approach in general simplifies calculations, but does not take into account specific cases of calibration, which can lead to unjustified increase of the value of expanded uncertainty of dose measurements during calibration of dosimeters in each specific point.

The calibrator should always, based on experience and skill, reduce the value of the uncertainty components of the measurement, so, for example, it is possible to:

1. increase the number of dose measurements to reduce the type A uncertainty component. As a rule, a value of 0.5 % is sufficient;
2. to calibrate the dosimeters at the reference calibration points to avoid additional uncertainty introduced by calculations of the reference dose by the square of the distance, i.e. $u_B(r_1)$, $u_B(r_2)$, $u_B(\mu)$;
3. reduce the interval between the reference calibration dates to reduce the contribution from the radionuclide source half-life error $u_B(T_{1/2})$. According to [10] it is sufficient to calibrate the reference facility once every two years;
4. use thermometers and barometers with the required accuracy to measure the ambient air temperature in the room of the reference facility and atmospheric pressure. As a rule, the uncertainty of measuring the ambient air temperature of 0.5 °C and the atmospheric pressure of 1 kPa is sufficient;
5. perform measurements at a sufficient distance from the collimator of the reference installation to reduce the influence of non-uniformity of the radiation field. According to [10] uniformity of the radiation field of 5% is sufficient;
6. calibration should be carried out under the required (normal) climatic conditions, i.e. normally from 15 to 25°C ambient air temperature, from 30 to 80 % relative humidity and from 86.0 to 106.7 kPa atmospheric pressure;
7. conduct calibration at the radiation background not exceeding the established norms. Usually, the ambient dose equivalent rate at the calibration point should not exceed 0.2 μSv/h or should be much lower than the dose at the open gate of the calibration facility.

It is important to study the operating documentation of the dosimeter to be calibrated under normal conditions for this dosimeter and to obtain a reliable result of the calibration factor and its expanded measurement uncertainty.

The calibration certificate specifies the uncertainty of measurement for each calibration point – the calibration factor.

REFERENCES

[1] Kozhemyakin, V. A. Modern reference calibration equipment for calibration of dosimetric equipment / V. A. Kozhemyakin [et al.] // Automated process control systems of nuclear power plants and thermal power plants: materials of the II International Scientific and Technical Conference, Minsk, April 27-28, 2021 / Belarusian State University of Informatics and Radioelectronics, Minsk, 2021, pp.125–126.

[2] ISO/IEC GUIDE 98-3:2008 Uncertainty of measurement – Part 3: Guide to the expression of uncertainty in measurement (GUM:1995)

[3] RMG 43-2001 Application of the “Guidelines for the expression of uncertainty measurements”.

[4] Pohodun A.I. Experimental Methods of Research. Measurement Errors and Uncertainties. Tutorial. SPb: SPbSU ITMO, 2006, 112 p.

[5] Efremova N.Y. Estimation of Uncertainty in Measurements: Practical Guide / N.Y. Efremova, Minsk: BelGIM, 2003, 50 p. [series “Guide to the Application of STB ISO/IEC 17025”].

[6] Estimation of uncertainty in analytical measurements: manual / N.N. Umarova [et al.]; Federal Agency on Education. Kazan. State Technological University, Kazan: KSTU, 2010, 82 p.

[7] ISO 13528:2015 Statistical methods for use in proficiency testing by interlaboratory comparison.

[8] STB 8083-2020 The system of ensuring the uniformity of measurements of the Republic of Belarus. State verification scheme for measuring instruments of kerma in the air, kerma power in the air, ambient, directional and individual dose equivalents, ambient, directional and individual dose equivalents of X-ray and gamma radiation.

[9] GOST R 8.804-2012 State system for ensuring the uniformity of measurements. State verification schedule for means measuring air kerma, air kerma rate, exposure, exposure rate, ambient dose equivalent, directional dose equivalent and personal dose equivalent, ambient dose equivalent rate, directional dose equivalent rate and personal dose equivalent rate and energy flux of X-ray and gamma radiation.

[10] ISO 4037-3:2019 Radiological protection X and gamma reference radiation for calibrating dosemeters and doserate meters and for determining their response as a function of photon energy. Part 3: Calibration of area and personal dosemeters and the measurement of their response as a function of energy and angle of incidence.

SECTION III
MEASUREMENT AND INFORMATION SYSTEMS AND TECHNOLOGIES

Method of Teraherz Spectroscopy for 3D Filament Nondestructive Testing and Its Metrological Aspects

Iurii Khoroshailo
dept. of Design and Operation of Electronic Devices
Kharkiv National University of Radioelectronics
Kharkov, Ukraine
yurii.khoroshailo@nure.ua

Nataliia Zaichenko
dept. of Microelectronics, Electronic Devices and Appliances
Kharkiv National University of Radioelectronics
Kharkov, Ukraine
nataliia.zaichenko@nure.ua

Olga Zaichenko
dept. of Design and Operation of Electronic Devices
Kharkiv National University of Radioelectronics
Kharkov, Ukraine
olha.zaichenko@nure.ua

Oleksandr Meniailo
dept. of Design and Operation of Electronic Devices
Kharkiv National University of Radioelectronics
Kharkov, Ukraine
oleksandr.meniailo@nure.ua

***Abstract*—This work is devoted to teraherz spectroscopy in time domain of filament for 3D printing and its metrological aspect. The subject of research is the thickness of the filament for 3D printing influence on. There was considered the refractive index determination, Fabry-Perot effect model and thickness of the filament for 3D printing influence on measurement uncertainty. The practical value lies in the possibility of using recycled materials for processing into filament for 3d printing, thereby solving environmental problems.**

***Keywords*—3d printing, time domain teraherz spectroscopy, refractive index, filament thickness, uncertainty**

I. INTRODUCTION

Additive technologies (3D printing) imply the process of combining (adding) the material from which an object is created according to its computer model. As a rule, for additive technologies, manufacturing happens “layer by layer” – in contrast to traditional “subtractive” technologies. “Subtracting” technologies are currently widely used technologies based on mechanical processing – removal (“subtraction”) of material from an array of workpieces. Thus, along with the traditional way – to produce something with the help of mechanical processing, gradually getting rid of everything superfluous by cutting, beating, drilling, milling, etc., currently, close attention is paid to the additive method of manufacturing based on the gradual addition of material and the creation of the necessary form [1].

The attractiveness of additive technologies is caused by a number of factors, first of all, they allow quickly make adjustments at any stage of the production process, adapt production to constantly changing market requirements, change the size of the produced batch at any moment depending on the increase or decrease in demand. 3D printing is used to produce a wide range of things, from prototype parts for avionics systems and industrial equipment, to a range of household items, gadgets and toys. However, in the manufacture of various products significantly affects their quality control of filament parameters.

Among the problems, the solution of which will increase the efficiency of using the potential inherent in the additive technologies, an important place is occupied by the issues of nondestructive testing or defectoscopy, its methods and models, metrology as well.

The most popular methods of 3D filament defectoscopy are ultrasonic spectroscopy, neutron radiography, optical nondestructive testing. Ultrasonic spectroscopy is usually understood as the use of phenomena associated with the diffraction of wave due to periodic changes in the density of the medium during the propagation of ultrasonic vibrations in it, but this term is also applicable to the methods of analyzing the frequency components of signals used in ultrasonic flaw detection [2].

Neutron radiography is a kind of radiographic method. Its advantage lies in the ease of interpretation of images and the ability to detect relatively small changes in the thickness and density of the material. Its disadvantages are also inherent in conventional radiography, for example, the inability to reliably detect cracks with a small extent in the direction of the radiation beam and the inability to provide detailed information about the quality of joints (soldering, riveting, gluing). When using the dependence of the attenuation of the neutron flux on the atomic number of the absorber material, in this case it is possible to obtain a satisfactory image of the junction. The optical nondestructive testing method is the simplest and most known, while it has the potential to further increase its accuracy.

There are different parameters characterizing 3D filament; refractive index is one of them. The refractive index we are interested in is the square root of the dielectric constant if the material does not have magnetic properties

In the microwave frequency range, one of the means of measuring the dielectric constant of substances is a six-port vector [3, 4] and scalar circuit analyzer[14-17], which is an additional option to traditional for six-port analyzers operations to determine power, complex reflectance and others.

The experience in material refractive index measurement in microwave domain and knowledge of its drawback led to the search for methods and means of defectoscopy in next to microwave frequency bands.

The work is devoted to the improvement of methods and models of terahertz spectroscopy in the time domain of filament for 3D printing.

The relevance of the topic of this study is confirmed by the large number of modern publications on this issue [1-9], which are devoted to a number of unsolved problemes. The subject of research in this paper is to determine the refractive index of the filament for 3D printing. The scientific novelty is to take into account the solidification of the filament in the manufacturing process. These factor leads to uncertainties, accounting which and correcting the measurement results, the accuracy of technological process control is increasing. The practical importance lies in the possibility of using secondary raw materials for processing into filament, thereby solving environmental problems.

II. Filament for 3D printing Properties as Uncertainty Source

PLA plastic is a material widely used in 3D printing. It is easy to use, and the products printed by this tilament thread differ in high operational characteristics. However, printing with this plastic requires compliance with a number of requirements for temperature and print speed. If you do not follow these rules, the product may deform

Shrinkage is the property of a polymeric material to decrease in volume during the printing process. The effect directly depends on how pure the chemical composition of the filament, as well as the melting point of the polymer and the temperature in the thermobox in the process of 3D printing. Errors may occur when printing with PLA plastic, which will eventually cause the finished model to shrink.

It is worth noting that the first layers of the product are more susceptible to shrinkage, as this area is subject to constant heating due to the energy transmitted by the printer table and the corresponding difference between the temperatures of subsequent layers. To avoid shrinkage and deformation of the PLA plastic model, it is recommended to follow the rules listed below: increasing adhesion, reducing printing speed can also reduce warping, to get rid of possible drafts, reducing the print temperature, reducing the print density. If the printing errors due to shrinkage may not be so noticeable visually, but present in the form of uncertainty, we will estimate the uncertainty.

Plastic thread suitable for printing is often used in two diameters: 1.75 mm and 3 mm. The choice of diameter depends on the extruder nozzle in the existing printer. Comes as a spool of wound plastic thread of one diameter

The temperature when plastic changes its aggregate states different for different plastics. The minimum is 180 °C for PLA, the maximum is 240 °C for ABS.

The thickness of the sample changes when applying heating, what causes the plastic physical state changes from hard to solid. The sample dimension changes are proportional to the temperature coefficient of linear expansion, which is the reference data Thermal expansion is a change in the linear size and shape of the body when its temperature changes. Quantitative thermal expansion of liquids and gases at constant pressure is characterized by the isobaric coefficient of expansion (volumetric coefficient of thermal extensions). To characterize the thermal expansion of solids, the coefficient of linear thermal expansion is additionally introduced. The branch of physics that studies this property is called dilatometry. Thermal expansion of bodies is taken into account in the design of all installations, devices and machines operating in variable temperature conditions

The basic law of thermal expansion states that a body with a linear size in the appropriate dimension expands by an amount equal to its temperature and in the absence of external mechanical forces

$$\Delta L = \alpha L \Delta T , \qquad (1)$$

where α is the coefficient of linear thermal expansion. Similar formulas are available to calculate changes in body area and volume. In the simplest case, when the coefficient of thermal expansion does not depend on temperature or direction of expansion, the substance will expand evenly in all directions in strict accordance with the above formula.

The temperature coefficient of linear expansion is $(8-10)\cdot 10^{-5}$ 1/K for ABS plastic.

III. Teraherz Spectroscopy Model and Means

The principle of operation of the time domain of the spectrometer (fig.1)

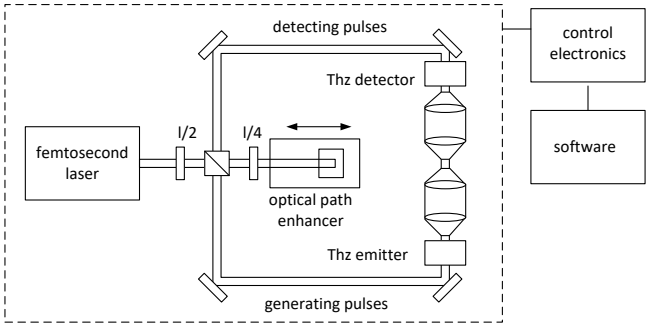

Fig. 1. Teraherz spectrometry plant

In this spectrometer, the laser beam is divided into two beams: generating and detecting. These beams pass different optical paths to the radiating and receiving antennas, respectively. One optical path has a variable length to control the delay of the pulse coming to the corresponding antenna (fig.1).

After the pulse is generated in the radiating antenna, the "detecting" pulse allows the corresponding antenna to measure the electric field strength. By varying the optical delay, the measurements are made at the right time. Later, frequencies are obtained from these points in time by means of Fourier transform. When the test sample is placed in the instrument, the received signal changes. To obtain information about the properties of the material, the two obtained spectra are compared.

Because the main use of time domain teraherz spectroscopy is in material characterization, a large amount of literature has been devoted to the subject of parameter extraction, i.e. to calculating the optical parameters of the materials studied from their THz transmission spectra. In common with other spectrometers, time domain teraherz spectroscopy measurements require comparison between the data recorded with the sample placed in the beam path and reference data recorded with the sample removed. First measurements of dielectric constants of materials were

demonstrated soon after the invention of time domain teraherz spectroscopy.

The main equation of terahertz spectroscopy is the dependence of the refractive index on various parameters, including the thickness of the sample

$$n(\omega) = n_0 - \frac{c}{\omega l}\arg\{H(\omega)\}, \quad (2)$$

where c is light velocity, l is sample thickness, n_0 is refractive index in the air, ω is circular frequency, H is relation [8-9]

$$H(\omega) = \frac{4n(\omega)n_0}{[n(\omega)+n_0]^2}\exp\left\{-k(\omega)\frac{\omega l}{c}\right\}\exp\left\{-j[n(\omega)-n_0]\frac{\omega l}{c}\right\}$$

$k(\omega)$ is extinction coefficient.

$$\arg\{H(\omega)\} = -[n(\omega)-n_0]\frac{\omega l}{c}$$

IV. Sample Thickness Influence on Refractive Index Measurement Uncertainty

The type A thickness uncertainty analytical expression is [10-11]

$$S^2_{n,l}(\omega) = \left[\frac{n(\omega)-n_0}{l}\right]^2 S_l^2, \quad (3)$$

where S_l^2 is thickness dispersion.

The type B thickness uncertainty is

$$S^2_{n,\delta}(\omega) = \left[\frac{n(\omega)-n_0}{l}\right]^2 \frac{\delta_l^2}{12}, \quad (4)$$

where δ_l^2 is obtained from publishing value.

The thickness of the sample can be determined in several ways, which can be classified into internal and external, i.e. measured in the framework of dilatometry or directly measured by terahertz spectroscopy so we get S_l^2 and δ_l^2 values for numerical estimation [6-9].

It is possible to estimate an error through the formula of an error of indirect measurements and here some components. Also called the formula for the accumulation of private errors.

There are many sources of error contribute to the variance of measured optical constant. The combined uncertainities for refractive index is esimated by adding variance and deviation

$$u_n(\omega) = k_p\sqrt{\frac{S^2_{n,E_{sam}}}{N_{E_{sam}}} + \frac{S^2_{n,E_{ref}}}{N_{E_{ref}}} + \frac{S^2_{n,l}}{N_l} + S^2_{n,\delta}} + f_{n,H} + f_{n,FP} + f_{n_0}, \quad (5)$$

where k_p is the coverage factor, $k_p = 1$ for standard uncertainty, $k_p > 1$ for expanded uncertainty, $S^2_{n,E_{sam}}$ and $S^2_{n,E_{ref}}$ are the amplitude-related variance sample and refered signals, $N_{E_{sam}}$ and $N_{E_{ref}}$ are the numbers of measurement for sample and reference signals, respectively, N_l is the number of measurement for the sample thickness, $S^2_{n,\delta}(\omega)$ is systematic uncertainty in sample thickness, $f_{n,H}$ is the effect of the phase difference on the refractive index deviation, $f_{n,FP}$ is the effect of reflections on the refractive index deviation, f_{n_0} is systematic error in air refractive index [8].

Uncertainty contribution values are sample thickness 1,8 10^{-3}, other uncertainty 10 time less, sample measurement noise and repeatability, sample alignement, air refractive index, and 100 time less reference measurement, transfer function, it means that sample thicknes uncertainty is dominant sourse of error [4].

V. Simulation and its result

The non excluded systematic error θ is determined from (1) is

$$\theta = \sqrt{\left(\frac{\partial \Delta L}{\partial L}\right)^2 (\Delta L)^2 + \left(\frac{\partial \Delta L}{\partial T}\right)^2 (\Delta T)^2}, \quad (4)$$

Standard uncertainty of B type uB for value depends on a priori information on value variability. If value is non-excluded systematic error with boundaries then its uncertainty is calculated by the formula [10-11]

$$u_B = \frac{\theta}{2\sqrt{3}}, \quad (5)$$

where $2\sqrt{3}$ is coefficient corresponding to the rectangular law distribution within the boundaries of the non excluded systematic error.

Calculations were carried out, which showed that at the temperature coefficient of linear expansion $\alpha = 9\cdot10^{-5}\ 1/K$, sample length (diameter) $L = 3\cdot10^{-3}\ m$, temperature change from melting temperature to room temperature with a temperature difference $\Delta T = 290 - 20^{\circ}C$, non-eliminated residue of uncertainty is $1.143\cdot10^{-4}$.

VI. Conclusions

In the course of the work, it was found that a change in the thickness of the filament caused by heating, leading to a change in the state of aggregation and described by the temperature coefficient of linear expansion, is an additional source of uncertainty. We have estimated the remaining residual systematic error. The standard uncertainty is $1.143\cdot10^{-4}$, extended one is $3.3\cdot10^{-5}$. Therefore, such an error should be taken into account in the calculation of the error budget.

There are directions for further development Firstly, taking into account the dynamics of solidification, that is, the rate of filament extrusion and quantifying its effect on the total error.

The condition for the applicability of the Fabry Perot effect, which is used in the model of terahertz spectroscopy in the time domain, is the parallelism of the opposite faces of the sample of the material under study, but the shape of the filament thread is usually cylindrical. The prismatic shape can be non-destructively shaped by using a rectangular nozzle of extruder or by machine flattening. The latter method is destructive and, moreover, is poorly combined with operational control, when the filament solidifies or vice versa melts. To preserve the cylindrical shape during the study, one can switch from terahertz spectrometry to terahertz imaging.

The idea of terahertz imaging is very simple. Terahertz radiation is focused by a lens or mirror. The sample under study is placed in a terahertz beam at its focus. Then scanning is carried out in a plane perpendicular to the beam. Terahertz radiation transmitted or reflected from each point of the sample is recorded by the detector. The set of points forms a terahertz pattern of transmission or reflection. One of future research direction is terahertz imaging with colorimetry combination [12, 13].

Another promising direction is related to the sample thickness, which will allow improving the model and measurement method in terahertz spectroscopy. The proposed approach uses an analogy with multimeters in the microwave range, namely, the phase distance between sensors in the microwave unit of a multiprobe microwave multimeter [14–17] is similar to the electrical path of the beam from one to the other face of a crystal in a terahertz spectrometer, as well as oriented graphs in the model multimeter is similar to the propagation of light in a sample in terahertz spectroscopy. With the caveat that directed graphs come from a cascade connection of graphical equivalents of scattering matrices that describe sensors, and the Fabry-Perrot effect [9] is physically observed in the sample under study.

If the thickness of the filament sample is selected during the production process by changing the extruder nozzle cross section, then a sample with such property can be obtained. In the describing the signal transformation in the sample model, in the expression for the electric field strength there is a factor responsible for the Fabry Perrot effect. Now this factor is treated as a series, and it is known that the series is limited by some member, and this can serve as a source of uncertainty. An alternative proposed approach is to compensate for the interference terms for Fabry-Perrot effect as in a multimeter accounting with opposite signes interference terms, like trigonometric function in sensors signals linearized equations system. This is where the mismatch uncertainty with U-shape probability distribution appears and is of interest from metrology point of view.

And one more perspective is associated with the presence of metal impurities in the filament, a possible further direction of research is sue from the fact that an electromagnetic wave passes through the dielectric and is reflected from the metal, and the main task is to distinguish the reflection from metal impurities from the reflection from the edges of the sample, which is present even in ideal pure filament.

REFERENCES

[1] P. I. Neyezhmakov, A. V. Prokopov, “On topical problems of metrology in the field of additive technologies,” Ukrainian metrological journal, 2016, (3), pp. 4-6.(in Russian).

[2] A. V. Prokopov, A. I. Shloma, “Analysis of the prospects for the use of non-destructive testing in the field of additive technologies,” Ukrainian Metrological Journal, 2017, (3), pp. 44-49.(in Russian)

[3] M. Naftaly, R. G. Clarke, D. A. Humphreys, “Metrology State-of-the-Art and Challenges in Broadband Phase-Sensitive Terahertz Measurements,” Proceedings of the IEEE, 2017, 105(6), pp.1-15.

[4] L. Oberto, M. Bisi, A. Kazemipour, A. Steiger, T. Kleine-Ostmann, T. Schrader, “Measurement comparison among time-domain, FTIR and VNA-based spectrometers in the THz frequency range,” Metrologia, 2017, 54(1), pp.77-84.

[5] F. Destic, C. Bouvet, ”Impact damages detection on composite materials by THz imaging,” Case studies in nondestructive testing and evaluation, 2016, 6, pp.53-62.

[6] T. D. Dorney, R. G. Baraniuk, D. M. Mittleman, “Material parameter estimation with terahertz time-domain spectroscopy,” JOSA A, 2001, 18(7), pp.1562-1571.

[7] L. Duvillaret, F. Garet, J. L. Coutaz, “Highly precise determination of optical constants and sample thickness in terahertz time-domain spectroscopy,” Applied optics, 199938(2), pp.409-415.

[8] W. Withayachumnankul, B. M. Fischer, H. Lin, D. Abbott, “Uncertainty in terahertz time-domain spectroscopy measurement,” JOSA B, 2008, 25(6), pp.1059-1072.

[9] W. Withayachumnankul, M. Naftaly, “Fundamentals of measurement in terahertz time-domain spectroscopy,” Journal of Infrared, Millimeter, and Terahertz Waves, 2014, 35(8), pp. 610-637.

[10] I. P. Zakharov, N. V. Shtefan, “Algorithms for reliable and effective estimation of type A uncertainty,” Measurement Techniques, 2005, Vol. 48, No. 5, p. 427-437.

[11] I .P. Zakharov, S. V.Vodotyka, E. N Shevchenko, “ Methods, models, and budgets for estimation of measurement uncertainty during calibration,” Measurement Techniques, 2011, Volume: 54, Issue: 4, pp. 387-399.

[12] Y. Horoshajlo, I. Sezonova, V. Chumakov, S. Efimenko, G. Levitskaya, “The Possibility of Using the Concept of Colorimetric Functions in Applied Research,” Proceedings of the International Conference on Advanced Optoelectronics and Lasers, CAOL, 2019, pp. 225–227.

[13] G. M. Suchkov, R. P. Migushchenko, O. Y. Kropachek, S. Y. Plesnetsov, Z. V. Bilyk, Y. E. Horoshailo, S. A. Efimenko, S. Boussi, Noncontact Spectral Express Method for Detecting Corrosion Damage to Metal Products, 2020, 56(1), pp. 12–19.

[14] O. Zaichenko, P. Galkin, N. Zaichenko, M. Miroshnyk, Six-port Reflectometer with Kalman Filter Processing of Sensor Signals Proceedings - 15th International Conference on Advanced Trends in Radioelectronics, Telecommunications and Computer Engineering, TCSET 2020, 2020, pp. 55–58,

[15] O. Zaichenko, M. Miroshnyk, N. Zaichenko, A. Miroshnyk, A. Multiprobe microwave multimeter signals iterative processing 30th International Scientific Symposium Metrology and Metrology Assurance, MMA 2020, 2020, pp.1-4.

[16] O. Zaichenko, P. Galkin, M. Miroshnyk, N. Zaichenko, A. Miroshnyk, . Application of Six-Port for Distance Measurement 2020 IEEE International Conference on Problems of Infocommunications Science and Technology, PICST 2020 Proceedings, 2021, pp. 97–100.

[17] O. B. Zaichenko, N. Y. Zaichenko, N. Y. “Systematization of the Formulas of Resonant Ferrite Isolator Loss,” Radio Electronics, Computer Science, Control, 2022, 1, pp.20-29.

Field of Captured Gamma Radiation with Energy up to 10 MeV for Metrological Support of Spectrometry and Dosimetry Instruments

Damian Komar
ATOMTEX SPE
Minsk, Republic of Belarus
komar_di@atomtex.com

Yulia Verhusha
ATOMTEX SPE
Minsk, Republic of Belarus
verhusha_ya@atomtex.com

***Abstract*— The use of dosimeters calibrated in reference fields with corresponding energies for correct estimation of dose loads for personnel working in high-energy gamma-radiation fields with energies above 3 MeV is required. The creation of reference fields with gamma-radiation energies up to 7 MeV is essential for photon radiation dosimetry at nuclear power plants, where a significant gross dose rate component is stipulated by the radiation with an energy of 6.13 MeV associated with the $^{16}O(n, p)^{16}N$ reaction in the water cooling loop. Apart from nuclear power plants, such tasks occur on electron accelerators, widely used for therapeutic, industrial and other purposes.**

The state verification schedule (Republic of Belarus and Russian Federation) stipulates the use of ^{241}Am (0.06 MeV), ^{137}Cs (0.662 MeV) and ^{60}Co (1.250 MeV) radionuclides for reference dosimetry measurements of gamma radiation in the range from 0.06 to 3 MeV. No standard calibration and verification is performed for nuclear physics equipment in bremsstrahlung with an energy above 3 MeV generated by accelerators. Dosimeters calibrated in the radionuclide sources fields may not measure the dose rate from high-energy gamma radiation correctly. At the same time, there is a nomenclature list of instruments with various detector types, where the energy range has to be expanded to 7 MeV or 10 MeV following the relevant research is carried out.

High-energy capture gamma-radiation fields with energies up to 7 MeV (titanium target) and up to 10 MeV (nickel target) to calibrate the energy scale and verify the energy dependence of developed spectrometric and dosimetric measuring instruments were generated by AT140 Neutron calibration facility for radiation monitoring instruments according to the requirements of international standard ISO-4037:2019.

The report presents the results of experimental studies. The standard dosimeter AT5350/1 with a highly sensitive ionization chamber TM32002 was used to determine the air kerma rate and ambient dose equivalent rate of gamma radiation.

Keywords—high-energy captured gamma-radiation fields, AT140 neutron calibration facility, titanium target, nickel target.

I. INTRODUCTION

Correct assessments of dose loads on the personnel working in the fields of high-energy gamma radiation with energies more than 3 MeV should be carried out by dosimeters calibrated in the reference fields with appropriate energies. Creation of reference fields up to 7 MeV is of essential importance for dosimetry of photon radiation at NPPs, where a significant component of the total dose rate is due to radiation from the $^{16}O(n, p)^{16}N$ nuclear reaction with energy 6.13 MeV flowing in the water cooling circuit. In addition to NPPs, such problems arise at electron gas pedals and high-energy X-ray machines, which can be used for therapeutic and industrial purposes. At such facilities, the energy of secondary photon radiation can reach several tens of MeV.

The expansion of energy range of gamma radiation dose rate measurements up to 7 MeV is also dictated by the requirements of international standards, such as ISO 4037-1 and IEC 61017 recommendations [2, 3].

Gamma radiation fields with higher (E>3 MeV) energies, suitable for instrument calibration, are obtained by nuclear reactions. This method of forming reference calibration fields requires a significant amount of expensive laboratory equipment, which is available to several leading national institutes. The $^{19}F(p, \alpha\gamma)^{16}O$ reaction can generate photons with energies of 6.13, 6.92, and 7.12 MeV [4] and the $^{12}C(p, p'\gamma)^{12}C$ reaction can generate photons of 4.44 MeV [5]. In such field formation schemes, targets made of special materials are irradiated with a beam of protons accelerated by the gas pedal field. The irradiated target is a source of gamma rays. Such schemes have been implemented in the National Research Council of Canada (NRC), National Institute of Metrology of Germany (PTB), Japan Atomic Energy Agency (JAEA), etc. [5-7].

Gamma rays with energies up to 10 MeV are emitted during radiation capture of a thermal neutron, i.e., a nuclear reaction (n, γ). The location of a titanium target in the thermal neutron flux from a nuclear reactor allows the formation of a reference field up to 7 MeV, and a nickel target up to 10 MeV [8]. Also, neutron flux with thermal energies can be obtained from radionuclide sources of fast neutrons [9-11].

The purpose of this work is to study by means of the Monte Carlo method as well as experimentally the spectral characteristics of the trapped gamma ray field formed by thermal neutron geometry, the neutron radiation calibration setup AT140 with titanium and nickel targets.

II. MATERIALS AND METHODS OF RESEARCH

It is possible to use radionuclide sources of fast neutrons to create a compact laboratory source of trapped gamma radiation with a stationary in time field. The flux of fast neutrons from a radionuclide source ($^{238}PuBe$, ^{252}Cf, $^{241}AmBe$) is slowed to thermal energies in polyethylene and directed to the target. In this approach, the simplest capture radiation source consists of a fast neutron source, a moderator, and a target.

A container-collimator with thermal neutron geometry of the neutron calibration facility (AT140, *ATOMTEX SPE*) forms

a collimated neutron beam with a significant component of thermal energy neutrons “Fig. 1”.

Fig.1. AT140 neutron calibration facility

A Monte Carlo model of a collimator container with a thermal insertion, premises, and ^{238}PuBe source of fast neutrons was developed [12, 13, 14]. In [11] the possibility of obtaining a trapped gamma ray source in “thermal” geometry with a ^{238}PuBe neutron source (type IBN-8-6) was investigated and variants of lead and polyethylene filters were proposed.

The gamma radiation field is formed in this case by 3 main sources:

1) Trapped radiation source from collimator materials and radiation scattered in the collimator.

2) Capture radiation source from the target.

3) Gamma radiation with an energy of 4.439 MeV accompanying the ^{9}Be(α,n)^{12}C reaction in the active part of the ^{238}PuBe - neutron source.

The features of the field produced in this way allow the trapped radiation from the target and the 4.439 MeV radiation to be used independently of each other using different filters “Fig. 2”.

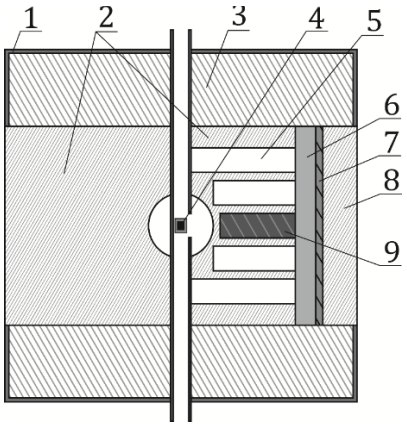

Fig.2. Monte–Carlo model of container–collimator with thermal neutrons geometry: 1 – aluminum casing; 2 – insert for thermal–neutron geometry; 3 – container–collimator; 4 – ^{238}PuBe fast–neutron source (IBN–8–6); 5 – air channels; 6 – lead; 7 – target; 8 – polyethylene; 9 – tungsten.

The central channel of the thermal insert is filled with tungsten to filter gamma radiation from the neutron source. The target is located in the collimator channel.

The international standard ISO 4037-1 recommends using titanium and nickel targets [2] for obtaining the reference gamma radiation field in the range up to 7 MeV and up to 10 MeV, for which the characteristics of gamma radiation capture lines are given in “Tab. 1”.

TABLE I. THE MOST INTENCE PROMPT NEUTRON CAPTURE GAMMA-RAY FOR TITANIUM AND NICKEL

Titanium target		**Nickel target**	
Photon energy, MeV	*Number of photons per 100 captures*	*Photon energy, MeV*	*Number of photons per 100 captures*
0,342	26,3	0,283	3,3
1,381	69,1	0,465	13
1,498	4,1	0,878	3,9
1,586	8,9	6,581	2,3
1,762	5,6	6,837	10,8
4,882	5,2	7,537	4,5
4,869	3,6	7,819	8,2
6,418	30,1	8,121	3,1
6,557	4,7	8,533	17
6,761	24,2	8,999	37,7

Titanium and nickel have separate lines with high gamma-quantum yield in their gamma capture spectra. Gamma radiation from structural and shielding materials must also be taken into account.

Targets in the form of disks (d=300 mm) made of titanium (plate VT 1-0 GOST 23755-79) 15 mm thick and nickel (nickel H-1 GOST 849-97) 10 mm thick.

III. RESULTS AND DISCUSSION

In the developed MCNP-4b model to determine the energy distribution of the flux density of trapped gamma rays at a given point, it is necessary to consider the propagation of both neutrons and photons. The active matter cell of an isotropic neutron source is the birthplace of neutrons in this problem, whereas gamma rays are secondary particles and are generated as a result of various interactions within the whole solution region of the problem. In MCNP-4b one can solve simultaneously the problem of neutron and gamma ray transport by including a special function mode N, P (mode N for neutrons, mode P for gammas). The gamma flux density was calculated for a sphere of 1 mm radius located 550 mm from the centre of the neutron source along the collimator axis, using the tally F4 map [12].

The energy distribution of photon flux density for a titanium target “Fig. 3” and a nickel target “Fig. 4” was obtained by Monte Carlo simulations (the result is normalised to the neutron yield from the source). The width of the energy interval is 50 keV.

The most intense lines are the titanium and nickel lines, the hydrogen capture line of 2.223 MeV, and the thermal neutron capture line of the ^{10}B nucleus by the ^{10}B(n,α)^{7}Li reaction with gamma ray release of 0.477 MeV [17]. The 4.439 MeV peak corresponds to inelastic scattering of fast neutrons by ^{12}C(n,n') ^{12}C* carbon nuclei [18]. There are no other fairly intense gamma-ray lines near the 6.418, 6.760 MeV lines for titanium and 8.533, 8.999 MeV for nickel.

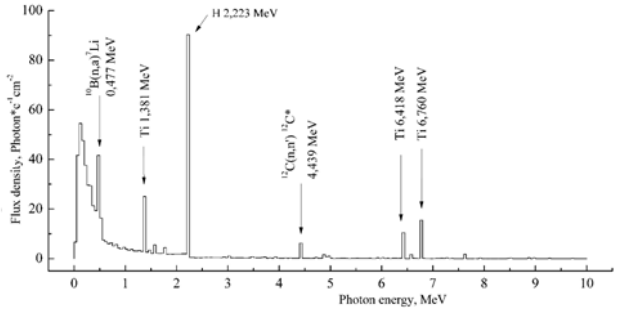

Fig.3. Spectrum of neutron capture gamma–ray for titanium target

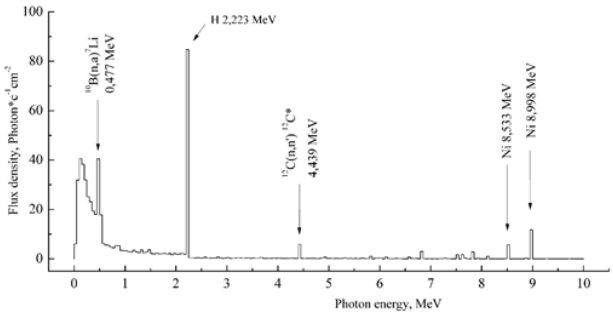

Fig.4. Spectrum of neutron capture gamma–ray for nickel target

A specialized spectrometric detection unit based on $LaBr_3$(Ce) crystal of dimensions Ø38×38 mm with nonlinear channel-energy conversion characteristic in the range up to 10 MeV (number of channels - 1024) was used for experimental investigation of spectral characteristics of the trapped radiation field. "Fig. 5" shows the mutual arrangement of the detection unit, collimator container and target.

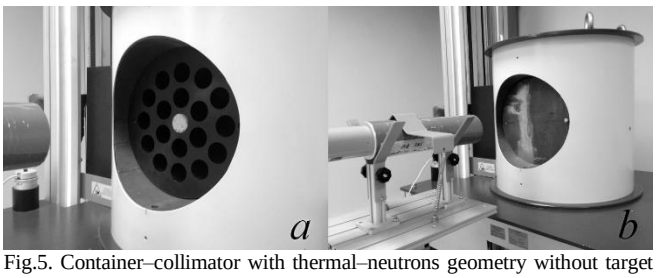

Fig.5. Container–collimator with thermal–neutrons geometry without target (*a*) and nickel target (*b*)

The gamma ray spectra were measured with a 5 cm polyethylene filter. A tungsten filter was placed in the central channel of the thermal insert. The experimental spectra, minus the intrinsic radioactivity of the $LaBr_3$(Ce) crystal and the background without neutron source are shown in "Fig. 6".

The 4.439 MeV total absorption peaks from the ^{238}PuBe neutron source and reference lines from the target, accompanied by pronounced peaks of single escape (SE) and double escape (DE). A 5 cm polyethylene filter was used to increase the emission intensity of the target against the rest of the spectrum.

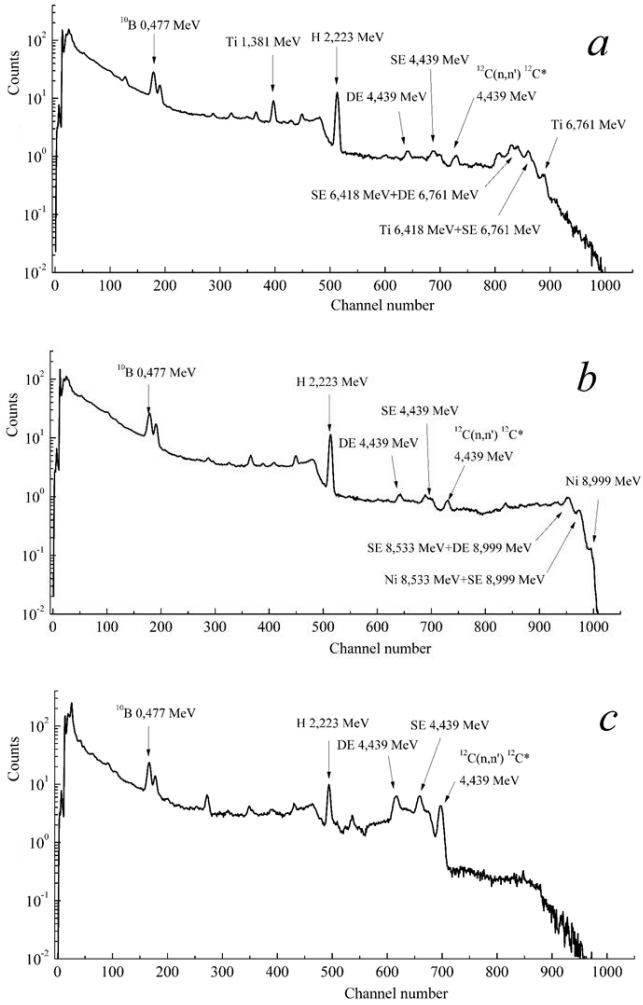

Fig.6. Experimental spectra for titanium target (*a*), nickel target (*b*) and bare ^{238}PuBe source (c)

From the hardware spectra obtained, it can be concluded that the spectrometric units can be calibrated in the trapped gamma ray field up to 10 MeV.

IV. CONCLUSION

Theplacement of titanium and nickel disks in the thermal neutron geometry collimator container channel allows the formation of a trapped gamma ray field with energies up to 7 MeV and up to 10 MeV. Monte Carlo simulations have shown that the most intense lines (except for target lines) correspond to thermal neutron capture by hydrogen and boron nuclei.

Experimental hardware spectra were obtained using a specialized spectrometric detection unit based on the $LaBr_3$(Ce) crystal of dimensions Ø38×38 mm with a nonlinear channel-energy conversion characteristic in the range up to 10 MeV. Analysis of experimental data has confirmed the possibility of calibration of spectrometers up to 10 MeV by trapped radiation lines.

REFERENCES

1) Bermann F. ed. Capture Gamma Ray Beam for the Calibration of Radioprotection Dosemeters between 5 and 9 MeV. Radiation Protection Dosymetry, 1990, no. 4, pp. 237–243. doi: 10.1093/oxfordjournals.rpd.a080623

2) International Electrotechnical Commission «Radiation Protection Instrumentation – Transportable, Mobile or Installed Equipment to Measure Photon Radiation for Environmental Monitoring» 23/10/2015 № IEC 61017 Ed.1.

3) International Standart «X and gamma radiation for calibrating dosimeters and dose rate meters and for determining their response as a function of photon energy « 15/12/1996 № ISO 4037–1.

4) Duvall K. C., Heaton H. T., Soares C. G. The development of a 6–7 MeV photon field for instrument calibration. Nuclear Instruments and Methods in Physics Research, 1985, vol. 10–11, no. 2, pp. 942–945. doi: 10.1016/0168–583X(85)90145–4

5) Guldbakke S., Schaffer S. Properties of high–energy photon fields to be applied for calibration purposes. Nuclear Instruments and Metods in Physics Research, 1990, vol. 299, iss. 1–3, pp. 367–371. doi: 10.1016/0168–9002(90)90806–H

6) Rogers D. O. A nearly mono–energetic 6–7 MeV photon calibration source. Health Physics, 1983, vol. 45, no. 1, pp. 127–137. doi: 10.1097/00004032–198307000–0001

7) Croft S., Bailey M. The determination of the adsolute responce function of a deuterated benzene total energy detector to 6,13 MeV γ–rays. Nuclear Instruments and Methods in Physics Research, 1991, vol. 302, no. 2, pp. 315–326. doi: 10.1016/0168–9002(91)90415–M

8) Bermann F. Étalonnage de détecteurs de radioprotection avec des gammas d'énergie supérieure à l MeV: utilisation de faisceaux de gammas de capture, Radioprotection, 1991, vol. 26, no. 3, pp. 493–513. doi: 10.1051/radiopro/1991017

9) Kroupa M., Granja C., Janout Z. Wide energy range gamma–ray calibration source. Journal of Instrumentation, 2011, vol. 6, no. 1, pp. 6–11. doi:10.1088/1748–0221/6/11/T11002

10) Rogers J. G., Andreaco M. S., Moisan C. A 7–9 MeV isotopic gamma–ray source for detector testing. Nuclear Instruments and Metods in Physics Research, 1998, vol. 413, iss. 2–3, pp. 249–254. doi: 10.1016/S0168–9002(98)00097–7

11) Komar D., Lukashevich R., Guzov V., Kutsen S. [Neutron capture gamma ray field with energy to 10 MeV for metrological support of radiation protection devices]. Pribory i metody izmerenii [Devices and Methods of Measurements], 2016, vol. 7, no. 3, pp. 296–304. doi:10.21122/2220–9506–2016–7–3–296–304.

12) Briestmeister J.F. ed. MCNP–A general Monte Carlo N–particle transport code, Version 4A. Report LA–12625–M, Los Alamos, NM: Los Alamos National Laboratory,1994, 736 pp.

13) Komar D.I., Kutsen S.A., Guzov V.D. [Monte–Carlo simulation metrological characteristics of the neutron calibration facility]. Ekologicheskij vestnik [Ecological proceedings]. 2016, no. 3, pp. 54–61.

14) Komar D., Kutsen S. [Influence of scattered neutron radiation on metrological characterictics of AT140 Neutron Calibration Facility]. Pribory i metody izmerenii [Devices and Methods of Measurements], 2017, vol. 8, no. 1, pp. 23–31. doi: 10.21122/2220–9506–2017–8–1–23–31.

15) Choi, H.D., Firestone, R.B., Lindstorm, R.B. Database of promt gamma–rays from slow neutron capture for elemental analysis, Vienna: International atomic Energy Agency, 2006, 252 p.

16) Kopecky, J. Ed. Atlas of Neutron Capture Cross Sections/ J. Kopecky. – Vienna: International atomic Energy Agency, 1997. – 370 p.

17) Ceberg C. P., Salford L. G. Neutron capture imaging of 10B in tissue specimens. Radiotherapy and Oncology, 1993, vol. 26, iss. 2., pp. 139–146. doi: 10.1016/0167–8140(93)90095–P.

18) Hugh, E. H. Neutron Inelastic Scattering in ^{12}C, ^{14}N and ^{16}O, Houston, Texas, 1959, 256 p.

19) Baldini A., Bemporad C., Cei F. A NaI activation method for the measurement of the weak thermal neutron field around the MEG experiment. Nuclear Instruments and Methods in Physics Research, 2007, vol. 570, iss. 3, pp. 561–564. doi: 10.1016/j.nima.2006.10.101.

20) Gardner R. P., Sayyed E., Zheng Y. NaI detector neutron activation spectra for PGNAA applications. Applied Radiation and Isotopes, 2000, Vol. 53, iss. 4–5, pp. 483–497. doi: 10.1016/S0969–8043(00)00198–6.

SECTION IV
MEASUREMENTS IN THE INDUSTRY

Design and manufacture of a device for working with a portable roughness device INSIZE ISR- C002, using additive printing

Kliment Georgiev
Technical University of Sofia, branch Plovdiv
Faculty of Mechanical Engineering;
Department: Mechanical and Instrument Engineering
Plovdiv, Bulgaria
k.georgiev@tu-plovdiv.bg

Pavlina Katsarova
Technical University of Sofia, branch Plovdiv
Faculty of Mechanical Engineering;
Department: Mechanical and Instrument Engineering
Plovdiv, Bulgaria
p_katsarova@abv.bg

Nikola Todorov
Liebherr Hausgeräte Marica EOOD
Plovdiv, Bulgaria
nikolatodorov9@abv.bg

Abstract — **A device for roughness tester INSIZE ISR-C002 has been designed and manufactured. It is designed to facilitate the operation of the roughness device. The developed design was designed using SolidWorks as an assembled unit and parts. To minimize the stresses received during operation, the proposed design was optimized by using SolidWorks Simulation. After the completion of the 3D model, a choice of material and technology of 3D printing was made. Then an additive 3D printing was used for its production. The developed device was used for experimental measurements in a training laboratory. Experiments prove its workability and applicability.**

Keywords— Design, fabrication, 3d printing, 3d modelling, device, surface roughness testing;

I. INTRODUCTION

The roughness of the surfaces of the parts affects their performance properties. Methods for assessing the roughness of surfaces are divided into two main groups: methods for qualitative assessment and methods for quantitative assessment. Qualitative assessment methods consist of comparing roughness samples against the controlled surface. Qualitative assessment methods are divided into two types: contact and non-contact. Profilographs, profilometers are used in the contact methods. Non-contact measurements use microscopes, laser interferometers and others.

There are many surface roughness parameters that can be found. They represent the geometric characteristics of the processed detail. Those parameters are defined in many international standards such as SIST EN ISO 4287:2000/AC:2008[1]. Surface roughness profile is determined by high pass filtering with a proper selection of the filtering length (cut-off length, l_r). There parameters are also known as surface heights. The surface roughness parameters are calculated from the filtered roughness profile. A typical surface roughness profile is shown in figure 1. The evaluation length ln (the assessed length) usually consists of an integral multiplication of the cut-off length. The height of the assessed profile at any position x can be obtained from a general function Z(x) to mathematically describe the surface. However, surface profiles measured with a profilometer are typically digitized. Discrete points (xi, i=1, ..., n) with an equal increment Dx and the corresponding surface heights (zi, i=1, ..., n) are used instead to describe the surface profiles [2]. Commonly used surface roughness parameters are defined below. Ra is the arithmetical average of surface heights, also known as the center line average of surface heights (CLA), and can be calculated as [2]:

$$Ra = \frac{1}{lr}\int_0^{lr} |z(x)dx \qquad (1)$$

Rq(RMS) is defined as the root mean square of surface heights, i.e [2].

$$Rq = \sqrt{\frac{1}{lr}\int_0^{lr} |z(x)^2 dx} \qquad (2)$$

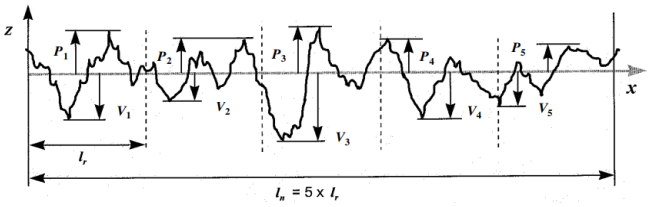

Figure 1. A typical surface roughness profile; according to Chang, W. R et al. (2001) [2].

Modern portable instruments for measuring roughness have high accuracy, can work in different production environments, but their basic devices do not allow the use of the full capacity of the instruments compared to their use in static environments. This complicates the work and requires more time for adjustment by the operator and worsens the accuracy of the results obtained.

The portable profilometer "INSIZE ISR - C002" measures the roughness of the parameters Ra, Rq, Rz, Rt, Rp, Rv, R3z, R3y, Rz (JIS), R_s, Rsk, Rp, Rsm, Rvk, Rsk, Mr1, Mr2, Ry (JIS), Rmax, range is 160μm, Speed 0.5mm / s, 1mm / s, Memory - 100 measurement results, Weight 400g, dimensions: 141x55x40mm [3].

Diagram of the device:

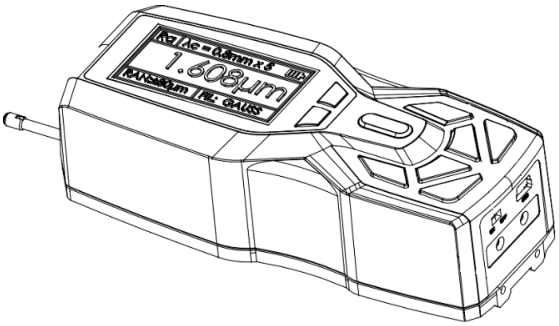

Fig 2. Portable profilometer INSIZE ISR - C002.

Advantage of the device is that it can be connected to a computer with software and a printer to illustrate the results or stored in it [3].

The disadvantage is the lack of a suitable device in the kit for use in complex and inaccessible measurements in laboratory and production conditions. The presence of a device for mounting the profilometer would lead to easy positioning, increase the ability to measure and more. This would improve and facilitate the work of the operator.

The development of technology in recent decades allows the use of additive printing technologies. They allow us to quickly, easily and cheaply develop prototypes and devices of different types, shapes and sizes. The variety of materials used in these technologies allow for the selection of suitable material that meets the characteristics and requirements of the model.

The materials used in the FDM technology parts are very close to conventional engineering polymers, so the suitability of the basic materials is not a problem. The main difference between the FDM part and the molding is the fact that it is built in layers, which means that the inherent strength of the part will be slightly lower in the 'Z' direction (vertically). The partial layers are relatively large - between 0.13 mm and 0.33 mm. This can lead to quite rough surfaces before surface treatment [4].

The presented report has developed a device to facilitate the operation of the profilometer in a dynamic environment, using modern materials and technology for additive printing. The introduction states that there is no such device for basing and adjusting the portable roughness device, but the 3D printing technologies are sufficiently accessible and reliable for its production.

II. MATERIALS AND METHODS

A. Materials

The choice of material must meet the requirements for dimensional accuracy, minimum execution time and wall thickness of the structure.

Some of the most important properties when choosing materials for 3D printing are: tensile strength, bending and tearing, modules of elasticity and flexibility, elongation, compressive strength, compressibility, moisture adsorption, thermal deformation temperature (HDT), point of Vika softening and coefficient of thermal expansion [5].

The types of materials used in 3D printing are extremely numerous, but the chosen technology for 3D printing limits us to a few. As we have no special requirements for the element itself for the initial prototype, we will use PLA filament with dimensions of 1.75 mm ± 0.03 mm as the most cost-effective material.

This material was chosen because of its less flexibility compared to other materials, the possibility of post- processing, the lack of odors when printing and the relatively low cost.

PLA - Polylactic acid - polylactide is one of the most common materials for 3D printing. It is harder than ABS, inflexible and does not require a heating platform. PLA is a biodegradable and ecological material, using cornstarch. The disadvantage is the low deformation temperature, which is 60 degrees. However, PLA is suitable for prototyping that does not have special requirements [5]. Table 1 presents the physical properties of PLA.

Table 1

Physical properties of PLA

Melting temperature	175-180 deg.
Working temperature (3d printer)	190-225 °C recommended 210 °C
Print bed temperature	45-70°C
Softening point	50-55 °C
Glass transition temperature	60-70 °C
Minimum wall thickness (recommended)	1.2 mm
Maximum layer thickness (recommended)	80% of the nozzle diameter
Density	1.24 g / s m³
Tensile strength	60 MPa
Bending strength	56 MPa
Hardness (Rockwell)	75-85
Shrinkage	1%
Turbidity (thickness 2 mm, transparent)	3-5%
Glitter G, U (for all types)	110
Degrees of water absorption	0.5-50%

B. Methods

The ISO / ASTM 52900 standard categorizes all different types of 3D printing. For the designed device a technology for 3D printing - modeling of fused deposits is chosen. It is an additive manufacturing method in which layers of materials are fused together into an object creation model. FDM is the most cost-effective way to produce custom thermoplastic parts and prototypes.

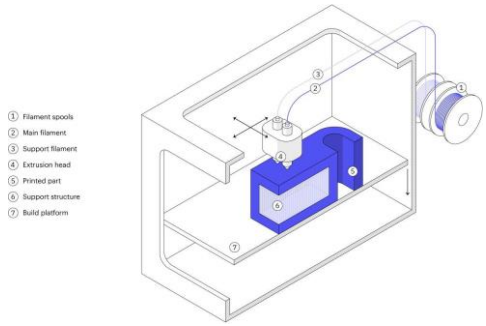

Fig. 3. Schematic diagram of FDM technology

A wide range of thermoplastic materials is available for FDM, suitable for both prototyping and some functional applications [6].

As a limitation, FDM has the lowest dimensional accuracy and resolution compared to other 3D printing technologies. FDM parts have visible lines, so for treatment on a smooth surface, subsequent treatment is often required. In addition, the adhesion mechanism of the layer makes FDM particles inherently anisotropic. They are weaker in one direction and are generally unsuitable for critical applications [7].

The device used is: Prusa i3 MK3S + with additional modification for better leveling of the printer bed.

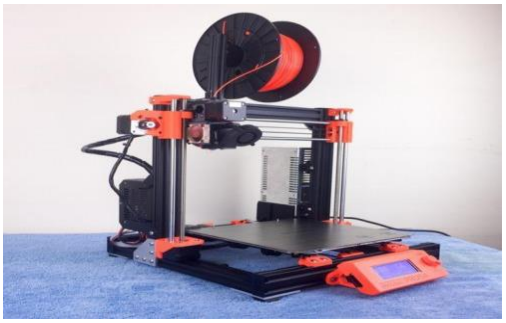

Фиг. 4. Опитна постановка

III. Design of a 3D Model of the Device in the SolidWorks Enviroment

A. The device must meet the following requirements for the appliance:

- Do not obstruct operation during measurement
- Be able to mount on different surfaces
- Be a design suitable for 3D printing.
- To allow adjustment of the device and its stability
- To ensure the necessary accuracy

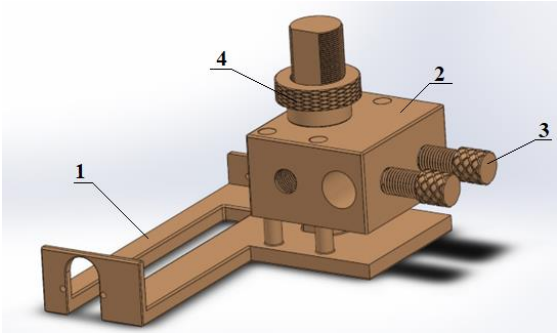

Fig 5. 3D model of the device

Fig. 5 shows a 3D model of the designed device in a SolidWorks environment. The device is designed considering the geometry of the instrument and its features, so as to facilitate the basing and bringing the instrument into readiness for measurement. The device consists of a base (1) to which the roughness tester is attached, a unit for fastening to a magnetic stand (2), locking bolts (3) and a height- adjusting nut (4). The purpose of the base is to ensure the stillness of the device without restricting the movement of the sensor. The mounting block is used to attach the appliance to a magnetic stand. The two bolts positioned in the block are used to attach the device and position it to the measuring stand. They are designed on the basis of bolt M12x1.5. The bolts are printed similar to the fixture.

B. Making the device

As it's noted, the Prusa i3MK3S+ 3D printer is used to make the device (prototype). Fig. 6 shows the positioning of the model on the printer table. The orientation of the part on the working table of the printer affects the strength of the part and obtaining good adhesion. Good adhesion plays an important role in the construction of the first layer. This can be improved by using a heating plate heated to 60 - 65˚ for PLA. The temperature of the printing table varies depending on the manufacturer of the material. The parameters set during the construction of the device are presented in Table 2.

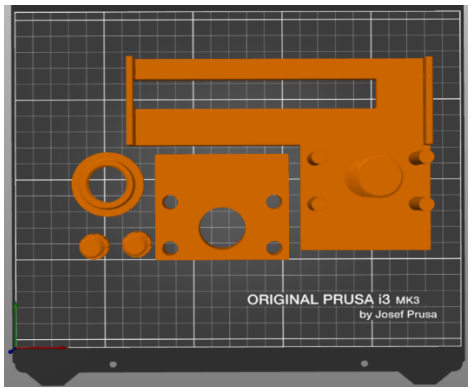

Fig. 6 - Location of the details on the printing table

Table 2

Parameters of the print

Parameters	Value
Layer height	0.15 mm
First layer height	0.2 mm
Filament	Generic PLA
Infill density	15%
Infill pattern	Gyroid
Top fill pattern	Monotonic
Bottom fill pattern	Monotonic
Filament diameter	1.75 mm
Nozzle temperature for the first layer	220°C
Nozzle temperature for the other layers	215°C
Bed temperature for the first layer	60°C
Bed temperature for the other layers	60°C
Brim	No

IV. Investigation of Threatened Cross Section And Stress

The study of endangered sections and stresses is performed using SolidWorks Simulation. Stress simulation - figure 7 and strain simulation – fig. 7 are presented.

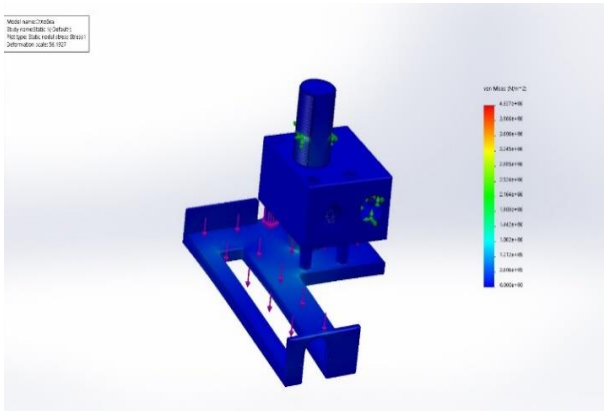

Fig. 7. Stress simulation.

The stress simulations show that the stresses in the 3D model are well distributed and no stress concentrators are observed.

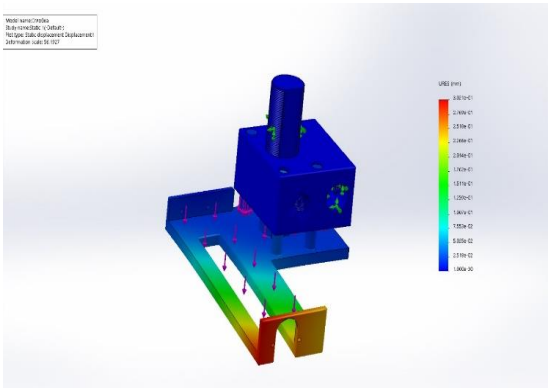

Fig. 8. Deformation simulation.

The deformation simulation in the 3D model shows the endangered areas. Bending at the front of the fixture is expected. The expected bending can be compensated by the way the profilometer is attached to the device through the designed bolts, which are part of the original equipment of the roughness tester.

V. Experimental Use Of The Manufactured Device In A Laboratory Inviroment

Fig. 9 shows the assembled device

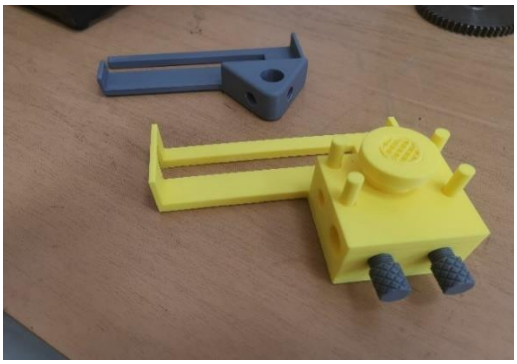

Fig. 9. Portable profilometer device.

It is easily mounted on the stand together with the device. As this determines the first requirement to be met. The screws hold it firmly to the object stand and hold the weight of the appliance.

Fig. 10 Measuring a reference with the device

Attaching the device itself to the magnetic stand, as well as leveling the appropriate height is much faster than the before. The designed screw gives a good result as the discrepancy is only -0.078 μm relative to the zero point of the device – fig. 11.

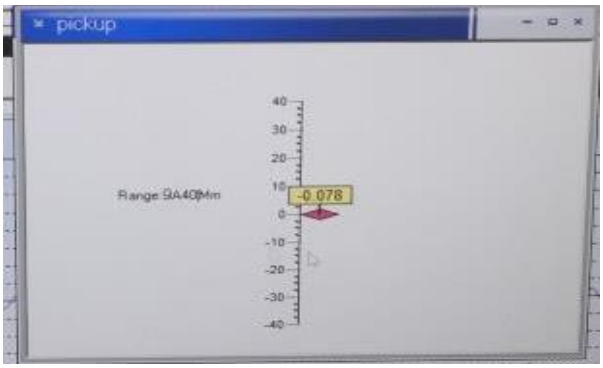

Fig. 11. Sensor positioning scale

After the preparation of the device, a test with reference roughness Ra = 1.20μm is performed, the device shows a value Ra = 1.264 μm which is about 6% error at the factory set to 10% at λc = 0.8mm x3. Fig. 10 shows a visualization of the results of the test, using software to connect and control the profilometer with a computer.

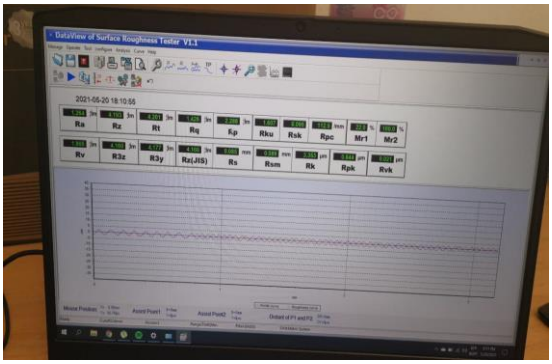

Fig. 12. Test results

As the step λc = 0.8mm x5 increases, the measurement error decreases. The device is firmly fixed and stable, it steps entirely on the platform, and there is no contact of the diamond needle with the hole of the platform. Bending during fastening is avoided by designing an arch above the channel

for the diamond needle which does not allow bending of the platform by the fastening forces of the two screws diagonally with which the device is fastened to the device. The results of the measurement are shown in Fig 12. For this purpose, special software is used with which the device for measuring roughness works.

VI. Conclusions

1) The designed device facilitates the work of the operator and increases the possibilities for measurement
2) The tests performed in laboratory conditions prove its indisputable operability
3) Additive printing technology can be used for fast and cheap production of functional prototypes and devices.
4) The accuracy and quality of the manufactured devices does not affect the accuracy of the obtained results.

Acknowledgment

The author/s would like to thank the Research and Development Sector at the Technical University of Sofia for the financial support."

References

[1] EN ISO 4287:2000 - Geometrical product specifications (GPS) - Surface texture: Profile method - Terms, definitions and surface texture parameters (ISO 4287:1997)

[2] Chang, W. R., Kim, I. J., Manning, D. P., & Bunterngchit, Y. (2001). The role of surface roughness in the measurement of slipperiness. *Ergonomics*, *44*(13), 1200-1216.

[3] http://www.insize.com/page-169-267.html.

[4] Mike Ayre. 3D printing for manufacture: a basic design guide. Available on 20.06.22 at: https://www.crucibledesign.co.uk/images/uploaded/guides/3d-printing-for-manufacture-a-basic-design-guide-download-original.pdf.

[5] Shahrubudin, N., Lee, T. C., & Ramlan, R. (2019). An overview on 3D printing technology: Technological, materials, and applications. *Procedia Manufacturing*, *35*, 1286-1296.

[6] Dudek, P. F. D. M. (2013). FDM 3D printing technology in manufacturing composite elements. Archives of metallurgy and materials, 58(4), 1415-1418.

[7] https://www.3dsolid.eu/2019/09/25/procesi-v-3d-printirane/. Available on july 2021.

Improvement of the Secondary standard of the electric power unit at industrial frequency

Sergii Shevkun
Scientific and Production Institute of Electromagnetic Measurements State Enterprise "UKRMETRTESTSTANDARD"
Kyiv, Ukraine
shevkun@ukrcsm.kiev.ua

Maryna Dobroliubova
Information and Measuring Technologies Department
Igor Sikorsky Kyiv Polytechnic Institute
Kyiv, Ukraine
m.v.dobroliubova@gmail.com

Olexii Statsenko
Department of Electromechanical Systems Automation and Electrical Drives
Igor Sikorsky Kyiv Polytechnic Institute
Kyiv, Ukraine
o.statsenko@kpi.ua

***Abstract*—The secondary standard of the electric power unit is used for adjustment and calibration of meters of electric power and electric energy which are a part of test and calibration units. These units are intended to be used at the output control, as well as in the metrological and calibration laboratories of enterprises producing meters of electric power and electric energy. Materials on modernization of the standard by inclusion of additional equipment in its structure that gives opportunity to improve metrological characteristics of this standard are presented. Modernization allows achieving the expansion of the dynamic range of the standard, as well as increasing its productivity and reducing the cost of work due to use of significant automation of the measurement process and results processing.**

Keywords—standard of electric power, calibration, electric power meter

I. Problem Statement

Current trends of energy cost increase (including electric energy), the desire for a mass transition to clean sources of electricity and the need to take comprehensive activities for reducing energy consumption for saving them require a significant increase of electric energy meters accuracy.

A large number of standard electric power and electric energy meters are used for setting up, testing, calibrating and verifying industrial and household meters. Standard meters of accuracy classes 0.1 and 0.05 include the following: MTE PTS 3.3; Applied Precision RS 2130, RS 2330, RS 1130, RS 1330; BX-33; MTE SWS 1.3, PWS 2.3 GENX, CHECKMETER 2.3 GENX; Itron SM 3050 [1-7].

The existing nomenclature of high-precision meters assumes the presence of a corresponding standard base that has the necessary accuracy, high productivity and a modern level of work automation to ensure their calibration.

For the calibration of standard meters, the SE "UKRMETRTESTSTANDARD" uses the Secondary standard of the unit of electric power for the industrial frequency range of VETU 08-08-01-08. This standard is used for setting up and calibrating electric power and electric energy meters that are parts of test and calibration units. These units are intended to be used at the output control, as well as in the metrological and calibration laboratories of enterprises producing meters of electric power and electric energy.

But the Secondary standard of the unit of electrical power for the industrial frequency range of VETU 08-08-01-08 due to long-term use has almost exhausted its resource and is morally obsolete. The low level of automation and numerous failures of the secondary standard lead to the fact that calibration on the Secondary standard VETU 08-08-01-08 is usually not carried out, and all electricity meters of accuracy classes 0.1 and 0.05 (more than 110 units annually) are calibrated on the National standard of units of electric power and power factor DETU 08-08-02.

The problem is that the almost continuous operation of the National standard DETU 08-08-02 significantly reduces its resource and can lead to the failure of its components at any moment.

The purpose of the article is to reveal ways to modernize the Secondary standard of the unit of electric power for the industrial frequency range VETU 08-08-01-08 to restore its resource, increase the level of automation and expand the dynamic range.

II. Main Content of Research

As a result of the analysis of ways to modernize the Secondary standard of the unit of electric power for the industrial frequency range VETU 08-08-01-08, a number of requirements for standard equipment, which must be part of the modernized standard, have been defined.

At first, to calibrate the entire nomenclature of three-phase electric power and electric energy meters in the full range of values, the standard should include three high-precision voltage sources and three high-power current sources - one for each phase.

Secondly, the standard should include a precision three-phase standard electric energy meter, which is constructively and by software compatible with the standard voltage and current sources mentioned above. The meter must create a single standard software-hardware complex with voltage and current sources, designed for high-precision calibration of electric power and electric energy meters.

Thirdly, the equipment of the standard should allow calibration of several meters simultaneously, in a high-performance automated mode with automatic documentation of calibration results.

Overview of the available nomenclature of standard equipment for measuring electrical quantities on the modern market, as well as the analysis of its characteristics, show that the three-phase power source PS3 [8] for calibrating standard electric energy meters produced by the company MeterTest, Poland, in conjunction with a three-phase reference standard

978-1-6654-8569-2/22/$31.00 ©2022 IEEE

RD-33 [9] produced by Radian Research, USA, meets the specified requirements.

The PS3 three-phase power source includes high-precision and high-power integrated voltage sources VIS-400 [10] and current sources CIS-600 [11] (3 units, 1 for each phase), as well as an ACU-3000 control unit.

The appearance of the three-phase power source PS3 is shown in Fig. 1.

Fig. 1. Three-phase power source MeterTest PS3

The PS3 three-phase power source is a stable alternating current and voltage source for use in standard three-phase calibration and test equipment. The general characteristics of the PS3 three-phase power source are as follows:

- wide dynamic range of generated voltages and currents, as well as permissible loads;
- high stability of parameters and minimal non-linear distortions;
- multi-level protection system;
- individual adjustment of each voltage, current and phase angle;
- automated control;
- generation of a significant number of harmonics, up to and including the 21st.

A wide range of output voltages and currents allows to set any phase angle, as well as harmonics generation. The PS3 power source is widely used to adjust, calibrate and test all types of energy meters, while showing stability of all electrical parameters and characteristics.

The ACU control unit provides the PS3 power source with precise regulation and control of direct loads with a wide range of parameters, from purely capacitive loads to resistive or inductive loads. This feature of the PS3 power source allows avoiding external load compensators. Digital feedback, controlled by an internal DSP, provides high stability in time, fast adjustment of the required output current and voltage values, as well as a low level of nonlinear distortion.

The high safety and reliability of the PS3 power source is ensured by the presence of multi-level protection, which provides protection against current overload, overvoltage, short circuit/open circuit, overheating, current leakage to the body parts and to the ground.

Full automation of adjustments and settings of the PS3 power source ensures high productivity of metrological works.

Power cascades of power amplifiers use PWM technology, providing high power with very little heat loss.

The standard configuration of the PS3 three-phase power source provides the generation of harmonics up to and including of 21st order.

The ACU-3000 control unit is designed for detection of short circuits between voltage and current circuits, control of emergency switches, control of tariff systems, signaling of dangerous voltage appearance on body parts and much more.

The MeterTest PS3 three-phase power source has the following metrological characteristics:

- Available output power for linear loads:
  - voltage sources model – 3 × 400 VA (VIS-400);
  - current sources model – 3 × 600 VA (CIS-600);
- Working voltage range – 3 × 0…350 V (Phase-Neutral)/3 × 0…600 V (Phase-Phase);
- Working current range – 3 × 1 mA…120 A;
- Frequency of the fundamental – 40…70 Hz;
- Harmonics – up to the 21st, user programmable;
- Phase angle range (independently for each voltage and current signal) – 0 °…360 °;
- Resolution of output current/voltage adjustment – 0.002 %;
- Resolution of phase angle adjustment – 0.001 °;
- Resolution of frequency adjustment – 0.001 Hz;
- Stability of the output current – ≤ 0.005 % (time base: 150 s);
- Stability of the output voltage – ≤ 0.005 % (time base: 150 s);

- Output voltage/current accuracy – according to the accuracy of the reference standard;
- Accuracy of the phase angle – according to the accuracy of the reference standard;
- Accuracy of the frequency – according to the accuracy of the reference standard;
- Total Harmonic Distortion (THD):
  - output voltage - <0.1 %;
  - output current - <0.3 %.

The MeterTest PS3 three-phase power source must be used in conjunction with the Radian Research RD-33 three-phase reference standard.

The appearance of the three-phase reference standard Radian Research RD-33 is shown in fig. 2.

Fig. 2. Three-phase reference standard Radian Research RD-33

The principle of operation of RD-33 counters is based on analog-to-digital conversion of instantaneous values of current and voltage input signals followed by software calculation of measured values from the obtained data array.

RD-33 meters consist of a block of primary current and voltage transducers, analog-to-digital converters, a microprocessor, memory devices, and an LCD that displays the measurement results. The keyboard on the front panel allows changing the operating modes and displaying of all measured values. Communication with an external PC is carried out using the RS-232 interface. The RD-33 meters are equipped with an input for connection to the pulse output of calibrated electric energy meters and a pulse output with a signal frequency proportional to the measured power value. There is an additional function "harmonic analyzer", which allows calculating of THD, as well as displaying the shapes of the curves and the vector diagram of the measured system of voltages and currents.

The Radian Research RD-33 three-phase reference standard has the following main metrological characteristics:

- voltage measurement range – 30…600 V;
- voltage measurement accuracy – ±0.01 %;
- alternating current measurement range – 0.02…120 A;
- alternating current measurement accuracy – ±0.01 %;
- measurement accuracy of active, reactive and total power and energy – ±0.01 %;
- frequency of the measured network – 45…65 Hz;
- frequency measurement accuracy – ±0.005 Hz;
- range of phase shift angle measurements – 0 °…360 ° or -180 °…180 °;
- accuracy of phase shift angle measurement – ±0.02 °;
- power factor ($cos\varphi$) – -1…+1;
- power factor measurement accuracy – ±0.01;
- uncertainty due to temperature dependence – ±0.001 %/°C;
- number of measured harmonics – up to 63;
- range of direct current measurements throw analog input – ±2 mA;
- direct current measurements accuracy – ±0.01 %;
- voltage of the additional power source – 60…600 V.

Thanks to the compatible software, the three-phase reference standard Radian Research RD-33 creates with the three-phase power supply MeterTest PS3 a single standard software-hardware complex designed for the calibration and testing of electric power and electric energy meters of accuracy classes 0.1 and 0.05 and worse.

Using of stationary multi-parameter test bench ASTeL as part of the standard allows simultaneous calibration of several meters - 6, 10 or more, depending on the type of stationary system [12-15].

The general view of the stand for calibrating 10 meters is shown in fig. 3.

Fig. 3. Stationary multi-parameter test bench ASTeL 3.2

The functional scheme of the modernized Secondary standard of the unit of electric power at the industrial frequency when calibrating 3-phase electricity meters MTE PWS 2.3 GENX is shown in Fig. 4.

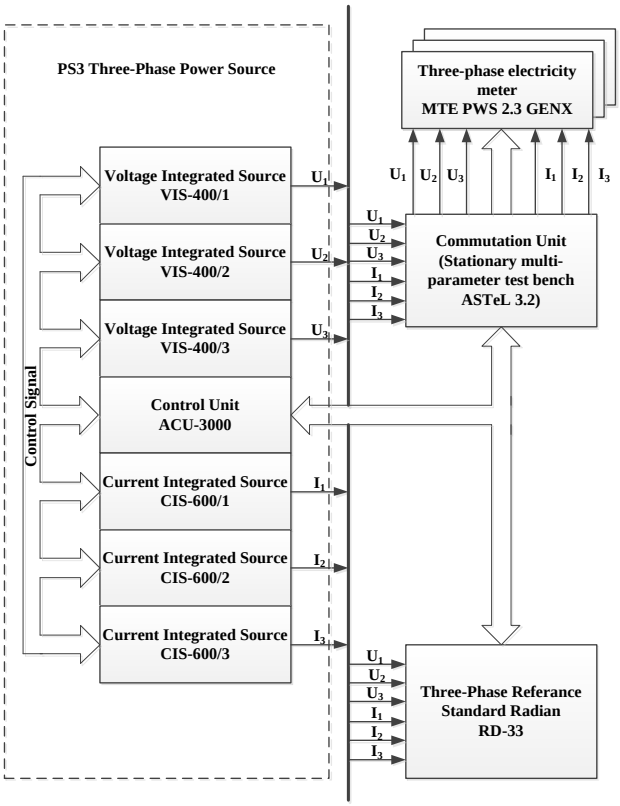

Fig. 4. Functional scheme of the modernized Secondary standard of the unit of electric power at the industrial frequency when calibrating 3-phase electricity meters MTE PWS 2.3 GENX

III. Conclusion

The article reveals ways to modernize the Secondary standard of the electrical power unit at industrial frequency range to restore its resource, increase the level of automation and expand the dynamic range.

To calibrate the entire nomenclature of three-phase electric power and electric energy meters in the full range of values, the standard should include three high-precision voltage sources and three high-power current sources - one for each phase.

The standard should include a precision three-phase standard electric energy meter, which is constructively and by software compatible with the standard voltage and current sources.

To implement the specified requirements, it is proposed to include a PS3 three-phase power source for calibrating standard electric energy meters produced by MeterTest, Poland, in conjunction with a three-phase reference standard RD-33 produced by Radian Research, USA.

The inclusion of a stationary measuring test system as a part of the standard will allow simultaneous calibration of several counters.

Thanks to the compatible software, the three-phase reference standard Radian Research RD-33 creates with the three-phase power supply MeterTest PS3 a single standard software-hardware complex, which will provide calibration and testing of electric power and electric energy meters of accuracy classes 0.1 and 0.05 and worse in the full range of values in high-performance automated mode.

References

[1] MTE. Meter Test Equipment. PTS 3.3 C. Available at: http://electrovymir.com/files/PoverochniePribory/lgmPTS33C.pdf (accessed: 23.01.2022).

[2] Reference Standard. Standard Meter of Electrical Power and Energy. Model RS 2130, RS 2330, RS 1130, RS 1330. Available at: https://www.appliedp.com/download/manual/rs_ug_en.pdf (accessed: 23.01.2022).

[3] VKh-33 Reference three-phase meter. Available at: https://tunic.com.ua/product/%D0%B2%D1%85-33-%D1%8D%D1%82%D0%B0%D0%BB%D0%BE%D0%BD%D0%BD%D1%8B%D0%B9-%D1%82%D1%80%D0%B5%D1%85%D1%84%D0%B0%D0%B7%D0%BD%D1%8B%D0%B9-%D1%81%D1%87%D0%B5%D1%82%D1%87%D0%B8%D0%BA/ (accessed: 23.01.2022).

[4] MTE. Meter Test Equipment. SWS 1.3. Available at: https://www.mte.ch/data/files/SWS%201.3%20English_R04%20(04.2003).pdf (accessed23.01.2022).

[5] PWS 2.3 GENX. Available at: https://www.lgmetering.kiev.ua/oborudovanie/smt/item/pws-23-genx.html (accessed: 23.01.2022).

[6] MTE. Meter Test Equipment. CheckMeter 2.3 genX. Available at: https://www.lgmetering.kiev.ua/files/mte/lgmCheckMeter23genx.pdf (accessed: 23.01.2022).

[7] SM 3050 (SM3050) Actaris, Itron. Available at: http://www.energoportal.net/tovar_5_38949.html (accessed: 23.01.2022).

[8] PS3. Three-Phase Power Source. Available at: http://www.meter-test-equipment.com/en/p/ps3-three-phase-power-source/ (accessed: 01.02.2022).

[9] Radian RD-33 Dytronic Three-Phase Reference Standard. Available at: http://www.measuretronix.com/en/products/radian-rd-33-dytronic-three-phase-reference-standard (accessed: 03.02.2022).

[10] VIS. Voltage Integrated Sources. Available at: http://www.meter-test-equipment.com/en/p/vis-voltage-integrated-sources/ (accessed: 01.02.2022).

[11] CIS. Current Integrated Sources. Available at: http://www.meter-test-equipment.com/en/p/cis-current-integrated-sources/ (accessed: 03.02.2022).

[12] Meter Test Equipment of ASTeL 2 series. Available at: https://pdf.directindustry.com/pdf/metertest/three-phase-meter-test-equipment-astel-32xx-series/112007-347219.html#open1068303 (accessed: 03.02.2022).

[13] Meter Test. ASTeL 3.2. Available at: https://www.directindustry.com.ru/prod/metertest/product-112007-1068303.html (accessed: 03.02.2022).

[14] ASTeL. Stationary Meter Test Equipment. Available at: https://www.caltech.se/files/2016-12/astel-system.pdf (accessed: 03.02.2022).

[15] Multi-parameter test bench ASTeL 3.2. Available at: https://www.directindustry.com/prod/metertest/product-112007-1068303.html (accessed: 03.02.2022).

SECTION VII
MEASUREMENTS IN THE ECOLOGY, BIOTECHNOLOGY, MEDICINE, AND SPORT

Using the colorimetric method in certain technologies

Khoroshailo Iurii Yevheniyovych
PhD in Technical Sciences
Kharkiv National University of Radioelectronics
Kharkiv, Ukraine
yurii.khoroshailo@nure.ua

Klyuchnyk Ihor Ivanovych
PhD in Technical Sciences
Kharkiv National University of Radioelectronics
Kharkiv, Ukraine
ihor.lkiuchnyk@nure.ua

Sezonova Irina Konstantinovna
PhD in Technical Sciences,
Kharkiv National University of Radioelectronics
Kharkiv, Ukraine
iryna.sezonova@nure.ua

Yarmak Ivan Mykolayovych
Postgraduate
Kharkiv National University of Radioelectronics
Kharkiv, Ukraine
yarmak26ivan01@gmail.com

Chernyakov Eduard Ivanovych
PhD of Physical and Mathematical Sciences
Kharkiv National University of Radioelectronics
Kharkiv, Ukraine

***Abstract*—A device is proposed for measuring color characteristics, which, using a measuring transducer, assigns to each radiation three signals proportional to color coordinates. Existing devices have many drawbacks, among them low speed, due to the use of inert elements, which makes it impossible to measure rapidly changing light fluxes. In this device, the authors tried to minimize the shortcomings. Also in this article, a mathematical model of the device is proposed. Attention is paid to the psychophysiological perception of color.**

Keywords—measurement, device, color, photodiodes, microcontroller, mathematical model, psychophysiology of vision.

I. Color Measurementt

Color measurement is a section of colorimetry, an objective way to determine the characteristics of the light flux emanating from a source of visible light (object) using optical devices (instruments) in order to exclude the subjective factor - the visual sensation from the action of light. Currently, when measuring color, after digitizing its characteristics, color information is processed, transmitted without a sample using numbers. There are two main measurement methods: Colorimetric and Spectral.

Measuring (reference) light emitted by the lamp is reflected by the sample and perceived by three photosensors. Filters that create spectral sensitivity in three color channels corresponding to standard spectral functions, and those that imitate the spectral sensitivity of the retina and correspond to the visual sensors of the eye. The sensor signal definition obtains standard XYZ digital values for red, green, and blue. They are then used for all other colorimetric calculations.

The limitations of this system are the incomplete modeling of several types of light, the lack of spectral reflectance values and metamerism measurements.

In recent years, in connection with the development of color television, multimedia programs for computers, animation developments, various training programs and simulators, interest in color measuring instruments has grown significantly.

Devices for measuring color have been used for decades. Gradually, they gain their place in everyday practice. Progress in this area depends on the development and production of new devices and methods for measuring color with wide operational capabilities, inexpensive and easy to use.

One of the most common color measurement tools used in the above areas is an electronic colorimeter, as it has the following advantages - the ability to express control, ease of operation, high probability (accuracy) of measurement. The capabilities of the electronic colorimeter far exceed the similar parameters of other color measuring instruments.

Thus, further study of the mechanisms of operation of the electronic colorimeter, the features of its application, is relevant and is of significant interest, both for developers of this type of device and for consumers.

However, one cannot fail to admit, and this is constantly noted by researchers, the development of tools and methods for measuring color is still in its infancy. There is no doubt the need to expand the range of tasks and situations, both from the point of view of practical needs, and in order to accumulate theoretical experience.

The vision of the world is carried out in the process of visual sensations and visual perception. In contrast to visual perception, visual sensations reflect only certain properties of objects and phenomena. Visual perception is a holistic reflection of objects and phenomena, i.e. in the aggregate of their properties, arising from the direct action of physical stimuli on the receptor surface of the eye. It is a complex activity of the visual analyzer system, including the processing of visual information (detecting an object, distinguishing and distinguishing its informative features and reuniting them into an integral visual image), its assessment (correlating the perceived image with perceptual and verbal standards), interpretation and categorization (adoption decisions about the class to which the object belongs) [1].

The development of visual perception depends on how smoothly and correctly its various components function - visual sensations or visual functions. Visual functions, being closely connected with each other, in mental activity form a single whole, called the act of vision. Its physiological basis is as follows: rays of light pass through the cornea of the eye, the lens, vitreous body and reach the retina. The cornea and lens not only transmit light, but also refract its rays,

acting as a biconvex lens. This allows you to collect them in a converging beam and direct them to the retina so that it produces a valid, but inverted (inverted) image of objects. In cones and rods located in the retina, light energy is converted into nerve impulses, which are carried through the optic nerves to the visual centers of the brain. Here, the energy of the nerve impulse is converted into a visual sensation. As a result, there are sensations of the shape, size, color of objects, their degree of remoteness from the eye, etc. The functional ability of the retina is not equivalent throughout its entirety. It is highest in its central part (central fossa of the macula), where the retina consists of highly differentiated receptors - cones. When examining any object, the eye is set in such a way that the image of the object is always projected onto the region of the central fossa [2]. On the rest of the retina, less differentiated receptors - sticks - dominate: and the farther away from the center the image of the object is projected, the less clearly it is perceived.

Vision has a dual nature: daytime vision is carried out by cones, and nighttime vision is performed by chopsticks. The rod device has a high photosensitivity, but is not able to convey a sense of color; cones provide uniform and color vision, but compared to sticks, they are noticeably less sensitive to low light and fully function only in good light. Three types of functional ability of the eye can be distinguished depending on the degree of illumination.

1. Daytime (photopic) vision is performed by the cone apparatus of the eye at high light intensity. It is characterized by high visual acuity and a clear, adequate perception of color.

2. Twilight (mesopic) vision is carried out by the rod apparatus of the eye at a low degree of illumination (0.1-0.3 lux). It is characterized by low visual acuity and achromatic (non-color) perception of objects. The lack of color perception in low light is well reflected in the proverb "all cats are sulfur at night."

3. Night (scotopic) vision is also carried out by the chopsticks in very low light and comes down only to the sensation of light.

Thus, the dual nature of vision requires a differentiated approach to assessing visual functions. Distinguish between central and peripheral vision.

Central vision is characterized by a person's ability to distinguish between the shape, small details and color of the objects in question. To recognize objects of the outside world, it is necessary to distinguish between them individual details. The finer the details distinguished by the eye, the higher its visual acuity. By visual acuity it is customary to understand the ability of the human eye to perceive separately points located at a minimum distance from each other. Due to the unequal distribution of cones in the retina, its various sections are uneven in visual acuity: with distance from the center of the retina, visual acuity decreases. Already at a distance of 10º from the center, it is equal to 0.2 and even more reduced to the periphery. Normal visual acuity in most adults is 1.

The maximum spectral sensitivity of cones of the so-called "standard observer" is 565 nm for red cones, 540 nm for green cones and 440 nm for blue cones, although there are disagreements on this issue between different authors and observed individuals. It should be noted that the sensitivity of the rods reaches a maximum at 495 nm - right in the middle between the blue and green flasks.

Chromatic colors include all tones and shades of the color spectrum. They are characterized by three qualities: 1) color tone (the color feature differs from other colors in the spectrum: blue, red, yellow, etc.); 2) saturation, determined by the proportion of the fundamental tone and impurities to it gray, which determines the color intensity; 3) the brightness or lightness of the color, the degree of proximity to white (light and darker colors). Various combinations of these characteristics give many shades of chromatic color [3]. A person is able to perceive about 180 color tones, and taking into account differences in brightness and saturation - more than 13 thousand.

Peripheral vision plays a large role in human life: it serves to orientate in space, has a high sensitivity in relation to moving objects, serves a person in low light conditions. The peripheral vision provided by the peripheral parts of the retina is determined by the size and configuration of the field of view - the space that is perceived by the eye (or eyes) with a fixed gaze. For achromatic (non-color) objects, the normal field of view (when viewed with both eyes) horizontally covers a space of 180 °, vertically - 110 °. The field of view of each eye has certain boundaries: outward - 90º, downward outward - 90º, downward - 60º, downward inward - 50º, inward - 60º, upward inward - 55º, upward - 55º and upward outward - 70º. In both eyes, the boundaries of the field of view are symmetrical.

The biophysical nature of vision is based on the interaction of individual molecules (retinoids) with radiation. These molecules are derivatives of retinol (vitamin A1), which is responsible for the yellow-orange color of the retina.

In rods there is only one type of retinoid - rhodopsin, and in cones many species are contained. In total, there are more than twelve different species, but four of them stand out, especially noticeable in cones [4]. It is rhodopsin 5, 7 and 9 and also a substance sensitive to ultraviolet waves - rhodopsin 11. However, it should be noted that the cornea, aqueous humor, lens and vitreous body absorb most of the ultraviolet radiation (UV). Red, green, and blue cones contain a mixture of all these retinoids, but in each type of flask, one type of retinoid is present in larger quantities, and in a proportion of 1000 times more than all the others.

In the cells of cones and rods there are thousands of membrane disks formed by plasma folds and on which 15 are attached by long chains of retinoid molecules. Thus, a real fractal space is formed for trapping light.

From the point of view of physics, all the molecules considered are similar. They consist of seven long chains of opsin surrounding a small but special molecule - 11-cis-retinal. When a photon collides with such a molecule, there is a 50% chance that it (the molecule) will "unfold" and turn into an isomer - trans-retinal.

In the dark, 11-cis retinal is firmly bound to the opsin protein. The interests of the photon leads to the isomerization of the 11-cis retinal to the trans retinal. Moreover, the complex opsin-trans-retinal through several chemical transformations quickly dissociates into opsin and trans-retinal. Rhodopsin regeneration depends on the interaction of pigment epithelial cells and photosensitive

cells. In case of blinding, rhodopsin is restored from visual purpura, that is, from retinoids of the pigment epithelium.

This phenomenon forms the basis of nervous information. In darkness, a constant input “dark” current flows in the outer segments of photosensitive cells [6]. As a result, the constant membrane potential of photosensitive cells is approximately - 40 mV. The input current in the dark is carried mainly by sodium ions, 16 following along the electrochemical gradient through the cationic channels of the outer segment of photosensitive cells. Under the influence of light, cation channels are closed. Thus, the value of the membrane potential shifts to the value of the equilibrium potassium potential, approximately - 80 mV. Accordingly, conditions arise for the appearance and translation of the visual signal along the axons of nerve cells.

II. MAIN PART

In this work, the authors propose a device for measuring the color characteristics of light reflected or transmitted through an optical medium.

The main element of this device is a measuring transducer, which associates with each radiation three signals proportional to the color coordinates[7].

Existing devices for measuring color characteristics have several disadvantages - low speed, due to the use of inert elements, which will make it impossible to measure rapidly changing light fluxes; insufficient accuracy of measuring the luminous flux, which has a weak power (poorly lit objects) due to the low sensitivity of the photoresistors, the inability to separate in space the measuring transducer and device; the inability to directly control the device due to the implementation of controls, etc.

In the developed device for measuring the color characteristics of objects, the authors tried to minimize the above disadvantages through the use of photodiodes and a microcontroller with built-in ADC, reference lighting LEDs and a color measurement method, which consists in determining the intensity of the three components of the input light flux by converting this data into a digital signal for subsequent recalculation of the signal color coordinates x and y for the color chart, which will uniquely characterize the color of the object , Expanding functionality by adding an interface device display facilities management, ability to save data to a memory card and the possibility of using the device in offline mode without involving a PC [8].

The device operates as follows: in a digital color measuring device, which contains three light filters, three photosensitive elements, a normalization amplifier, a microcontroller, the light flux passing through the filters enters the photosensitive elements, which are connected to the inputs of the normalized amplifiers, according to the invention, as photosensitive elements photodiodes are used, in addition, he has additionally introduced two normalization amplifiers, the inputs of which are connected to the photodiodes, and the outputs with analog microcontroller inputs, reference lighting LEDs that are connected to the outputs of the microcontroller, control buttons that are connected to the inputs of the microcontroller, a liquid crystal indicator, which is connected to the outputs of the microcontroller, and a memory card that is connected to the outputs of the microcontroller(Picture 1).

The authors suggest a mathematical model of a device for measuring color [9].

Formally we set the following problem. In the Hilbert space L_2 [a, b] a system of functions u_1 (x), …, u_n (x) is given, it is required to define linear combinations with a set of coefficients $\{\alpha_{ji}\}$ (i=1,n)(j=1,n) for which the differences between given curves $h_j(x)$ and linear combinations

$$g_j(x) = \sum_{i=1}^{h} \alpha_{ji} U_i(x) \tag{1}$$

were minimal.

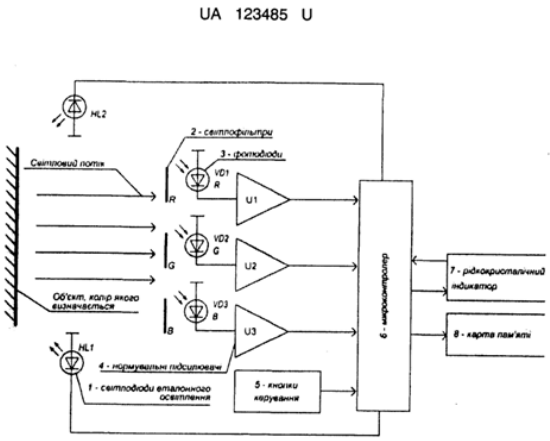

Pic 1 - Digital portable color measurement device

It is clear that with such a statement in the metric space L_2 [a, b], the measure of the deviation is simply the metric of this space, that is

$$\Delta = \int_a^b (g_j(x) - h_j(x))^2 dx \tag{2}$$

To find the root-mean-square deviation, consider a linear combination $\sum_{i=1}^{h} \alpha_{ji} U_i(x)$ for which

$$\int_a^b (h_j(x) - \sum_{i=1}^{h} \alpha_{ji} U_i(x)) f_m(x) dx = 0, \quad m = 1, \ldots, n \tag{3}$$

The existence of a given linear combination follows from the fact that the coefficient α_{ji} is uniquely determined from the system of linear equations

$$\sum_{i=1}^{h} \alpha_{ji} \int_a^b U_i(x) \cdot U_m(x) dx = \int_a^b h_j(x) U_m(x) dx \tag{4}$$

It is not difficult to see that the matrix of this system is a Grane matrix for a set of functions u_1(x), …, u_n(x)that are linearly independent, hence its determinant is not equal to zero. It is easy to show that expression (2) reaches its minimum on this linear combination [10]. Indeed, for some other linear combination $\sum_{i=1}^{n}\alpha'_{ji}U_i(x)$ we consider expression (2) with allowance for (3). Then we get

$$\begin{aligned}&\int_a^b (h_j(x)-\sum_{i=1}^{n}\alpha'_{ji}U_i(x))^2dx=\\ &=\int_a^b (h_j(x)-\sum_{i=1}^{n}\alpha_{ji}U_i(x)+\sum_{i=1}^{n}(\alpha_{ji}-\alpha'_{ji})U_i(x))^2dx=\\ &=\int_a^b (h_j(x)-\sum_{i=1}^{n}\alpha_{ji}U_i(x))^2dx+\\ &+\int_a^b (\sum_{i=1}^{n}(\alpha_{ji}-\alpha'_{ji})U_i(x))^2dx\geq\\ &\geq\int_a^b (h_j(x)-\sum_{i=1}^{n}\alpha_{ji}U_i(x))^2dx\end{aligned} \tag{5}$$

which indicates the validity of our statement.

We take an approximation of the integrals of system (4) on an arbitrary set of points $(x_1,...,x_q)\in[a,b]$.

Then

$$\int_a^b U_i(x)\cdot U_m(x)dx=\sum_{k=1}^{q}U_i(x_k)\cdot U_m(x_k) \tag{6}$$

We denote by

$$\sum_{k=1}^{q}U_i(x_k)\cdot U_m(x_k)=(U_i,U_m) \tag{7}$$

Then system (4) will have the form

$$\begin{aligned}&\alpha_{j1}(U_1,U_1)+...+\alpha_{jn}(U_n,U_1)=(h_j,U_1)\\ &.....\\ &\alpha_{j1}(U_1,U_n)+...+\alpha_{jn}(U_n,U_m)=(h_j,U_n)\end{aligned} \tag{8}$$

In this case, the minimum value Δ in expression (2) will be determined

$$\Delta=\sum_{k=1}^{q}(\sum_{i=1}^{n}\alpha_{ji}U_i(x_k)-h_j(x_k))^2 \tag{9}$$

Taking into account the fact that α_{ji} is solution of the system (8), then we finally obtain

$$\lambda=\frac{\begin{vmatrix}(U_1,U_1) & ..... & (U_n,U_1) & (h_j,U_1)\\ ..... & ..... & ..... & .....\\ (U_1,U_n) & ..... & (U_n,U_n) & (h_j,U_n)\\ (h_j,U_1) & ..... & (h_j,U_n) & (h_j,h_j)\end{vmatrix}}{\begin{vmatrix}(U_1,U_1) & ..... & (U_n,U_1)\\ ..... & ..... & .....\\ (U_1,U_n) & ..... & (U_n,U_n)\end{vmatrix}} \tag{10}$$

III. Conclusion

The results obtained confirm that the device developed by the authors has a number of advantages over its analogues, which allows color measurement with higher accuracy. This color measurement method can be used in space, medical, forensic, etc.

References

[1] Bogdanovich L. B., Burian V.A., Rautman F.I. Hudozhestvennoe konstruirovanie v mashinostroenii [Artistic design in mechanical engineering]. Kiev, Tehnika Publ., 1976. 183 p.

[2] Varlamov R. G., Strukov O. D. Elementy hudozhestvennogo konstruirovaniya i tehnicheskoy estetiki [Elements of artistic design and technical aesthetics]. Moscow, Soviet Radio Publ., 1980. 96 p.

[3] Lyutov V. P., Chetverkin P. A., Golovastikov G. Yu. Tsvetovedenie i osnovyi kolorimetrii : uchebnik i praktikum dlya akademicheskogo bakalavriata [Color science and bases of colorimetry: a textbook and a practical work for academic baccalaureate]. Moscow, Yurayt Publ., 2018. 222 p.

[4] Braham G. Psihologiya tsveta [Psychology of color]. Moscow, AST, Astrel, 2009. 158 p.

[5] Murakhovsky V. I., Simonovich S. V. Bolshaya kniga tsifrovoy fotografii [The Big Book of Digital Photography]. Pemza, Peter Publ., 2012. 304 p.

[6] Churkin A. V., Uvarova R. M., Shashlov A. B. Osnovy svetotehniki.Uchebnik [Fundamentals of lighting technology]. Moscow, MGUP Publ., 2002. 310 p.

[7] Shashlov B. A. Tsvet i tsvetovosproizvedenie [Color and color reproductions]. Moscow, MGAP, The World of the Book Publ., 1995. 245 p.

[8] Gurevich M. M. Fotometriya(teoriya,metody,pribory) [Photometry (theory, methods, devices)]. Leningrad, Energoatomizdat 1983. 415 p.

[9] Horoshajlo Y. E., Semenov S. G., Limarenko V. V. Pat 107317, Ukraina, Cifrovoj datchik dlya izmereniya cveta. 2016.

[10] Khoroshaylo Y. E., Sezonova I. K., Colorimetry. Proceeding of COAL 2005 2nd International Conference on Advanced Optoelectronics and Lasers V2. Yalta, 2005. 254p.

The measurement and effect of laser radiation on the human body

Vera Golian
Department of Software Engineering
Kharkiv National University of Radio Electronics
Kharkiv, Ukraine
0000-0001-5981-4760

Nataliia Golian
Department of Software Engineering
Kharkiv National University of Radio Electronics
Kharkiv, Ukraine
0000-0002-1390-3116

Iryna Afanasieva
Department of Software Engineering
Kharkiv National University of Radio Electronics
Kharkiv, Ukraine
0000-0003-4061-0332

Kyrylo Halchenko
Department of Software Engineering
Kharkiv National University of Radio Electronics
Kharkiv, Ukraine
0000-0001-9418-1399

Viktor Kazmirchuk
Institute of Microbiology and Immunology
National Academy of Medical Sciences of Ukraine Mechnikov
Kharkiv, Ukraine
imiamn@amnu.gov.ua

***Abstract*— The intensive implementation of laser radiation in biological research and practical medicine has been studied. The unique properties of the laser beam have opened up wide possibilities for its application in various fields: surgery, therapy and diagnostics. The clinical observations have shown the effectiveness of ultraviolet, visible and infrared laser spectra for local application on pathological niduses and for affecting the entire body.**

Keywords*— *laser, laser radiation, laser control, laser and health, quantum generator, laser diagnosis

I. INTRODUCTION

Over the past 15 years, the mechanisms of action have been largely disclosed and refined. The impact of low-intensity lasers leads to a rapid subsidence of acute inflammatory phenomena, stimulates reparative (restorative) processes, improves tissue microcirculation, normalizes overall immunity, and increases the resistance (stability) of the body. At present it has been proven that low-intensity laser radiation has a pronounced therapeutic effect. A laser or optical quantum generator is a technical device that emits light in a narrow spectral range in the form of a focused, highly coherent, monochromatic, polarized beam of electromagnetic waves. Depending on the nature of the interaction of laser light with biological tissues, there are three types of photobiological effects:

- Photo destructive effect, due to which the thermal, hydrodynamic, photochemical effects of light causes tissue destruction. This kind of laser interaction is used in laser surgery.
- Photophysical and photochemical effects, due to which the light absorbed by biological tissues excites atoms and molecules in them causing photochemical and photophysical reactions. The use of laser radiation as a therapeutic one is based on this type of interaction.
- Non-disturbing effect, when the biological substance does not change its properties in the process of interaction with light. These are effects such as scattering, reflection and penetration. This type is used for diagnostics (for example, laser spectroscopy).

II. PURPOSE AND OBJECTIVES OF THE STUDY

The purpose of the paper is to study a very wide area of modern medicine - the application of laser radiation to restore the health of a human being.

The first studies have shown that laser radiation is selectively absorbed by the pigment substances contained in the cells. The pigment melanin absorbs light most actively in the violet area, porphyrin and its derivatives, i.e., red, so oxyhemoglobin absorbs in the range of 542 and 546 nm, reduced hemoglobin absorbs in the range of 556 nm, and the enzyme catalase absorbs in the range of 628 nm. Taking into account the key role of catalase in many links of energy production, one can understand the wide therapeutic range of the helium-neon laser (HNL) and its universal normalizing effect on biological processes in the body. Absorption of laser energy also occurs by various molecular formations that do not have specific pigments and photobiological targets. Water absorbs visible light and the red part of the spectrum. This changes the structural organization of the water layer in membranes and changes the function of the thermolabile channels of the membranes. The biological structures of the body have their own electromagnetic fields and free charges, which are redistributed under the influence of photons of the HNL radiation, which leads to direct “energy pumping” of the irradiated organism. Primary chemical reactions are accompanied by the appearance of free radicals in a small amount, which, in turn, trigger the processes of oxidation of biological substrates, which have a chain character. This fact allows us to understand the switching (trigger) mechanism of multiple amplification of the initial effect of LILR. Thus, the mechanism of action of low-power lasers on tissues in the visible and infrared areas is based on processes occurring at cellular and molecular levels. Low-intensity laser irradiation stimulates the metabolic activity of the cell. Stimulation of biosynthetic processes can be one of the important points that determine the effect of low-intensity laser radiation on the most important functions of cells and tissues, vital processes and regeneration (recovery). HNL leads to an increase in the content of DNA and RNA in the nuclei of human cells, which indicates the intensification of transcription processes (divisions). This is the first step in the process of protein biosynthesis. This brings up the question of triggering

978-1-6654-8569-2/22/$31.00 ©2022 IEEE

mutations. However, it has been proven that the frequency of chromosomal mutations in human cells caused by chemical mutants decreases when exposed to HNL. HNL has an antimutagenic effect, activates DNA synthesis and accelerates the recovery processes in cells exposed to neutron flux or gamma radiation. This allows to use laser radiation in oncology, in hazardous industries, in military medicine, both as a preventive and therapeutic factor along with medicines.

A. Indications for laser therapy have been developed taking into account the pathogenetic mechanism of the action of laser radiation on the body.

Internal diseases: Ischemic heart disease, hypertension, chronic nonspecific lung diseases, gastric and duodenal ulcers, biliary dyskinesia, colitis, chronic pancreatitis, acute and chronic (non-calculous) cholecystitis, adhesive disease.

Diseases of the musculoskeletal system: Osteochondrosis of the spine with radicular syndrome, inflammatory diseases of bones and joints of metabolic etiology in the acute stage, arthritis and arthrosis, diseases and traumatic injuries of the musculoskeletal system (myositis, tendovaginitis, bursitis).

Diseases of the nervous system: Neuritis and neuralgia of the peripheral nerves, trigeminal neuralgia, neuritis of the facial nerve, cerebrovascular insufficiency.

Diseases of the genitourinary system: Chronic salpingo-oophoritis, tubal infertility, chronic nonspecific prostatitis, urethritis, cystitis, weakening of sexual function.

Diseases of ENT - organs: Chronic inflammation of the paranasal sinuses, pharyngolaryngitis, tonsillitis, otitis media, subatrophic and vasomotor rhinitis.

Surgical diseases: Postoperative and non-healing wounds, trophic ulcers, keloid scars (in the subacute stage), injuries (mechanical, thermal, chemical), osteomyelitis, anal fissures, purulent abscesses, mastitis, vascular diseases of the lower extremities.

Skin diseases: Itching dermatosis, trophic ulcers of various origins, inflammatory infiltrate, boils, eczema, neurodermatitis, psoriasis, atopic dermatitis.

Dental diseases: Stomatitis, gingivitis, alveolitis, pulpitis, periodontitis, paradontosis, odontogenic inflammation of the maxillofacial area.

Laser therapy has the features of a pathogenetically substantiated method. When applying it, it is important to take into account not only the general condition of the body, the specifics of the pathological process, its clinical manifestations, stages and forms of diseases, but also concomitant diseases, age and professional characteristics of the patient. The most effective use of laser therapy is in the functionally reversible phases of the disease, although new techniques are also used in more severe manifestations of the pathological process, with pronounced morphological changes. It can be used in conjunction with laser therapy and other physiotherapeutic factors, physiotherapy exercises, massage, no more than 2 factors a day. As mentioned earlier, the complex use of laser therapy with medications is much more effective, especially in acute stages. The total effectiveness of laser therapy ranges from 50 to 85%, in some cases up to 95%.

III. Modern Sources of Radiation and Equipment for Low-Intensity Laser Therapy

Since the earliest times, the Sun has been perceived as a source of light, heat and life. The use of natural light for medicinal purposes is probably as old as mankind itself. Sunlight and water have always been the closest and most accessible remedies for a human being. The first mention of the conscious use of sunlight for preventive and therapeutic purposes that has come down to us dates back to the reign of Pharaoh Amenhotep IV in Egypt (presumably from 1375 to 1358 BC). There are reports about the healing properties of the Sun in the papers of Herodotus, Hippocrates, Aulus Cornelius Celsus, Claudius Galen, Abu Ali ibn Sina, etc. One can say that the Sun is the first source of radiation in phototherapy, which has a wide spectral range, unstable radiation power, unstable degree of polarization. At the end of the last century there appeared artificial light sources, which had a narrower spectral range, stable radiation power, due to which it became possible to receive a much more pronounced and stable therapeutic effect than with sun therapy. In addition, scientists made research on the phenomena of photo and biological activation with the appearance of a more controlled means of exposure. First of all, the success of phototherapy is associated with the name of the Danish physiotherapist Nils Ryberg Finsen (N.R. Finsen, 1860-1904), who proposed to concentrate the sun's rays, while excluding the visible and infrared parts of the spectrum for the treatment of skin tuberculosis (lupus), as well as to treat skin smallpox with red light. In 1903, he was awarded the Nobel Prize in Medicine for the development of a new method of treatment. The second half of the 20th century was marked by the appearance of lasers - light sources with new properties, such as: monochromaticity, coherence, polarization and directivity. This fact didn't escape observation, and in the mid-1960s, the study of photobioeffects caused by low-intensity laser radiation (LILR) began. One of the first issues was comparing the monochromatic radiation of a He-Ne laser and the broadband light of a red lamp. V.M. Inyushin [6, 7] and other researchers convincingly showed the advantages of laser radiation as a means of therapeutic action, which largely determined the further development of low-intensity laser therapy as an independent area of physiotherapy.

The classification of lasers according to various parameters [4, 8] is given below.

- Physical (aggregate) state of the working substance of the laser: gas (helium-neon, helium-cadmium, argon, carbon dioxide, etc.); excimer (argon-fluorine, krypton-fluorine, etc.); solid-state (glass, yttrium aluminum garnet, etc., doped with various ions); liquid (organic dyes); semiconductor (gallium arsenide, gallium arsenide phosphide, lead selenide).
- Method of excitation of the working substance: optical pumping; pumping due to gas discharge; electronic excitation; charge carrier injection; thermal; chemical reaction; etc.
- The wavelength of the laser radiation. If the emission spectrum is concentrated in a very narrow wavelength range (less than 3 nm), then it is customary to consider the radiation to be monochromatic and its technical data indicate a specific wavelength corresponding to the maximum of the spectral line. The radiation wavelength is determined by the material of the

working substance, but it can vary within small limits, for example, depending on the temperature. The same wavelengths can be generated by different types of lasers, for example, around l = 633nm the following lasers are at work: He-Ne, dye lasers, gold vapor, semiconductor lasers (AlGaInP).

- According to the nature of the emitted energy, continuous and pulsed lasers are distinguished. The concepts of a pulsed laser and a laser with modulation of continuous radiation should not be confused, since in the second case we get, in fact, intermittent radiation of various frequencies and shapes, but with a maximum power that does not exceed the value in continuous mode or exceeds it slightly. Pulsed lasers, on the other hand, have a high pulse power, reaching 107 W or more for some types, but the pulse duration is extremely short, and the average power per period is small.

- The characteristic of the average power of lasers is very important. High-power lasers have more than 103 W; low power lasers have less than 10-1 W. Intermediate values are not of great interest to us from the point of view of the issue under consideration. Lasers for medicine should be approached from the point of view of their impact on a biological object. In some cases, "low power" of 100 mW can be very large. In the scientific papers on laser therapy [1], it is suggested to conventionally subdivide low-intensity laser irradiation into "soft" ones - up to 4 mW/cm?, "average" ones - from 4 to 30 mW/cm? and "hard" ones - more than 30 mW/cm?. In the treatment process, "soft" radiation is used for reflexology at the points of classical acupuncture, "medium" radiation is used for influencing superficially located pathological foci, or on the projection area of certain organs. "Hard" low-intensity irradiation, in particular, of a helium-neon laser, is recommended for use in dentistry in the treatment of certain diseases of the oral cavity and teeth. However, the question remains open regarding the energy classification of therapeutic pulsed lasers, which must be considered comprehensively from the standpoint of the biological effect of laser radiation, taking into account not only the average output power, but also the level of pulsed power, pulse duration, and time of exposure to laser radiation.

- Depending on the degree of danger of the generated radiation for service personnel, lasers are divided into four classes: Class 1. Laser products are safe under the intended operating conditions. Class 2. Laser products that generate visible radiation in the wavelength range from 400 to 700 nm. Eye protection is achieved by natural reactions, including the blink reflex. Class 3A. Laser products are safe for viewing with the naked eye. For laser products that generate radiation in the wavelength range from 400 to 700 nm, protection is achieved by natural reactions, including the blink reflex. For other wavelengths, the danger to the unprotected eye is no greater than with Class 1 laser products. Direct observation of the beam emitted by Class 3A laser products with optical instruments (i.e., binoculars, telescope, microscope) can be hazardous. Class 3B. Direct observation of such laser products is always dangerous. Visible scattered radiation is usually harmless. Note: Conditions for safe observation of diffuse reflection for laser products of class 3B in the visible region: the minimum distance for observation between the eye and the screen is 13 cm, the maximum observation time is 10 s. Class 4: Laser products that produce hazardous scattered radiation. They can cause skin damage and also create a fire risk. When using them, one must take special precautions. This gradation is defined by GOST R 50723-94: Laser safety. General safety requirements for the development and operation of laser products [3].

- For carrying out a treatment process, such a characteristic of the laser as the angular divergence of the beam is often important. It is measured in degrees, minutes of arc (1/60 of a degree), seconds of arc (1/60 of a minute), or radians (1_ = p / 180 > 0.0175 rad). Gas lasers have the smallest divergence - about 30 arc seconds (> 0.15 mrad). The beam divergence of solid-state lasers is about 30 arc minutes (> 10 mrad), for semiconductor lasers: in a plane parallel to the p-n junction it is from 10 to 20 degrees (depending on the type of laser); in a plane perpendicular to the p-n - transition it is about 40 degrees.

- The coefficient of performance (COP) of the laser. There are theoretically possible (quantum output) and real (overall) efficiency factors. The latter is determined by the ratio of the laser radiation power to the power consumed from the pump source. For gas lasers, the total efficiency factor is 1-20% (helium-neon is up to 1%, carbon dioxide is 10-20%,), for solid-state lasers it is 1-6%, for semiconductor lasers it is 10-50% (in some designs it is up to 95%). It becomes clear why only semiconductor lasers can be used in autonomous and portable therapeutic equipment. Gas lasers are diverse according to the type of the medium used: He-Ne, CO, CO2, N, Ar and others. This determines a very wide range of wavelengths at which generation is obtained. Pumping is carried out by creating a glow discharge in the tube, which is possible only at very high supply voltages. Of all types of lasers, they have the smallest spectral line width - up to 10-7 nm. Excimer lasers are a type of gas lasers that operate on compounds that can only exist in an excited state - halogens and inert gases (KrF, ArF, etc.). They emit in the ultraviolet region of the spectrum. Solid-state lasers are mainly yttrium aluminum garnet (YAG) doped with rare-earth metal ions (Nd, Er, Ho, etc.). Actually, these ions are the source of radiation, and the garnet is only a matrix for their correct location in space.

Solid-state lasers can be both pulsed and continuous, they operate at an average power level. Dye lasers (a liquid solution of special dyes is used as a working medium) are characterized by the fact that they can be tuned according to the wavelength in a wide spectral range. Semiconductor lasers occupy a special place due to their design features and physical principles of operation. The small dimensions of the laser are determined by the high efficiency and the need to provide a high pump current density in order to achieve the inverse population. For semiconductor lasers, pumping is carried out with a small current (tens of mA) when a voltage of about 2 - 3 V is applied, while for other laser types thousands of volts are required. It should be noted that we take into account

exclusively injection semiconductor lasers pumped by a direct current passing through a diode structure (laser diode). The disadvantage of semiconductor lasers is the large divergence of radiation, which limits its use in other areas, except for laser therapy. Semiconductor lasers operate in the wavelength range from 0.63 to 15 microns. The most widely used, both in therapy and in surgery, are the lasers in the near infrared (IR) region (l = 0.78-0.93 μm) based on a Ga1-xA1xAs crystal. Recently, semiconductor lasers based on AlGaInP (l = 0.633-0.64 μm) have become increasingly widespread, replacing traditional HeNe lasers. The lasers with a wavelength of 0.67 μm and an average power of up to 10 W are also successfully used for photodynamic therapy (PDT). It is reported that the production of green (l = 0.53 μm) and blue (l = 0.42 μm) semiconductor lasers based on Zn1-xCdxSe with a power of several milliwatts and an MTBF of up to 1000 hours has begun .

The apparatus used in medicine, in addition to the lasers themselves, also contain: a device for modulating the radiation power of continuous lasers or a master oscillator for pulsed lasers; a timer that sets the operating time; indicator or radiation power meter (photometer); a tool for delivering radiation to an object (light guides), etc. Semiconductor lasers are the most promising in LILT. Small dimensions, low supply voltages, a wide range of radiation wavelengths and powers, the possibility of direct radiation modulation, relatively low cost - all this allows us to state that semiconductor lasers are unrivaled in this field of medicine. Currently, dozens of laser therapy devices (LTD) are produced: stationary and portable; multidisciplinary and highly specialized; using lasers of various types and their combinations, etc. Over the years of laser therapy development, the requirements for equipment have also been formed, which were formulated in a generalized form relatively recently. In accordance with the increase in the level of laser medicine, the requirements for modern LTD have also grown significantly, the next stage in the development of laser therapeutic equipment as a direction in medical instrumentation has come - the formation of a single targeted policy in the development and production based on the closest possible cooperation between the researchers of various specialties, practitioners and manufacturers. Universality is one of the fundamental principles embedded in the modern "tool" of a doctor or researcher. The main goal of universality is to meet the numerous, sometimes conflicting requirements of doctors for the equipment at minimal cost. The block principle of the equipment development allows to combine the incompatible. The equipment developed on the basis of this principle is divided into three parts: the base unit, radiating heads and nozzles. The principle of universality was fully implemented in the development of LTD "Mustang". The base unit - the basis of each set, is essentially a power supply and a control unit. Its main functions are setting radiation modes: frequency, time, power. Most models make it possible to control several radiation parameters, the main of which is power (average or pulsed). The basic blocks differ in functionality and can be conditionally divided into two types: with a fixed set of parameters and an arbitrarily set. Working according to well-known methods, when the treatment procedure is carried out by a nurse with a large flow of patients, it is most preferable and convenient to use LTD, in which the principle of "fixed frequencies" is applied. On the front panel of such a base unit there is a row of buttons with an indication above each frequency that will be automatically set after pressing the button. In this case an important attribute is a light indication of switching on, which allows you to make sure that the mode is set correctly. The operating time (timer) is selected in the same way. This principle is implemented in the LTD "Mustang" models - 016, 017, 022. A small number of fixed parameters set by such devices leads to limitations, which are to a certain extent eliminated by the presence of basic blocks that allow the doctor to set the necessary parameter values personally (LTD "Mustang" - 024 and 026 models). A visual representation of the selected values is provided by 40 digital indicators of various types. Devices of all types must have an indicator or a radiation power meter (photometer). One, two or more radiating heads can be connected to one block, but two-channel devices are the most common. As a rule, in the arsenal of a modern doctor there are several types of heads that allow you to maximize the possibilities of laser therapy. In this case, the use of various types of switches, distributors, splitters, etc. is very convenient, because there is no need to change the head with each procedure and you can adjust their power independently. You can quickly connect any of the heads, and at the same time you can use two or more of them in any combination, for example, red and infrared lasers. The interchangeability of radiating heads and nozzles allows each doctor, according to a specific task, to create his own, optimal set of equipment or organize multifunctional, highly efficient treatment rooms. The ease of control is necessary in any equipment, including medical ones. The criterion for evaluating the ease of control is the time to think about the actions associated with changes in settings and the number of errors made in this case. The ease of LTD control is closely related to its ergonomics. The work of the medical staff should be ensured in such a way that all attention is focused on the patient, on the fulfillment of the main task, i.e., high-quality treatment, the functioning of LTD should not distract the attention of the doctor. The control of laser radiation parameters is extremely important for the validity of the applied methods of treatment and the correct dosage, which ensures the most high-quality and effective treatment, as well as for addressing the issues of patient and physician safety. Based on these tasks, it is necessary to control the following parameters: 1. The length of the radiation wave. This parameter is determined by the type of laser and is indicated in the documentation by the manufacturer. Additional indication is not required. 2. Frequency of repetition of radiation pulses or modulation frequency. It is set by a switch of any of the types listed above on the panel of the base unit (control unit). Information about the exact value of the frequency is presented either by a digital indicator in the form of specific numbers, or by fixing a discrete switch in the desired position. It should be noted that in the second case, each discrete mark must necessarily contain information about the specific value and dimension of the parameter, for example, 80, 150, 300 Hz. It is not allowed to use abstract values of the type: 1, 2, 3: with the manufacturer's recommendation to find out the real value of the parameter in the passport or instruction manual. In addition to the fact that it is simply inconvenient, the probability of an error when setting the exposure parameters, also increases significantly. 3. Working time (timer). In addition to the requirements that apply to the frequency indication, it is also necessary to provide sound indication of the beginning and end of work. 4. Radiation power. Due to the fact that the effect of LILR is dose-dependent, and the radiation power can vary significantly due to many reasons: ambient temperature, supply voltage, etc. There is a need for

mandatory control of the radiation power to more accurately determine the dose of exposure. If the drop in power of lasers in the visible range of radiation can be somehow noticed, for infrared lasers (radiation invisible to the eye) the problem of power control and safety issues is even more acute. A wide range of power recommended for various diseases and techniques requires the presence of a power level regulator, and, in this case, the control over these changes is simply necessary.

The radiating heads are connected to the base unit directly or through a splitter. They consist of one or more semiconductor lasers (LEDs are less commonly used) and an electronic control circuit that sets the laser pump current and also ensures the head adjustment to a unified power supply from the unit. Sometimes the electronic circuit provides other functions. It should be noted that it was the semiconductor laser that made it possible to create a system of remote emitting heads and to fully implement the block principle of developing modern equipment for low-intensity laser therapy. Matrix radiators constitute a special class of heads and autonomous devices. When considering the nozzles, only special magnetic ones are used (MM-2, MM-3). In medical practice, matrix emitting heads and autonomous devices containing 10 pulsed infrared lasers are mainly used [2]. The mass-dimensional parameters of the equipment are by no means always of decisive importance. The priority is often given to the characteristics that ultimately allow you to get the best therapeutic effect: versatility, the ability to change and control radiation parameters, ease of control, etc. The problem of the dimensions and weight of the apparatus is acute in the case when its systematic movement is required. Such situations most often arise in the following cases: 1. Working conditions of a doctor: on a floating vessel, on board an aircraft, in mobile outpatient clinics, in isolated teams (duty points, search teams, expeditions), in field conditions, etc. Rural and private practitioners also face the problem. 2. In the cases, when under periodic medical supervision patients carry out their procedures independently. This is especially true in the treatment of severe chronic patients, whose movement is difficult, as well as the patients who are far from medical institutions, which makes it possible to continue the course of treatment on weekends and holidays. In these situations, portable devices with minimal dimensions and weight, operating both from the mains (via an adapter) and from a battery, are preferable. In the first case, the minimum size and weight lead to the loss of versatility for the doctor and, as a result, to the limitation of laser therapy possibilities; and in the second case, the simplicity of such devices is even more appropriate, because it allows you not to worry about its incorrect use by the patient. At the same time, the capabilities of portable devices may well be enough for a practicing doctor. Autonomous portable laser therapy devices use both matrix emitters (LTD “Muravei”) and single emitters, which have the advantage of using various attachments (magnetic and optical) [9]. They are indispensable when working with intracavitary instruments (ENT, dental, etc.), but such LTDs have manifested themselves especially well in reflexology. For example, for laser acupuncture, a special LTDs “Motylyok” have been developed, which include a corresponding nozzle (A3). Besides, the specialized direction of their application is determined by the use of lasers with the most effective radiation wavelengths for acupuncture of 0.63 and 1.3 μm (optical attachments for intracavitary laser therapy). Historically, helium-neon lasers (l = 0.63 μm) were the first to be used in LILT. The radiation with this wavelength penetrates the tissues to an insignificant depth and it is possible to influence the internal organs only with the help of an appropriate light guide instrument. At present, with the advent of pulsed infrared semiconductor lasers and especially matrix emitters based on them, the use of nozzles has often been abandoned in favor of non-invasive irradiation on the projection of the diseased organ.

It is possible to significantly expand the range of intensities that do not violate the harmony of internal biorhythms with the time synchronization of the impact on the biosystem. In principle, it is possible to achieve the non-mismatching effect of LILR at all levels by matching the time characteristics of the affecting radiation with the periods of all endogenous biorhythms, but due to fundamental difficulties, the implementation of such a regimen is limited to a prior determination for each patient of at least 3 frequencies of internal rhythms. The use of semiconductor lasers provides small dimensions and user convenience [5, 6, 8]. The specialization of some apparatus highlights other requirements than universality, which is not always exclusively necessary. To some extent, this has already been shown on the example of autonomous vehicles. In 1982-1989 there have been reports of the effectiveness of intravenous blood irradiation (ILBI) for the treatment of patients with angina pectoris and acute myocardial infarction.

ACKNOWLEDGMENT

The designing of highly specialized complexes, which, as a rule, combine several ways of the laser radiation impact on a human body, equipped with powerful methodological support, make it possible to most effectively realize the possibilities of physical medicine in the treatment of one or two diseases. The example of this instrumentation area are the devices for intravenous blood irradiation, specialized according to the method of exposure. The development and widespread implementation of LILT techniques based on exposure to several wavelengths of monochromatic radiation (blue, green, red and infrared) can be implemented by means of semiconductor lasers, small-sized and versatile devices, with the corresponding wavelengths of radiation. There is a possibility of exposure to all wavelengths simultaneously or in any combination of different emitters. The replacement of CW lasers for generating nanosecond pulses with a peak power of 1-10 W and an average power that is 2-3 orders of magnitude less than that of CW lasers used today. Again, the only possible sources of radiation in this case are exclusively semiconductor injection pulsed lasers with different wavelengths of radiation. The implementation of a multi-frequency mode of laser radiation modulation by the entire hierarchy of endogenous rhythms of a particular patient (or the maximum possible set) covers the range from ontogenesis (10-10 Hz) to the frequencies of the optical range of electromagnetic waves (10-14 Hz), which are used for exposure. In other words, in order to obtain the maximum effect, it is important to take into account the age of the patient and to vary with different wavelengths of radiation. Between these extreme points of the frequency hierarchy of the life organization, there are many characteristic ranges successfully studied today and which must be taken into account in the multi-frequency regime of LILR exposure.

REFERENCES

[1] I. Baybekov, A. Kasymov and V. Kozlov, Morfologicheskiye osnovy nizkointensivnoy lazeroterapii. Tashkent: Ibn Siny, 1991.

[2] V. Gribkovskiy, Poluprovodnikovyye lazery. Mn: Universitetskoye, 1988.

[3] V. Grimblatov, Sovremennaya apparatura i problemy nizkointensivnoy lazernoy terapii. Kyiv: Primeneniye lazerov v biologii i meditsine (Sbornik), 1996, pp. 123-127.

[4] V. Inyushin, Lazernyy svet i zhivoy organizm. Alma-Ata, 1970.

[5] V. Inyushin, P. Chekerov, S. Hill and T. Ghoshal, Biostimulation through laser radiation and bioplasma. [Cph.]: The Danish Society for Psychical Research, 1978.

[6] S. Moskvin, A. Radayev and M. Ruchkin, "Novyye vozmozhnosti portativnykh lazernykh terapevticheskikh apparatov “Motylek”", Mezhd. nauch.-prakt. konf. “Primeneniye lazerov v meditsine i biologii", vol., pp. 111-113, 1996.

[7] S. Moskvin, "Lazernaya terapiya kak sovremennyy etap razvitiya gelioterapii (istoricheskiy aspekt)", Laser medicine, vol. 1, no. 1, pp. 45-49, 1997.

[8] L. McKibbin and R. Downie, "TREATMENT OF POST HERPETIC NEURALGIA USING A 904 nm (INFRARED) LOW INCIDENT ENERGY LASER: A CLINICAL STUDY", LASER THERAPY, vol. 3, no. 1, pp. 35-39, 1991. Available: 10.5978/islsm.91-or-05.

[9] M. Titov and S. Moskvin, "Optimization of the parameters of biostimulator “Mustang” in respect to the light scattering properties of the tissues", SPIE`s Symposium “Biomedical Optics Europe`93”, 1996.

Measurement of Impulses Along the Cellular Structures of Fibers Using a Radio Physical Model

Mykolay Kundenko
State Biotechnological University
Kharkiv, Ukraine
n.p.kundenko@ukr.net

Igor Chaly
State Biotechnological University
Kharkiv, Ukraine
ivchaly@gmail.com

Kateryna Yablunovska
Mykolayiv National Agrarian University
Mykolaiv, Ukraine
yablunovskayakaterina@ukr.net

Yury Megel
State Biotechnological University
Kharkiv, Ukraine
megel_ye@mail.ru

Andrii Rudenko
State Biotechnological University
Kharkiv, Ukraine
andrey0911r@gmail.com

Vitalii Mardziavko
State Biotechnological University
Kharkiv, Ukraine
vitalijmardzavko@gmail.com

***Abstract*—Almost all the features of the functioning of biological objects of flora and fauna are determined by electromagnetic interaction, therefore, the modern development of agricultural production cannot be imagined without the use and development of new electromagnetic technologies. In this article, the processes in a grain cell are studied during the passage of short electrical impulses in a wide range of parameters. In the course of the study, the change in potentials in cell membranes during the propagation of impulses along the fibers was considered. Traditional basic physical mechanisms of membrane conductivity were used, namely the conductivity of sodium, potassium and calcium ions. To study the change and passing processes of the charge of the outer membrane under the action of an external electric field, an equivalent circuit has been developed that simulates a cell of a grain crop. This equivalent scheme also takes into account the nucleus of the cell. The external environment is described by resistance and capacitance. On the basis of which, a modification of a number of basic radio physical models of the functioning of a grain cell and a solution to the problem of resonant frequencies in the development of an electrophysical installation are proposed. The results of the action of an electrical impulse on cells show the intensity of the impulse action as a result of the development of fluorescence of individual cells. As a result, the effect of cell destruction by short pulses of the electric field is effective in cleansing from pathogenic microbes.**

Keywords—electrical impulse, cell membrane model, fluorescence, electromagnetic interaction, cell structure

I. INTRODUCTION

To date, the topical issue is the deepening of the study of cellular connections when interacting with a magnetic field, which is one of the methods for processing grain crops. In the works of the authors [1-7], cells are studied, which consist in changing various states and fast transitions between them under types of external influence with controlled parameters. However, the question of specific electromagnetic effects on the cell remains not fully resolved.

The main results in the field of theoretical studies of cellular activity are related to the study of the dynamics of individual cells and the application of methods of the theory of neural networks that describe cells. One of the important results of these studies is that the dynamics of cells in a collective is somewhat more regular than the dynamics of individual cells [1-2].

II. ANALYSIS OF PREVIOUS STUDIES

Let us consider the change of potentials in cell membranes [3] with time during the propagation of impulses along the fibers. In the simplest case, in addition to the time variable t, we also consider the spatial variable *x*. In this case, the excitation can propagate along this coordinate.

Using the notation: $\varphi(x,t)$ - this potential difference across the membrane of the nerve fiber, $i(x,t)$ - the current flowing through the fiber and $ji(x,t)$ - the ion flux flowing through the membrane, we obtain the dynamics equations [4]:

$$\frac{\partial\varphi(x,t)}{\partial x} = -r\,i(x,t), \tag{1}$$

$$\frac{\partial i(x,t)}{\partial x} = -c_i\frac{\partial\varphi(x,t)}{\partial t} - j_i(x,t), \tag{2}$$

where c_i – specific capacity of the membrane; r – specific resistivity; x – coordinate along the nerve fiber along which the potential impulse propagates.

Differentiating equation (1-2), we obtain from the system of equations of the first order one equation of the second order:

$$\frac{\partial^2\varphi(x,t)}{\partial x^2} = r\,c_i\frac{\partial\varphi(x,t)}{\partial t} + r\,j_i(x,t), \tag{3}$$

So the equations for the membrane potential have the form of a nonlinear diffusion equation. The usual diffusion equation:

$$\frac{\partial^2\varphi(x,t)}{\partial x^2} = \frac{\partial\varphi(x,t)}{\partial t}, \tag{4}$$

has solutions that lead only to the violation of the initial states in the form of localized impulses and, as is well known, does not contain solutions in the form of propagating disturbances and waves (formally, we can say that the propagation velocity of disturbances is infinite).

978-1-6654-8569-2/22/$31.00 ©2022 IEEE

As is known, in [5-7], adding a nonlinear term to the diffusion equation leads to a new nonlinear diffusion equation, which is now known as the Kolmogorov, Petrovsky and Piskunov (KPP) equation, and to the emergence of a finite velocity of propagation of disturbances. KPP equation was obtained to describe the distribution of genes in a population. At the same time, Huxley obtained an exact solution in the form of a traveling wave for his model of the nonlinear equation of potential diffusion:

$$\frac{\partial^2\varphi(x,t)}{\partial x^2}=\frac{\partial\varphi(x,t)}{\partial t}+F(\varphi), \tag{5}$$

$$F(\varphi)=\varphi(\varphi-1)(\varphi-a), \tag{6}$$

Note that in the KPP equation, the nonlinearity was not cubic, as for a pulse propagating through fibers, but quadratic [6]:

$$F(\varphi)=\varphi(\varphi-1), \tag{7}$$

As well as the solution of the KPP equation does not have the form of a solitary wave, but the form of a moving front. One of the characteristic features of nerve fibers is the existence of a refractory time, during which the nerve fibers lose their excitability and do not respond to external stimuli. Dynamic equation describing the behavior of a nerve impulse was proposed in [8,9]. In these works, a $R(x,t)$ variable is used- a recovery variable associated with the refractoriness of the nerve fiber and the ion current model is presented in the following form:

$$j_i(x,t)=F(\varphi(x,t))+R(x,t), \tag{8}$$

$$\frac{\partial R(x,t)}{\partial t}=\varepsilon(\varphi(x,t)+a-bR(x,t)), \tag{9}$$

Here the parameter ε determines the rate of change in refractoriness $R(x,t)$. After combining equations (1-2) and (7-9) into a single system, we obtain the following dynamic equations (called FitzHugh-Nagumo equations) for a nerve impulse [7]:

$$\frac{\partial\varphi(x,t)}{\partial t}=\frac{\partial^2\varphi(x,t)}{\partial x^2}-F(\varphi(x,t))-R(x,t),$$

$$F(\varphi)=\varphi-\theta(\varphi-a), \tag{10}$$

$$\frac{\partial R(x,t)}{\partial t}=\varepsilon(u(x,t)-bR(x,t)), \tag{11}$$

where θ – theta Heaviside function:

$$\theta(x)=\begin{cases}1, & x\geq 0\\ 0, & x<0\end{cases}$$

For $\varepsilon = 0$ equation (10 - 11) is reduced to the KPP equation associated with gene diffusion.

Thus, modern ideas about the propagation of excitation along the network of nerve fibers is associated with nonsingular solutions of partial differential equations.

III. Purpose of the Study

Purpose of the study is modification of a number of cell functioning basic radiophysical models under conditions of specific external electromagnetic influences.

IV. Research Methods and Results

The pulsed electromagnetic field acts mainly on the transport processes in the membrane. In our model, the external environment (cytoplasm) is considered as a homogeneous conducting medium with a resistance of the order of 100 Ohm·cm [1]. The outer membrane of the cell consists of a double lipid layer with a capacity of the order of 10^{-6} F/cm^2 [3] and a resistance exceeding that of the cytoplasm.

To study the evolution of the outer membrane charge under the action of an external electric field, an equivalent circuit has been developed that simulates a grain cell (see Fig. 1).

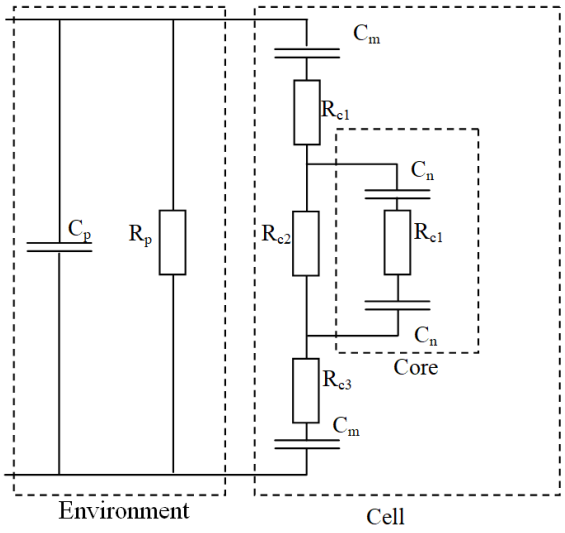

Fig. 1. Equivalent scheme of a cell with a nucleus in the medium.

This equivalent circuit also takes into account the cell nucleus. The external environment is described by resistance and capacitance.

For an acting electric field pulse with a characteristic duration exceeding the relaxation time of the dielectric constant of the cytoplasm, the capacitive part of the impedance is insignificant. The cell membrane is modeled by a capacitance, and the cytoplasm by resistance, the conductivity of the membrane is modeled by a voltage-dependent resistor.

When a voltage pulse is applied to a cell, a charge builds up in the membrane and the potential applied to the membrane increases. The characteristic relaxation time of the membrane charge of a spherical cell can be written as [4]:

$$\tau_c=\left(\frac{1+2V}{1-V}\frac{\rho_1}{2}+\rho_2\right)Ca, \tag{12}$$

where V – the volumetric concentration of cells, ρ_1 – the resistance of the medium, ρ_2 – the resistance of the cytoplasm, Ca – membrane capacity per area unit, and 2a – the diameter of the cell.

For typical cells with a diameter of 10 μm and a relatively low volume concentration, the characteristic membrane charging time is 75 ns. The amplitude of the electric field E_{cr} required to charge the membrane to the critical potential U_{cr}, leading to the destruction of the membrane has the form [5]:

$$E_{cr} = U_{cr} \Big/ \left(f\, a \left(1 - \exp\left(-\tau / \tau_c\right)\right)\right), \qquad (13)$$

where τ_c – the characteristic time of membrane charging, f – factor determined by the shape of the cell, and W_{cr} – the energy required for membrane breakdown [6]:

$$W_{cr} = E_{cr}^2 \tau / \rho_1 = K\tau / \left(1 - \exp\left(-\tau / \tau_c\right)\right), \qquad (14)$$

where K – constant.

With a sufficient increase in the amplitude of the electric pulse, this method can also be applied to bacteria with cell sizes less than one micron. It is considered that the resistors, capacitors and inductors included in the radiophysical model of the cell can be considered linear, and their parameters lend themselves to a rigorous description. The impedances of these components are calculated using the following relations: for resistors with resistance R: $Z=U/I=R$, for capacitors with capacity C: $Z=U/I= (j2\pi fC)^{-1}$, for inductors with inductance L: $Z=U/I= j2\pi fL$,at frequency f. Here Z,U,I – are complex quantities. In reality, all of these components have parasitic resistance, parasitic capacitance, and parasitic inductance. These spurious components usually have little effect at low frequencies, but at high frequencies, their contribution can become dominant.

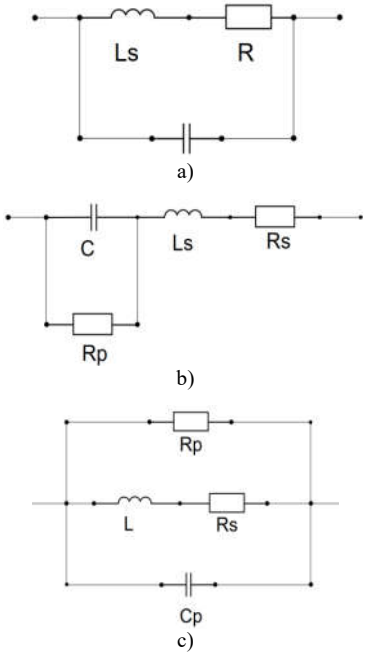

Fig.2. Model of the impedance: a) of the equivalent circuit resistor; b) capacitors of the equivalent circuit; c) for inductive load in the model of a living cell.

In Fig. 2,a shows a lumped impedance cell equivalent resistor model. Here R is the nominal resistance in Ohms, L_s - is the parasitic series inductance in Henry and C_p is the parasitic parallel capacitance in Farads; parasitic components appear due to the presence of the terminals of the resistor and the peculiarities of its design. At a frequency f in Hz, the impedance of the resistor is:

$$Z = U/I = \left[\left(R + j2\pi f L_s\right)^{-1} + j2\pi f C_p \right]^{-1}, \qquad (15)$$

In Fig. 3 shows a typical curve of the dependence of the impedance of resistors on frequency.

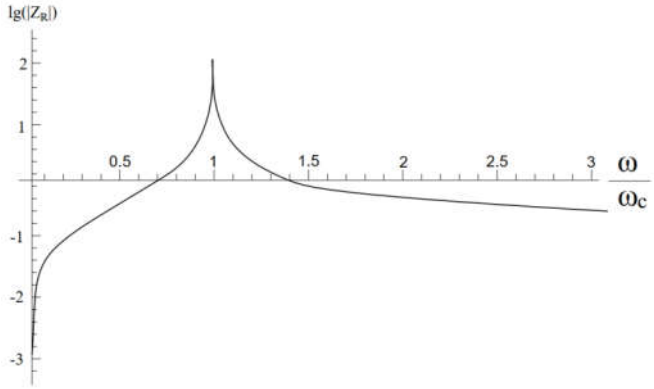

Fig.3. Typical curve of the dependence of the impedance of resistors on frequency in a living cell model.

The presented curves have two features: the impedance of high-resistance resistors does not depend on frequency at first, and then decreases, while the impedance of low-resistance resistors does not depend on frequency at first, then it rises sharply, forming a peak, and then falls.

By setting different values of R_s, L_s, C_p, you can find out that $R \approx 1.55 (L_s/C_p)^{1/2}$. By setting different values, you can find out which is the lowest resistance that does not result in an impedance curve peak. Therefore, let's say that the parameter is the critical resistance of the resistor. If the resistor`s resistance is $R \geq R_c$, the approximate expressions for the impedance will be:

$$|Z| \approx R \quad \text{at} \quad f \leq \left(2\pi R C_p\right)^{-1},$$

$$|Z| \approx \left(2\pi f C_p\right)^{-1} \text{ at } f > \left(2\pi R C_p\right)^{-1}. \qquad (16)$$

At $R \geq R_c$ L_s and C_p are resonatingat the frequency $f_c = 1/2\pi\left(L_s C_p\right)^{1/2}$. Then the impedance can be approximated by formulas:

$$|Z| \approx R \quad \text{at} \quad f < R/2\pi L_s,$$

$$|Z| \approx 2\pi f L_s \quad \text{at} \quad R/2\pi L_s \leq f \leq f_c/3, \qquad (17)$$

rising to

$$|Z| = \left[\left(L_s/RC_p\right)^2 + L_s/C_p\right]^{1/2} \quad \text{at} \quad f = f_c, \qquad (18)$$

and then dropping to:

$$|Z| \approx (2\pi f C_p)^{-1} \quad \text{at} \quad f > 3f_c. \tag{19}$$

As with resistors, parasitic components appear due to the presence of terminals on the capacitor and due to the peculiarities of its design.

In Fig. 2,b shows a lumped impedance model for capacitors in the equivalent circuit of a cell. As in the case of resistors, parasitic components appear due to the presence of terminals on the capacitor and due to the peculiarities of its design. At frequency *f*, the impedance of the capacitor is:

$$|Z| = U/I = \left(j2\pi fC + 1/R_p\right)^{-1} + j2\pi fL_s + R_s, \tag{20}$$

In Fig. 4 shows the curve of the dependence of the impedance of the capacitors on the frequency.

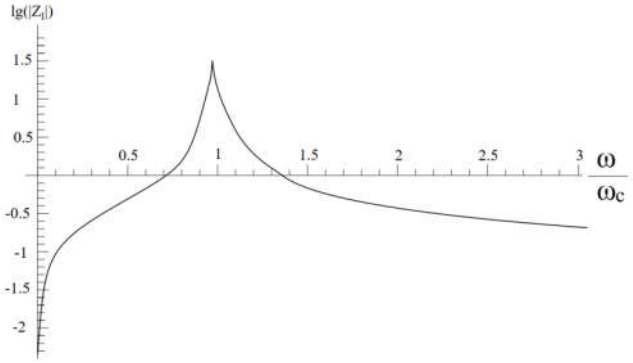

Fig.4. The curve of the dependence of the impedance of capacitors on frequency in the model of a living cell.

With large series resistances R_s plateau is observed on the impedance curve near the natural resonance frequency $f_c = 1/\left[2\pi(CL_s)^{1/2}\right]$, and with small series resistances R_s a sharp dip occurs at this frequency. By analyzing the capacitor impedance equations, it is easy to find that the fastest and smoothest transition from capacitive behavior ($f \le f_c$) to inductive behavior ($f \ge f_c$) occurs at $R_c \approx 1.41(L_s/C)^{1/2}$. Therefore, let`s say that the resistance R_c is the critical series resistance of the capacitor. If the series resistance of a capacitor $R_s \ge R_c$, its impedance can be approximated by the expressions:

$$|Z| \approx (2\pi fC)^{-1} \quad \text{at} \quad f < (2\pi R_s C)^{-1}$$

$$|Z| \approx R_s \quad \text{at} \quad (2\pi R_s C)^{-1} \le f \le (R_s/2\pi L_s)$$

$$|Z_L| \approx 2\pi fL_s \quad \text{at} \quad f > (R_s/2\pi L_s) \tag{21}$$

If $R_s \ge R_c$, then *C* and L_s resonates near the frequency f_c in this case, the expressions for the impedance will be as follows:

$$|Z| \approx (2\pi fC)^{-1} \quad \text{at} \quad f < f_c/3, \tag{22}$$

decreasing to

$$|Z| \approx R_c \quad \text{at} \quad f = f_c, \tag{23}$$

and then rising to

$$|Z| \approx 2\pi fL_s \quad \text{at} \quad f > 3f_c. \tag{24}$$

Typically, the resonant frequency is much higher than the operating frequency of the circuit. For capacitors with high capacitance, this is quite difficult to achieve. One simple solution to this problem is to connect small, high quality capacitors in parallel with large capacitors. This method also helps to compensate for the increase in series resistance as the oxide capacitor ages and thereby maintains the filtering efficiency of the circuit. In Fig. 2,c shows a lumped impedance model for inductors in the equivalent circuit of a cell.

Thus, at frequency *f*, the impedance of the inductor is:

$$|Z| = U/I = \left[\left(j2\pi fL + R_s\right)^{-1} + 1/R_p + j2\pi fC_p\right]^{-1}, \tag{25}$$

A typical curve of the dependence of the impedance of inductors on frequency is shown in Fig. 5.

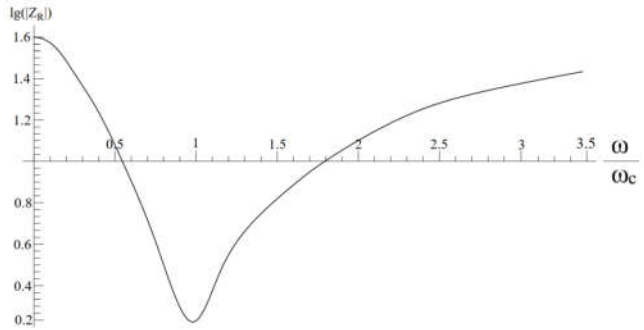

Fig.5. The curve of the dependence of the impedance of the inductors on the frequency in the model of a living.

Standard high-frequency inductors R_s have a range of 0.2 Ohm < R_s < 5 Ohm, and parasitic capacitance is in the range of 1.5 *pF* < C_p < 4*pF* [10].

Let us consider the equivalent circuit of a cell under the action of a pulsed broadband signal (see Fig. 6).

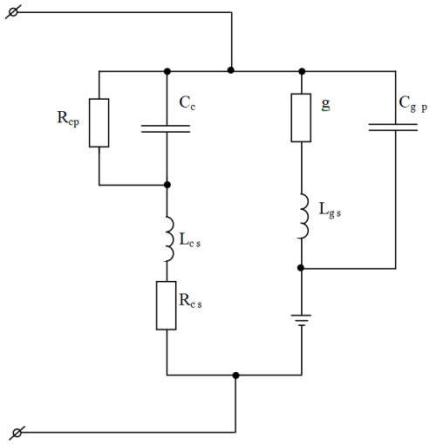

Fig.6. Equivalent circuit of a cell under the action of a pulsed broadband signal.

From the analysis of the circuit it follows:

$$\omega_1 \approx \frac{1}{\sqrt{L_{cs}C_c}}, \quad \omega_2 \approx \frac{1}{\sqrt{L_{eff}C_{eff}}}, \quad \omega_3 \approx \frac{1}{\sqrt{L_{gs}C_{gp}}}. \quad (26)$$

where $L_{eff} = f_L(L_{cs}, L_{gs})$; $C_{eff} = f_C(C_{gp}, C_c)$, then $\omega = n\omega_1 + k\omega_2 + m\omega_3$.

To analyze the circuit`s operation we calculate its total impedance depending on the frequency:

$$Z_{total} = Z_{totre} + jZ_{totim}, \quad (27)$$

here Z_{totre} is the real part of the impedance, and Z_{totim} is the imaginary part.

A typical dependence of the impedance modulus on frequency, calculated according to (27), is shown in Fig. 7.

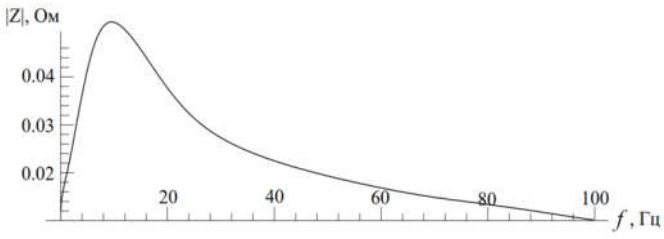

Fig.7. Dependence of the impedance modulus on frequency.

In accordance with the scheme, a pulsed broadband signal will necessarily find one of the natural frequencies of the cell, which will be in resonance with a frequency from a wide spectrum of the influencing signal. For this to happen, the duration of the external impulse of action on the cell must satisfy the following relation:

$$\omega_3 < \frac{2\pi}{\tau_p} < \omega_1, \quad (29)$$

If the pulse duration τ_p is much longer than the specified value, then such a pulse affects the cell in the same way as a quasi-constant electric field. Such impulses can be called long in relation to the impact on a given cell.

Our optimization calculations lead to several sets of parameters for - the Rose models [10,11]. For example, here are two typical sets:

- $a = 1.5$, $b = 3.5$, $c = 1.01$, $\varphi_0 = -1.6$, $s = 4.966$, $r = 3.5$;
- $a = 1.0$, $b = 3.0$, $c = 1.0$, $\varphi_0 = -1.6$, $s = 3.96$, $r = 3.0$.

These parameters most closely correspond to experimental studies, which show that seeds of corn, wheat and other agricultural plants have resonant frequencies in the range of 50-60 GHz. The agreement with experiment is clearly seen from the analysis of potential oscillations spectrum. The spectrum for oscillations with the first set of parameters is shown in Fig. 8,a and with the second in Fig. 8,b.

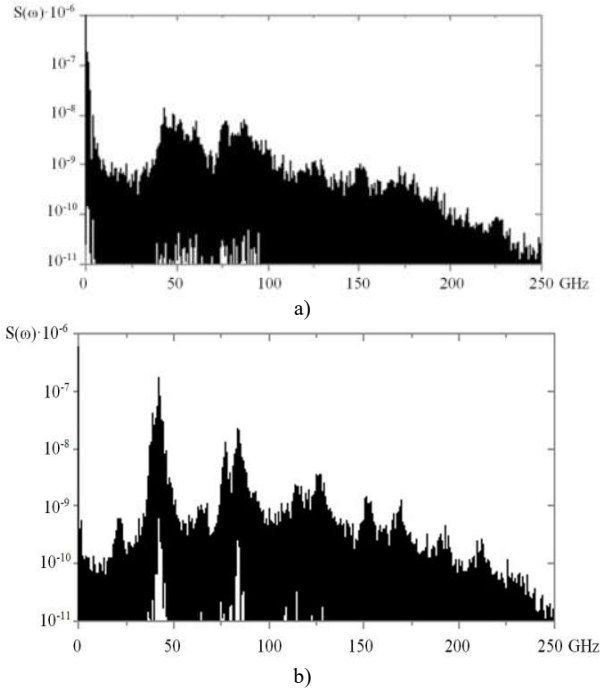

Fig.8. Spectrum of vibrations a) with the first set of parameters; b) with the second set of parameters.

Note that the experiments carried out on animal cells showed similar results [4]. The sequence of radio pulses used has a spectrum that covers the range of resonant frequencies of cells, therefore, the effect of these pulses on the cellular structures of plants and animals is highly effective. The above model of a cell in the form of a nonlinear oscillatory system was written on the basis of a radiophysical oscillatory circuit, which is shown in Fig. 9.

When a voltage pulse is applied to a cell, a charge builds up in the membrane and the potential applied to the membrane increases. The characteristic relaxation time of the charge of a spherical cell membrane can be written as:

$$\tau_c = \left(\frac{1}{2}\frac{1+2v}{1-v}\rho_1 + \rho_2\right)Ca, \quad (30)$$

where v is the volumetric concentration of cells, ρ_1 – is the resistance of the medium, ρ_1 – is the resistance of the cytoplasm, C – is the membrane capacity per unit area, and 2a is the cell diameter.

For typical cells with a diameter of 10 μm, and a relatively low volume concentration (typical for experiments on cells), the characteristic membrane charging time is 75 ns. The amplitude of the field required to charge the membrane to a critical potential leading to the destruction of the membrane:

$$E_{cr} = V_{cr} \Big/ \left(f\left(1 - \exp\left(-\tau/\tau_c\right)\right)\right), \quad (31)$$

where τ is the pulse duration, f is a factor determined by the shape of the cell, and V energy required for membrane breakdown:

$$W = E_{cr}\frac{2\tau}{\rho_1} = K\tau \Big/ \left(1-\exp\left(-\tau/\tau_c\right)\right), \qquad (32)$$

where K – is constant, W – is minimum for a pulse duration τ in 1.25 times longer than the characteristic membrane charging time τ_c.

The results of the electric pulse action on cells are shown in Fig. 9. The bright parts of the photos show the intensity of the impulse exposure as a result of the development of individual cells fluorescence. The effect of cell destruction by short pulses of an electric field is effective in cleaning liquid media from pathogenic microbes. The proposed method of liquid sterilization can be used in medicine and in various sectors of the national economy.

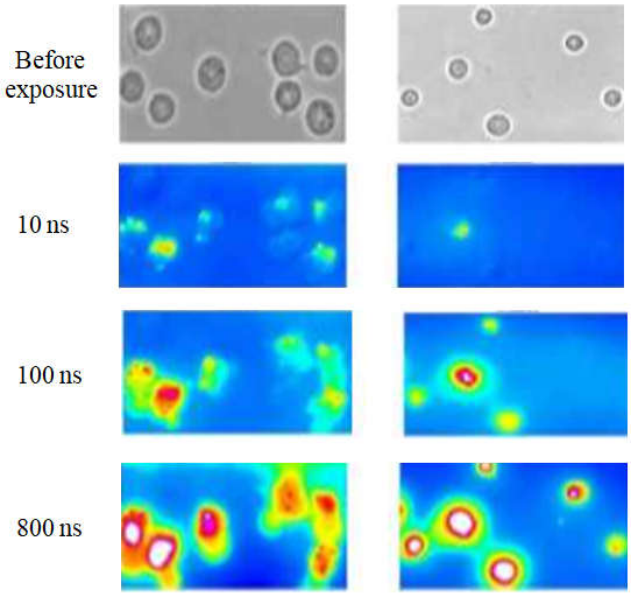

Fig.9. Photos of cells before exposure (top photo) and photos of cells exposed to pulses with an amplitude of 60 kV / cm and a duration of 10 ns, 100 ns, 800 ns.

Determination of processing modes and their specificity requires the continuation of theoretical and experimental studies. For the development of the proposed technologies, it is necessary to create generators of short electric pulses in a wide range of parameters.

V. Conclusion

The result of the research is the modification of a number of basic radio physical models of cell functioning under conditions of specific external electromagnetic influences, which will help in the development of an electrophysical installation. It can be said that under the influence of a short pulse in standard radio physical models, all passive elements must be replaced by circuits, and naturally there is the possibility of the emergence of several resonant frequencies with broadband interaction, as well as nonlinear mutual resonances. The frequency curves are considered regardless of the parameters of the inductors in the range from 0.2 to 0.5 Ohm, taking into account parasitic components. Spurious bandwidths and delays were taken into account, as well as spurious frequency components up to the fourth harmonic. It is shown the interaction of an electrical impulse with a cell, and the consequences of this process. From what we saw the efficiency of electromagnetic processing and found further ways of research.

Also, as a result of the results obtained, it can be seen that one of the methods for controlling the properties of the cell, as well as the method of destruction (or treatment) can be the use of external EM pulsed exposure to force the transport of substances through the cell membrane directed along the gradient of potentials and concentrations. Thus, it has been proven that the transport of substances across the cell membrane is a controlled probabilistic process of continuous movement of molecules and ions through the cell in two directions - from the environment surrounding the membrane and to the environment of the membrane. These phenomena may be associated with analytical dependence.

References

[1] B. Drukarch, H. Holland, M. Velichkov, and J. Geurts, "Thinking about the nerve impulse: A critical analysis of the electricitycentered conception of nerve excitability," *Progress in Neurobiology*, vol. 3, no. 169, pp. 172–185, 2018.

[2] A. Varekhov, "Potentiometric measurements of the transmembrane potential of cells using penetratingions," *Scientific Instrumentation*, vol. 25, no. 1, pp. 27–35, 2018.

[3] C. E. Morris and P. F. Juranka, "Nav channel mechanosensitivity: activation and inactivation accelerate reversibly with stretch," *Biophysical Journal*, vol. 93, no. 3, pp. 23–24, 2017.

[4] L. A. Katicheva, L. M. Surova, O. N. Sherstneva, A. V. Bushueva, E. V. Glinskaya, and V. A. Vodeneev, "Changes in the electrical resistance of the plasmalemma of higher plant cells during the generation of variable potential," *Bulletin of the Nizhny Novgorod University*, vol. 1, no. 3, pp. 150–154, 2018.

[5] M. Kundenko, V. Mardziavko, and A. Rudenko, "Stability of Self-Consistent States of Flow in a Short-Circuited Diode in a Mode with a Through Passage of Particles," in *IEEE International Conference on Information and Telecommunication Technologies and Radio Electronics 2021, UkrMiCo*, Kyiv, Ukraine, Dec. 23, 2021. 2021, pp. 275–278.

[6] O. D. Lipko, "Mathematical model of propagation of nerve impulses with regard hereditarity", *Vestnik KRAUNC*. Fiz.-Mat. Nauki,vol. 17, no. 1, pp. 33–43, 2017.

[7] G. V. Muratova and M. A. Belous, "Modeling of brain activity based on the Hodgkin-Huxley model," *Engineering Bulletin of Don*, vol. 43, no. 4, pp. 107–123, 2016.

[8] A. Denisov, P. Bulay, P. Taras, and S. Cherenkevich, "Cognitive processes and biological neural networks," *Science and innovation*, vol. 154, no. 12, pp. 29–35, 2015.

[9] N. OmaNfor and M. Mokoli, "Dynamics of Nerve Pulse Propagation in a Weakly Dissipative Myelinated Axon," Journal of Modern Physics, vol. 7, no. 10, pp. 1166–1180, 2016.

[10] A. Rosas and K. Lindenberg, "Pulse propagation in granular chains: The binary collision approximation," *International Journal of Modern Physics*, vol. 31, no. 10, pp. 142–156, 2017.

[11] H. E. Rajapakse and L. W. Miller, "Time-Resolved Luminescence Resonance Energy Transfer Imaging of Protein–Protein Interactions in Living Cells," Methods in Enzymology, vol. 505, pp. 329–345, 2012.

Metrology in healthcare equipment – the portuguese reality

Flávio Vitória
Coimbra Polythecnic – ISEC
Rua Pedro Nunes, Quinta da Nora,
3000-199 Coimbra, Portugal
a2019114252@isec.pt

Fernanda Coutinho
Coimbra Polythecnic – ISEC
Rua Pedro Nunes, Quinta da Nora
3000-199 Coimbra, Portugal
ISR – University of Coimbra
Rua Silvio Lima- Polo II
3030-290 Coimbra, Portugal
fermaco@{isec,isr.uc}.pt
ORCID 0000-0002-9693-2966

Jorge Santos
Serviço de Utilização Comum dos Hospitais - SUCH
Parque da saúde de Lisboa, Avenida do Brasil,1749-003 Lisboa, Portugal
jorgesantos@such.pt

Abstract — Metrology is unquestionably an important scientific area, with very direct relevance for consumer rights, by virtue of being essential for ensuring the safety and quality of products and services. The main purpose of this paper is to provide an overview and assessment of the metrological reality in Portugal. For this purpose, several aspects of applied metrology are addressed. We present a brief overview of the legal framework and description of the entities responsible for developing, supervising, and coordinating metrological activities, as well as the accreditation of specific conformity assessment activities. A brief description and characterization of the primary and secondary laboratory network will also be provided, including an analysis of the spectrum of accredited metrological control capabilities. Furthermore, we will focus our discussion on the reality of metrology for healthcare equipment, which is of note because its regulatory demands may be considered comparatively light in face of the high level of criticality of healthcare activities.

Keywords — healthcare, applied metrology, Portugal.

I. INTRODUCTION

The human being has felt the need to measure and quantify phenomena since the beginning of civilization. This necessity remains nowadays, and several decisions are made, on a daily basis, based on information from measurement processes. This situation applies to various areas of our society, such as healthcare, construction and industry. However, the quality of these decisions is closely related to the quality of the deciding information, which can be a determining factor to distinguish a good decision from a bad decision. [1]

From a technical and scientific perspective, measurement procedures are based on a series of rules that must be strictly followed, so that the value of the measurand quantity can be obtained correctly, to achieve a result as accurate as possible. To the science dedicated to the study of these rules is given the name of metrology. [2, 3]

As a consequence of the increasing technological development, new measurement instruments have been introduced in healthcare, enabling the optimization of clinical activities and providing essential data for the effective and efficient prevention, diagnosis, treatment and monitoring of pathologies. [1, 3]

This information is critical for the well-being and safety of patients, and also for the effectiveness of the services carried out by healthcare providers. However, measured values may present some variability and errors caused by factors such as the conditions of use of the device, the age of the device, among others. Disregard for these measurement errors can thus lead to errors with potentially critical and life-threatening consequences, because it can lead to misdiagnosis and incorrect treatment of patients. Therefore, the existence of procedures that ensure the correct functioning of measuring devices used in healthcare has become extremely important. These procedures aim to ensure the credibility and accuracy of the results.

There is a growing concern about the impact of errors caused by incorrect measurements in healthcare activities. This concern is starting to increase awareness of the importance of metrology for healthcare services. This prompts the need for an appropriate legal and regulatory framework to be created to ensure proper metrological traceability for measuring equipment [1].

The purpose of this document is to give the testimony of the current situation of metrology in Portugal, with emphasis on the healthcare sector.

Section II briefly discusses the relevance of metrology for healthcare equipment. Section III outlines the metrological organization structure in Portugal, also assessing the installed metrological service capacity from the perspective of the specific needs of different types of healthcare equipment. Section IV discusses the state of healthcare metrology practice in Portugal, including a characterization of awareness and demand for metrological services, analysis of available metrological capacity for different types of healthcare equipment, and also of obstacles to overcome for achieving a more widespread practice of metrological control. We conclude in Section V.

II. FOR HEALTHCARE EQUIPMENT

In healthcare contexts, poor quality measurements can have very detrimental and undesirable consequences, such as:

- Syringe pumps administering wrong dosages of drugs in medical treatments;
- Defibrillators applying incorrect levels of energy, unnecessarily injuring the patient by applying excessive energy, or failing to function as intended by providing insufficient power;
- Diagnosis errors, based on poor quality measurements of parameters such as in blood pressure;
- Subjecting patients to improper levels of radiation;
- Improper storage conditions of drugs and medical samples (blood, tissues, etc);

Some of these effects might be furthermore amplified in neo-natal and paediatric healthcare, due to the smaller

admissible margins of error for diagnosis and treatment for these type of patients.

It is apparent then, that metrology is instrumental to ensure high quality healthcare, patient safety and avoid medical errors.

Metrological control can also ultimately reduce the costs associated to healthcare. By improving diagnosis and treatment quality, unnecessary treatments can be avoided and accurate diagnosis can be made, ensuring the timely identification of medical conditions that might deteriorate and consume additional healthcare resources in the future.

In addition to minimizing clinical risks and exposure to legal liability, proper metrological control can provide opportunities for improving equipment management. The level of metrological drift between consecutive calibrations may be indicative of functional deterioration, which can inform the adaptation of maintenance strategies, or even suggest the controlled replacement of aging equipment. Another important aspect is that even in the undesirable scenario of metrological verification failure, which is of course to be avoided due to the criticality of healthcare services, traceability information may allow the re-evaluation of decisions made using the poor quality measurements, allowing for mitigation of potentially negative consequences.

The COVID-19 global epidemic has further confirmed and amplified the need of strong metrological control, not only due to the increased reliance and demand for life support equipment, but also because it is necessary to meet stringent and demanding cold chain temperature requirements for ensuring effective and efficient vaccine distribution. In fact, the World Health Organization reports in a 2005 study [4], that two of the main factors contributing to the waste of approximately 50% of all produced vaccines in 2005 were exposure of closed vials to excessively high or low temperatures, caused by failure in the cold chain temperature control.

These issues are still largely relevant today, or even more, as the wastage of vaccines hampers the ongoing COVID-19 vaccination efforts. News report that the French Directorate General of Health has stated that it is operating with the cautious estimate of a 30% wastage rate [5], while in Germany some inoculations were refrained after uncertainty arose about whether the cold chain had been maintained [6]. Similar issues were also reported in other countries, including Portugal.

III. Organization and Structure of National Metrology Institutions

The main objective of every measurement system is to obtain comparable, credible and exact results. An hierarchic structure, represented in *Figure 1*, is used to create a chain of standards that will ultimately connect calibration standards used in accredited laboratories to the SI standards managed by the *International Bureau of Weights and Measures* (BIPM) [7].

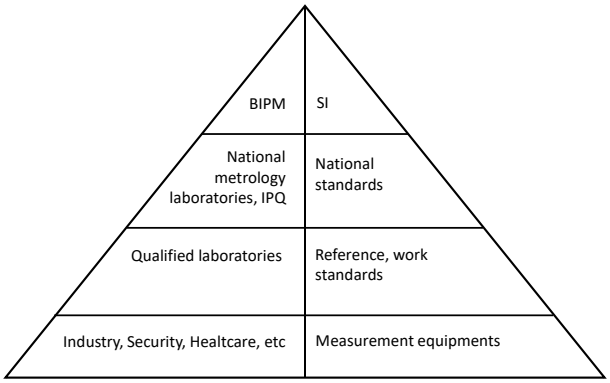

Figure 1-Hierarchic structure of metrological institutions.

In Portugal, the National institution for the regulation of metrological activity is *Instituto Português da Qualidade* (IPQ), the Portuguese Institute of Quality. This institution is classified as a National Metrology Institute (NMI), which puts it in the second layer of the previously shown pyramid, and is also part of the national standardization body, being responsible for the coordination of the quality system in the country [8].

The *Laboratorio Nacional de Metrologia* (LNM), the National Laboratory of Metrology, is an IPQ unit that is responsible for metrology. It has responsibilities in legal, applied and scientific metrology, including realizing the national standards of measurement units, participating in international metrological organizations and projects, managing traceability of national laboratories, providing formation, and regulating metrological activities [9]. The LNM maintains standards for all relevant parameters, except for ionizing radiation, sea water (silicia) and sediments (mercury), which are ensured by two designated laboratories.

The accreditation of metrology laboratories is subject to European legislation (ISO/IEC 17025:2017), to harmonise its operation across member countries [10, 11]. The responsibility of the *Instituto Português de Acreditação* (IPAC), the Portuguese Institute for Accreditation. IPAC is the national accreditation body, being a member of international institutions, such as the European cooperation for Accreditation (EA) and the International Laboratory Accreditation Cooperation (ILAC). To ensure impartiality, IPAC relies external evaluators and experts. These external collaborators are the ones who qualify and monitor entities for metrological procedures [9, 12].

Proceeding down the layers presented in the pyramid of Fig. 1 we will find the primary and secondary laboratories. Primary laboratories are the ones whose standards are calibrated directly from the standards of the NMIs, originating less accurate standards, but still with a very good quality. An example of a primary laboratory in Portugal is the *Instituto de Soldadura e Qualidade* (ISQ), the Welding and Quality Institute, which is the laboratory with the most encompassing offer of metrology services of the country.

Secondary laboratory standards are calibrated using the primary laboratories' standards, which leads to a further loss of accuracy with respect to the national standard. Secondary metrology laboratories provide services such as quality control for industry.

IV. METROLOGY FOR HEALTHCARE EQUIPMENT IN PORTUGAL

A. *Awareness and Demand for Metrology Services in Healthcare*

Medical devices are not subjected to legal metrology requirements, except for weighting and radiation devices. Nevertheless, there are some healthcare institutions that recognize the importance of metrological control and perform regular calibration.

There is one single hospital in Portugal that has an in-house accredited metrology laboratory for calibration of some of its medical devices. This institution is the *Centro Hospitalar Universitário de São João*, in Oporto, which is one of the largest hospitals in Portugal, with approximately 736 000 medical consultations and 47 000 programmed surgeries in 2020 [13]. This laboratory has been accredited in 2018 for the following parameters:

- Mass;
- Pressure, concerning blood pressure monitors;
- Volume, concerning micropipettes;
- Velocity and acceleration, concerning the rotation of centrifuges [14].

A few other major hospitals (e.g. *Hospital de Santa Maria* and *Hospital de Santo António*, in Lisbon) also perform metrological control, relying on external providers rather than an in-house laboratory for metrological services.

However, most healthcare entities (there are 238 public and private hospitals) are satisfied with conducting only preventive and corrective maintenance activities on medical equipment, neglecting to perform the necessary calibration, with the exception of laboratorial equipment. This is concerning, since maintained (and even new) equipment is not necessarily calibrated to a satisfactory degree.

B. *Installed Capacity of Metrological Services for Healthcare*

There is a reasonable number of metrology laboratories in Poortugal. However, from the eight entities accredited for metrological control of healthcare equipment, only one (the ISQ laboratory) covers metrology procedures for life support equipment. This is one of the main metrological laboratories in Portugal and provides calibration services for the following parameters of life support equipment:

- Ventilators / nebulizers / flow meters / secretion aspirators – volume, flow, oxygen, pressure and inspiration time;
- Defibrillators – energy, synchronism, charging time, leakage current, power and return electrode monitoring;
- Electrocardiographs – amplitude, beats per minute and frequency;
- Vital signs monitors / blood pressure monitors / oximeters – pressure, cardiac rhythm, oximetry and cardiac rhythm through oximetry;
- Infusion systems – flow, pressure and volume. [15]

A more detailed analysis of the number of metrological verification organisms accredited to calibrate different types of medical equipment, reveals the scenario in *Figure 2*.

It is possible to highlight that some types of equipment have very few accredited laboratories for calibrations. For some types of equipment there is only one option. This is due to poor demand for these services, but may be a cause of concern, because competition is an important factor that drives companies to improve their services, offering more and better options to the customers. It can also have negative consequences in the future, if the metrological awareness increases and the regulatory framework imposes stricter metrological control guidelines, the demand for control services will increase beyond what the installed capacity may offer.

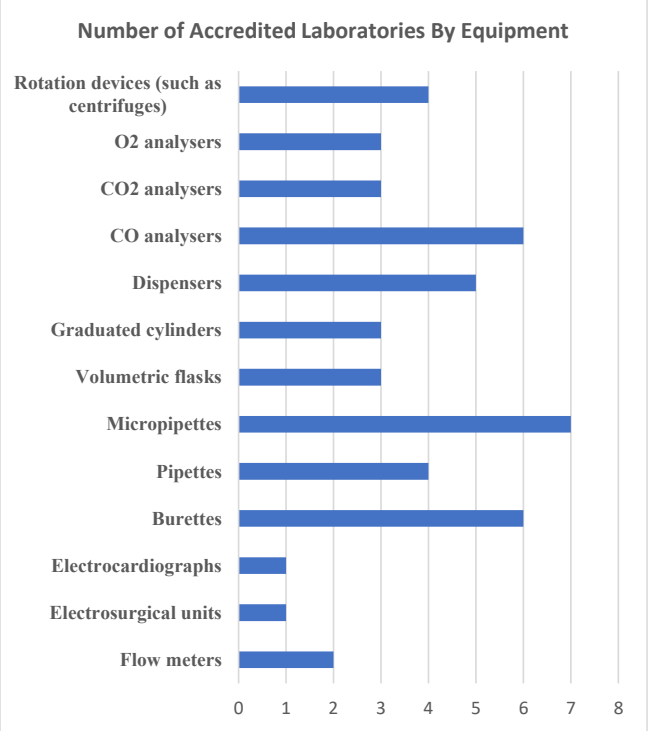

Figure 2 – Installed Metrological Service Capacity for Different Types of Healthcare Equipment

C. *Obstacles to the Increased Adoption of Metrological Control*

Because most medical equipment is not subjected to legal metrological requirements, the adoption of proper calibration procedures is currently dependent on the decisions of healthcare institution managers. Although there is currently an increasing awareness of the issue and the value of metrological control, as demonstrated by some of the larger hospitals taking significant measures to implement such policies, by and large a practice that is not yet adopted by most healthcare institutions.

Current efforts and funding in the healthcare sector are mainly concentrated on addressing and managing the COVID-19 epidemic. This diverts attention from other issues, including considering the organizational and processual changes and benefits involved with setting in place the required calibration efforts.

Furthermore, it can be said that further sensibilization may be required to debunk some common misconceptions, such as:

- *Calibration is too expensive, or reduces availability of equipment, or offers little benefits* – The converse is true. Lack of calibration leads to poor quality

service and increased costs for the consumer and healthcare services, as outlined in Section II. Calibration data can also potentially provide relevant data for predictive maintenance approaches, thereby lowering overall maintenance costs. It also provides relevant information concerning management and replacement of aging equipment. For example, a significant drift in results between consecutive calibrations might indicate that the quality of operation is quickly deteriorating and that further maintenance or even equipment substitution may be in order.

- *Calibration is not required if proper maintenance is performed* – Maintenance alone typically does not involve metrological control.
- *Acquiring new equipment can be a cheaper alternative to calibrating old equipment* – New equipment is seldom calibrated, and if calibrated, it is typically by non-accredited laboratories of the manufacturer. Therefore, new equipment should also be calibrated by accredited laboratories to ensure measurement traceability.

In order to reverse this situation, informational strategies might be implemented, such as increasing the number of workshops, seminars and formations in the area, promoting awareness of the importance of metrological control. These actions should specifically target important healthcare stakeholders and decisors. A promising strategy may be resorting to demonstrations of the benefits gained by the few leading institutions that have already decided to implement metrological control processes.

Notwithstanding all the above considerations, the lack of a legal framework regulating calibration of medical devices is the major hurdle preventing a more widespread adoption of metrological control. Without such regulations, calibration efforts will always be contingent on the voluntary adoption and support by healthcare institutions management. However, this support is not only challenging to obtain due to the common misconceptions outlined above, but it is also volatile by virtue of being vulnerable to changes of strategic orientations, substitution of decision-makers, budgeting considerations and conjunctural concerns.

V. Conclusion

Metrological control is very important for improving the quality of healthcare services. It ensures the reliability of data used to perform the diagnosis and treatment of patients, and also provides the opportunity to improve the management of installed equipment, informing potential adjustments of maintenance strategies or equipment replacement.

Portugal has a reasonably developed hierarchy of metrological laboratories, however, there is a currently not enough diversity of offer concerning the metrological services required for some types of medical equipments. Further competition could prove beneficial for the entire sector.

Currently a few large healthcare institutions have taken the lead and voluntarily established systematic calibration procedures, however this is not yet the case for most institutions. Low awareness, common misconceptions, and focus on the current pandemic are currently obstacles for a wider dissemination of the practice.

Improving this awareness with important stakeholders and decisors is therefore necessary, and the leading institutions might function as inspiring role models for others to follow. Nevertheless, the adoption of metrological control would benefit greatly from increased regulatory and legal requirements, developed both at national and transnational level.

References

[1] Sectoral Comission on Health (CS/09), Metrology in Health – Good Practices Guide - 1st. Ed. (ISBN 978-972-763-160-5), 1ª ed., Caparica: Portuguese Institute for Quality, 2018, p. 31.

[2] Joint Committee for Guides in Metrology, International vocabulary of metrology – Basic and general concepts and associated terms (VIM) - 3rd Edition, BIPM, 2012.

[3] M. C. Ferreira, "A importância da metrologia na saúde," *Gazeta de física,* vol. 36, no. 1, p. 32, May 2013.

[4] World Health Organization, "Monitoring vaccine wastage at country level," 2005. [Online]. Available: https://apps.who.int/iris/bitstream/handle/10665/68463/WHO_VB_03.18.Rev.1_eng.pdf. [Accessed 20 May 2021].

[5] T. Vey, "Covid : la France anticipe-t-elle réellement 25 à 30% de pertes sur ses vaccins ?," Le Figaro, 06 01 2021. [Online]. Available: https://www.lefigaro.fr/sciences/covid-la-france-anticipe-t-elle-reellement-25-a-30-de-pertes-sur-ses-vaccins-20210106. [Accessed 30 05 2021].

[6] M. Tantussi, "Cold chain doubts delay COVID-19 vaccinations in some German cities," Reuters, 26 12 2020. [Online]. Available: https://www.reuters.com/business/healthcare-pharmaceuticals/cold-chain-doubts-delay-covid-19-vaccinations-some-german-cities-2020-12-27/. [Accessed 30 5 2021].

[7] C. H. Page e P. e. Vigoureux, The International Bureau of Weights and Measures 1875–1975: NBS Special Publication 420, Washington, D.C.: National Bureau of Standards, 1975.

[8] IPQ, "Instituto Português da Qualidade," a. [Online]. Available: http://www1.ipq.pt/PT/Pages/Homepage.aspx. [Accessed 16 May 2021].

[9] IPQ, "Principais atribuições do departamento de metrologia," b. [Online]. Available: http://www1.ipq.pt/pt/metrologia/apresentacao/atribuicoes/Paginas/Atribuicoes.aspx. [Accessed 16 May 2021].

[10] IPAC, "A acreditação," [Online]. Available: http://www.ipac.pt/ipac/funcao.asp. [Accessed 18 May 2021].

[11] ISO/IEC, "17025:2017 - General requirements for the competence of testing and calibration laboratories," ISO/IEC, 2017.

[12] IPAC, "Apresentação do IPAC," [Online]. Available: http://www.ipac.pt/ipac/contactos.asp. [Accessed 18 May 2021].

[13] Centro Hospitalar Universitário de São João, E.P.E., "Relatório & Contas 2020," 03 May 2021. [Online]. Available: https://portal-chsj.min-saude.pt/uploads/document/file/928/R_C_2020.pdf. [Accessed 27 May 2021].

[14] IPAC, b. [Online]. Available: http://www.ipac.pt/pesquisa/ficha_lac.asp?id=M0114. [Accessed 27 May 2021].

[15] IPAC, a. [Online]. Available: http://www.ipac.pt/pesquisa/ficha_lae.asp?id=L0610. [Accessed 27 May 2021].

SECTION VIII
METROLOGY PRACTICE

Factors Affecting Contrast in Laser Marking of Non-Metal Materials

Simeon Tsenkulovski
dep. "Mechanical Engineering and Instrumentation"
Technical university-Gabrovo
Gabrovo, Bulgaria
s.tsenkulovski@advanced-technology.eu

Ivan Mitev
dep. " Economics"
Technical university-Gabrovo
Gabrovo, Bulgaria
imitev@tugab.bg

Georgi Karlovski
dep. "Mechanical Engineering and Instrumentation"
Technical university-Gabrovo
Gabrovo, Bulgaria
g_karlovski@abv.bg

Abstract— In the present study, the factors that influence the contrast in laser marking of non-metallic materials are considered. Four main groups of factors related to the type of processed material, the type of laser used, the technological characteristics of the process, as well as factors related to the complex action in marking the studied materials are considered.

Keywords—laser marking, non-metallic materials, image contrast.

I. INTRODUCTION

Laser marking is a non-contact effect in the structure of the processed material, resulting in a lasting contrast image. On the surface of the product with this method can be applied information in the form of: inscriptions, identification symbols (letters and numbers), bar codes, matrix codes (2D), special characters, serial numbers, images, decoration and so called [10]. In practice, with the help of a laser, it is very easy to create a random image of your own design.

Lasers are used to engrave and mark a wide range of organic and inorganic materials [2,3,4,9]. The laser marking has good contrast, is durable and indelible, and cannot be altered or destroyed. The laser marking system can be easily integrated into production lines and stand-only stands [8].

Today, all organic and inorganic polymers can be marked, in one way or another, by laser radiation. When the laser beam is focused on the material being processed for marking, its energy is absorbed by the surface layer and heated. As a result of a reaction caused by heat and depending on the type of material, different results can be obtained [1,6,7]:

- color change by carbonization or bleaching;
- evaporation of the surface layer of material with a thickness of parts of microns to hundreds of microns;
- changing the structure by melting the surface.

Controllable laser parameters, such as the amount of energy applied to the part, change the surface according to a given model, which affects its appearance without undesirable damage to the material. In recent years, laser technology has become increasingly popular and is used as a substitute for traditional finishing processes in industry [5,7].

In the present study the aim is to trace the influence of the factors related to the technological process of laser marking on the contrast of the marking of non-metallic materials used mainly in the production of medical products.

II. EXPERIMENTAL PART

The quality of the laser marking is determined to the greatest extent by the contrast - k *, which characterizes the brightness range of the image and is expressed by the ratio between its maximum and minimum brightness. The contrast is determined by the difference between the background brightness - L_f, and the image brightness - L_x, divided by the background brightness in percentages (1).

$$k^* = [(Lf - Lx) / Lf]. 100 \quad (1)$$

The visual perception of the marking is determined by the objective nature of color perception. Determining the color organoleptically, i.e. with the eyes, is not unambiguous. This is due to the fact that the color vision of human beings is subjective and depends on various factors:

- eye fatigue - when the eyes are concentrated for a long time on one or a combination of colored objects;
- is the emotional state of the observer - the emotional state or past experiences involving colors can cause the observer to perceive colors differently ;
- t type of lighting - Different light sources affect the colors perceived by people - Poor lighting in low light energy prevents the correct perception of the actual colors of the material, direct sunlight gives a slight yellow tint to all colors, indirect sunlight can give a slight blue tint);
- the intensity of the lighting;
- the age of the observer - with age the visual acuity decreases;
- biological defects of color perception - color blindness and spectral composition of light.

The marking has a certain threshold (limit) contrast k^*_{pr}, above which it can be read. Threshold contrast characterizes the ability of the eye to distinguish brightness differences and depends on a number of factors whose dependence is represented by (2) .

$$k^*_{pr} = (f_{(p)} / L_f). (A / \alpha + B)^2 \quad (2)$$

where: L_f - background brightness, *nt* ;

978-1-6654-8569-2/22/$31.00 ©2022 IEEE

$f_{(p)}$ - probability function to distinguish;
p - probability of differentiation;
α - angular size of the object in angular minutes;
A and B - constants depending on brightness in the background.

The threshold contrast is different when the marking is perceived visually through the eyes and automatically through electronic devices. According to various studies, a good marking for perception by the human eye is when there is a threshold contrast $k *_{pr} = 50\%$. Scientific instruments, such as spectrophotometers, are designed to measure color based on the fact that each color has a specific wavelength. Minimum 20% threshold contrast to the background is sufficient for reading by electronic readers of 2D code marking and bar codes [10]. Automated reading of markings with e-readers has a number of advantages over the visual, such as greater accuracy, the ability to create a database, fast analysis of information and avoid all the shortcomings of the subjective factor. For this reason, the requirements for contrast of the marking, compared to the visual perception, are lower.

The main factors influencing the quality of laser marking of non-metallic materials can be summarized in four directions: material properties, type of laser source, process parameters and complex factors

In turn, the factors that are determined by the type of processed material are grouped into optical and thermophysical.

For the process of laser marking of non- metals materials of special their optical characteristics and coefficients are important and their interrelation: reflectivity - R; absorption capacity - A; transmission capacity - D; reflection coefficient - ρ; absorption coefficient - α and transmission coefficient - β ;

The laser effect on the substance in incident radiation is different for different non- metallic materials and is related to the reflection and absorption of radiation. When a parallel beam of rays falls on a smooth non- metallic surface, it is reflected, and the rays are also parallel to each other. If the surface is rough, the incident parallel beam of rays is reflected in different directions and is diffuse reflection. Reflective ability is a dimensionless quantity, can have a value between 0 ÷ 1 and is a function of the wavelength of laser radiation R = f (λ) - fig.1.

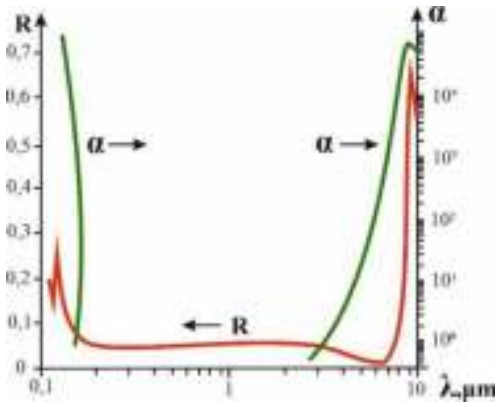

Fig. 1. Dependence of the reflectivity - R and the absorption coefficient - α, on the wavelength λ when marking samples of SiO_2

Therefore, roughness of the wavelength order significantly increases the penetration depth of the laser radiation.

The reflection coefficient of radiation - ρ , is another optical characteristic of the marked material. It is the ratio of the intensity of the reflected - Ir , and the incident radiation - Io .

For the absorption capacity, analogous physical laws of the incident laser radiation from the wavelength λ are in force. The higher the absorbency of the material, the lower the power of the incident laser radiation is required to carry out the laser marking process . Polymers are a good absorber of laser light - fig. 2.

Polymers absorb light very differently from metals . From the near ultraviolet zone to the near infrared zone - visible light, absorption is very low - uncolored polymers are transparent. Therefore, it can be concluded that YAG lasers with a wavelength close to the infrared zone are not suitable for processing polymers. However, carbon CO_2 and excimer lasers absorb light well and are applicable to organic materials. The most commonly used for polymer processing is the CO_2 system, while the Excimer laser can be used and has satisfactory results only if it has high pulsed energy and a very small focal spot.

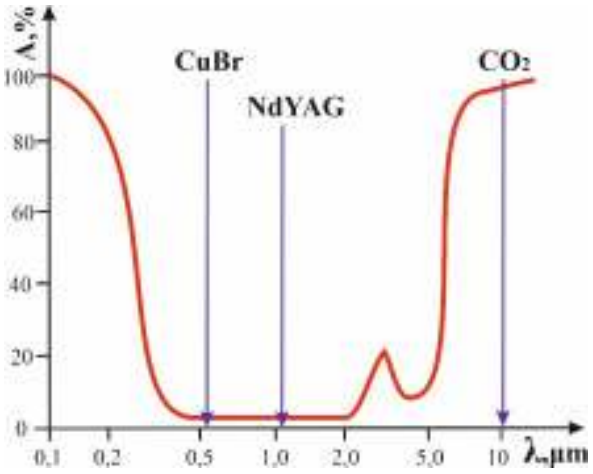

Fig. 2. The absorbency of polymeric materials as a function of wavelength A = A (λ) in some types of lasers

The coefficient of absorption of radiation - α, is an important optical characteristic that affects the contrast of the marking. It is a function of wavelength and temperature (3).

$$\alpha = (4\pi . k^{/} . n) / \lambda \qquad (3)$$

where: λ- wavelength;
n - refractive index;
$k^{/}$ - extinction of the substance .

The ratio of the intensities of the transmitted light - I, and the initially transmitted light - Io is called the transmittance coefficient - β, and is given as a percentage.

Depth of penetration - $\delta = \alpha^{-1}$, is the distance that light travels in matter at decreasing intensity. It should be borne in mind that the avian penetration depth in polymers , in contrast

to metals , is dominated by thermal, even with prolonged exposure to light flux.

In the process of laser marking of non-metallic materials heat is transferred to the treated area and therefore it is important to consider the main thermophysical characteristics of the treated material such as: coefficient of thermal conductivity - k ; specific heat capacity - s and coefficient of thermal conductivity - a.

Thermal conductivity depends on the type, structure and properties of the processed material. It is estimated by the coefficient of thermal conductivity, measured in $Wm^{-1} K^{-1}$ and shows the amount of heat that passes through a material with an area of one square meter and a thickness of one meter for one second, with a temperature difference of one degree [10]. The heat treatment of non- metallic materials causes changes in their micro and macro structure. Compared to metals, polymers show lower thermal conductivity and lower melting temperature ($100 \div 300^0$C). This short interval is a disadvantage because overheating and carbonization of the surface becomes very easy. There are polymers in which the depth of melting increases with increasing laser beam velocity. This is unexpected at first glance. This effect can be observed in polymers that have a tendency to carbonize. This happens when the speed is slow, the laser beam stays in the same place for a longer period of time, so in this layer the size of the carbonized material will be higher. As a result, the amount of laser light absorbed and the depth of melting will be reduced. When using a higher speed, the carbonation depth will be smaller and the total treated depth will be higher.

The coefficient of thermal conductivity - k, depends on the composition and structure of the material, the temperature -T and the pressure - p [3]. According to some experimental studies, the coefficient of thermal conductivity decreases with increasing temperature. When optimizing the process of marking non- metallic materials, it is necessary to study the dependence k = k (T):

$$K(T) = k_0 + b.(T - To) \quad (4)$$

where: k_0 - value of the coefficient of thermal conductivity at $T_0 = 273{,}15$ K,
b - experimentally established constant .

The heat capacity - C, shows how much heat must be transferred or taken to a body to raise its temperature by 1^0 K m, when heated and measured in JK^{-1} . When receiving the same amount of heat, different materials increase their temperature by different values. The specific heat capacity - c, is a material constant that determines the amount of heat that is absorbed or released by one kilogram of substance to change its temperature by one kelvin and is measured in $J.kg^{-1} K^{-1}$. The density of substances in the solid and liquid state does not change noticeably during the thermodynamic processes that take place and the mass can be considered constant. If he is famous the specific heat factor for a material, the amount of heat required to heat a substance to a certain temperature can be determined (5).

$$\Delta Q = c.m.\Delta T = c.m.(T_2 - T_1) \quad (5)$$

where: ΔQ - amount of heat;
$T = (T_2 - T_1)$ - temperature difference;
m - mass.

The coefficient of thermal conductivity is a complex characteristic that shows how fast the temperature of a layer of material equalizes and connects the coefficient of thermal conductivity - k, the specific heat capacity - c and the density of the material - ρ. It is related to the length of thermal diffusion and this relationship is expressed by (6).

$$l_d^2 = \alpha . t_d \quad (6)$$

where: t_d - time of thermal diffusion.

The contrast of the marking of non-metallic materials also depends on the following characteristics of the laser source: wavelength of the laser source - λ; diameter of the minimum focal spot - d_f; average power - P; pulse power - P_p ; pulse duration - τ; pulse repetition frequency - ν; surface density of laser radiation power - q_s ; diffraction number - M^2 and laser beam quality parameter - BPP .

The main characteristic of each laser is the wavelength - λ. It determines the ability to focus the laser beam , as well as the absorption and reflection ability of the relevant material. Absorption coefficient, penetration depth and Relay length - ZR, are also functionally dependent on λ. We have experimentally proved that lasers with a wavelength in the visible and far infrared region of radiation are suitable for marking textile and polymeric materials, such as $\lambda = 0.578 \div 10.6\mu m$.

With the help of focusing optics - with lenses or mirrors, for each laser system, the laser beam is focused on the treated surface in a spot with a certain diameter, called the diameter of the minimum focal spot - d_F. It depends on the wavelength, the diameter of the incident beam, the focal length, the parameter M^2 and is calculated from (7) [2,13].

$$d_F = M^2 . [(4.\Lambda . F) / (\pi . D)] \quad (7)$$

Depending on the focal length of the same diameter of the output laser beam, a minimal focal spot with different diameters can be obtained, and the larger the focal length, the larger the focused spot and vice versa - with short-focus lenses focal spot with smaller diameter.

The average power for marking non-metallic materials does not need to be large, power in the range of $10 \div 50$W is sufficient. Marking it is carried out with laser sources operating in pulsed mode for which the following are important: *pulsed power - P_p; pulse energy - E_p; pulse duration and pulse frequency.*

Surface power density - q_s is determined in Wm^{-2} and is a major factor influencing structural or the phase transformations of the material in the zone of influence during marking (8).

$$q_s = P / S = (4.P) / (\pi . d^2) \quad (8)$$

where: S - the area of the working spot;
d - diameter of the working spot.

The average power, and therefore the power density, of each laser source is specified in the manufacturer's technical specifications and cannot be changed. In order to obtain the optimal contrast of the marking for the specific processed material, it is necessary to determine the working intervals of the change of $q_{S.}$

The quality of laser radiation is a complex characteristic for each specific laser source and depends on : the parameter of laser beam quality (BPP-Beam Parameter Product), diffraction number - M^2, divergence angle - θ, diameter of the minimum focal spot - d_F, focal length - f, Rayleigh length - Z_R [3,11].

The divergence angle for laser sources from the visible and infrared range has values of 0.1÷10 mrad and is determined by the limit - $\lambda / \pi.r_{F.}$

The number of diffraction - M^2, is defined by standard EN ISO: 11145 and is introduced in order to take into account the increase in the radius of the minimum focal spot from the theoretical value in the Gaussian intensity distribution. The closer M^2 is to one, the better the laser beam. For laser marking of non-metallic materials it is necessary to select a laser source with a parameter in the range $M^2 \in [1,1; 2]$.

There are two main factors related to the technological process that affect the contrast in laser marking of non-metallic materials - speed of marking and defocusing.

The speed of marking is decisive for the quality of marking [11-14]. The higher the speed, the shorter the exposure time of the laser beam and the lower the energy absorbed by the material in the impact area. On the other hand, the higher the speed of the laser beam, the higher the efficiency of the technological process. It is important to know the type of material being processed and how it absorbs light energy, which is transformed into heat. Taking into account the other factors influencing the technological process, it is necessary to find the optimal speed of the laser beam for the respective material in order to realize the marking with the required contrast. The relationship between the velocity - v, the beam motion and the absorbed energy - E , is given by (9) , and the exposure time - t, of the radiation until the temperature of the treated material changes to a set value of (10) [6, 12,14] .

$$V = (A. P. d) / E \quad (9)$$

$$t = \frac{\pi^3.k^2.r^4(T-T_0)^2}{4.a.A^2.P^2} \quad (10)$$

where: A - absorption capacity;
P - average power of incident laser radiation;
d - diameter of the working spot;
k - coefficient of thermal conductivity;
To - mbient temperature;
a - coefficient of thermal conductivity.

The focusing of the laser beam is realized with an optical system for focus or defocus mode (Δf ″+″ above and "-" below the surface of the sample. The relationship between defocus (Δf) and the diameter of the working spot is linear, namely with increasing the defocus increases and the diameter of the spot.

Factors of complex importance for the contrast in laser marking of non-metallic materials are: linear energy density - LPE; linear pulse of density - LIP; efficient energy - E_{ef} and volumetric density of the absorbed energy - E_{ρ}.

The relationships between the factors of the three groups discussed above are described by factors of a complex nature (LPE, LIP, E_{ef} and E_{ρ}) and are expressed by (11 ÷ 14).

$$LPE = (A. P) / V \quad (11)$$
$$LIP = \nu / V \quad (12)$$
$$Eef = (A. P. N) / V^2 \quad (13)$$
$$Ep = (A. E) / \quad (14)$$

Heating, melting or evaporation occurs in the laser area depending on the energy absorbed, which can be quantified by dependence (14).

III. CONCLUSION

From The following experiments and the results obtained in them can be formulated the following more important conclusions:

It has been confirmed that the factors influencing the contrast in laser marking of non-metallic materials are: *the type of processed material; used the laser source, the technological process and complex influencing.*

The main factors influencing the contrast depending on the marked non-metallic material are conditionally grouped into two categories - optical and thermophysical.

It was found that the type of laser source used affects the quality of contrast when marking non-metallic materials by : *wavelength of the laser source - λ; diameter of the minimum focal spot - d_F; average power - P; pulse power - P_p; pulse duration - τ; pulse repetition frequency - ν; surface density of laser radiation power - q_s; diffraction number - M^2 and laser beam quality parameter - BPP .*

It has been confirmed that when marking non-metallic materials by technological factors, the most significant is the influence of the *speed of marking and defocusing.*

IV. REFERENCES

[1] LATI Industria Termoplastici SpA, Italy, Laser Marking of Thermoplastics, 05.01.2016

[2] L. Lazov,, Hr. Deneva, P. Narica, Laser Marking Methods, ISSN 1691-5402 , © Rezekne Higher Education Institution (Rēzeknes Augstskola), Rezekne ,2015.

[3] I.Mitev, Industrial Materials , ECS-PRESS, Gabrovo, 2017, ISBN 978-954-490-556.

[4] I. Mitev, Materials and blanks - part 1 (Materials), Credo - 3M, Gabrovo, 2021, ISBN 978-619-7100-44- 0

[5] I.Mitev, Materials and blanks - part 1II (Unconventional electrotechnological processes for obtaining blanks) , Credo - 3M, Gabrovo, 2021, ISBN 978-619-7100-46-4

[6] I.Mitev, I., Unconventional electrotechnological processes , EX-PRESS, Gabrovo, 2020, ISBN 978-954-490-698-7

[7] I.Mitev, Modern industrial technologies - part II / Electrophysical and electrochemical methods for forming / , EX-PRESS, Gabrovo, 2016, ISBN 978-954-490-413

[8] D.Schuőcker, Handbook of the Eurolaser Academy, Chapman & Hall, London, 1998

[9] M.Štěpánková et.al , Impact of laser thermal stress on cotton fabric. Fibers and Textiles in Eastern Europe , Vol.18, N3, p.70-73, 2010

[10] www.dapramarking.com/data-matrix.htm 2D Data Matrix Code Products

[11] D. Dichev, D. Diakov, R. Dicheva, I. Zhelezarov, O. Kupriyanov. Analysis of instrumental errors influence on the accuracy of

instruments for measuring parameters of moving objects. XXXI International Scientific Symposium "Metrology and Metrology Assurance 2021", September, 2021, Sozopol, Bulgaria. DOI: 10.1109/MMA52675.2021.9610855

[12] D. Dichev, I. Zhelezarov, R. Dicheva, D. Diakov, H. Nikolova, G. Cvetanov. Algorithm for estimation and correction of dynamic errors. XXX International Scientific Symposium "Metrology and Metrology Assurance 2020", September, 2020, Sozopol, Bulgaria. DOI: 10.1109/MMA49863.2020.9254261

[13] D. Dichev, H. Koev, D. Diakov, N. Panchev, R. Miteva, H. Nikolova. Automated System for Calibrating Instruments Measuring Parameters of Moving Objects. 59th International Symposium ELMAR, September 18-20 th, 2017, Zadar, Croatia, pp. 219-224. DOI: 10.23919/ELMAR.2017.8124472

[14] D. Dichev, I. Zhelezarov, N. Madzharov. Dynamic Error and Methods for its Elimination in Systems for Measuring Parameters of Moving Objects. Transactions of Famena, vol. 45, issue 4, 2021, pp 55-70. DOI: 10.21278/TOF.454029721

Determination of the penetration depth of laser marking of polymeric materials

Simeon Tsenkulovski
dep. "Mechanical Engineering and Instrumentation"
Technical university-Gabrovo
Gabrovo, Bulgaria
s.tsenkulovski@advanced-technology.eu

Ivan Mitev
dep. " Economics"
Technical university-Gabrovo
Gabrovo, Bulgaria
imitev@tugab.bg

Georgi Karlovski
dep. "Mechanical Engineering and Instrumentation"
Technical university-Gabrovo
Gabrovo, Bulgaria
g_karlovski@abv.bg

Abstract - This publication examines the penetration depth of laser radiation generated by a 50W fiber laser when marking polymeric materials. The statistical error at penetration depth 0.5 mm and scattering ± 0.1 mm was determined. Samples of 10 to 400 details were studied, and the obtained experimental results are presented in tabular and graphical form. Keywords — non-metallic materials, laser marking, depth of penetration

I. INTRODUCTION (*HEADING 1*)

In the recent years, a modern and very promising method for marking almost any material or product has entered the practice - laser marking [5,6,7]. It is most often applied as an alphanumeric code or as an image formed directly on the surface. The laser beam causes structural or phase changes in the processed material and may include one or a combination of the following processes: carbonization, bleaching, depigmentation, coating modification, melting, evaporation and others. Compared to traditional techniques, laser marking has a number of advantages, the most important of which are [1,2,8,9]:

- *very good quality;*
- *high efficiency;*
- *low operating costs;*
- *accessibility, even for uneven surfaces;*
- *no contact method;*
- *controlled by computer;*
- *high precision;*
- *reproducibility of results, both for large series and for single pieces;*
- *high speed and performance (up to several hundred characters per second)*

The method is cost-effective, provides an indelible mark, it is easy to read, difficult to copy or replace, contains unique information and does not change the functionality of the product in any way, is environmentally friendly and does not pollute the environment [1,10]. All this leads to a constant expansion of its application. Many traditional methods for marking industrial materials require significant amounts of energy, water and other consumables. Compared to them, laser technology is suitable for achieving good results at low cost.

During the recent years, the use of lasers for marking of non-metallic materials has increased due to the speed, accuracy and flexibility of this modern technology [1,2]. At the same time, however, this technology has not been sufficiently studied and the information in the scientific literature for the management and control of these processes is scarce. There are no scientific aspects which can be found regarding laser marking of non-metallic products, although it is increasingly used. The huge variety of polymers [3,4] creates a number of difficulties in the application of laser marking and raises the need to seek a scientific approach to solve them. The thermal, optical and mechanical properties of the various polymers make this area interesting and challenging for optimizing and managing the process for their labeling. In order to obtain the desired results and quality of the marking, it is necessary to control the process by adjusting the parameters of the laser system according to the characteristics of the specific material.

Having this in mind, the goal of the presented research is to trace the scattering and statistical error in determining the depth of penetration of laser marking at different speeds of polymeric materials.

II. EXPERIMENTAL PART

Samples of polyvinyl chloride (PVC) were tested. It is an amorphous polymer and in its initial state is a white powder with a density of 1.4 g / cm3 [3] Occurs in two modifications: soft - w and hard - h. In practice, the most widely used are products made of PVC and containing plasticizer (plastics), and PVC containing stabilizer (potassium stearate) and small amounts of plasticizers (viniplasts). Typical for this type of plastics is that they have a relatively low heat resistance and at temperatures above 140ºC, if they do not contain stabilizers, they begin to disintegrate. When applying the marking, a laser system was used, the schematic diagram of which is shown in Fig.1.

978-1-6654-8569-2/22/$31.00 ©2022 IEEE

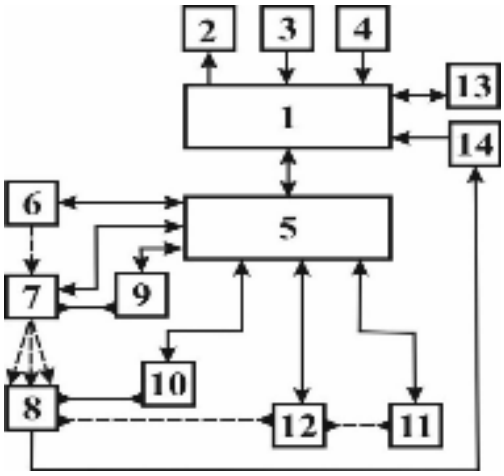

Fig.1. Scheme of the experimental installation: 1 – computer; 2 – monitor; 3 – keyboard; 4 – mouse; 5 – controller; 6 – source of laser beam; 7 – scanning device; 8 – piece; 9, 10, 11, 12 – electromechanical devices for movement on X, У, Z and rotating around vertical axis; 13 – server and 14 – barcode reader.

In the process of testing, the marking was done with a fiber laser with a power of 50W and a scanning head with a working space in the XY coordinate plane with dimensions 140x140mm.

The tests were proceeded under the following conditions of laser marking: penetration depth of 0,5mm and speed of 0,300 and 0,150 mm /s.

The measurements of the depth after the laser marking are done with ultrasonic depth gauge for non-metallic materials type „PosiTector 200 B“, on the samples of 10 up to 400 pieces of batch of 1000 pieces. The testing results are shown in tables 1 – columns 2 and 3, for the both tested speeds of the marking, and the scattering of the experimental results at a tolerance ±0,1mm, in column 4.

The statistical error in the measurements is calculated by the formula 1, and the results are shown in column 5 [11, 12].

$$\sigma = Sx/\sqrt{n} \qquad (1)$$

where: Sx – deviation from the set value, mm;
n - sample size, pcs.

The graphical interpretation of the experimental results for the scatter versus the baseline value is presented in Figures 1 and 2, respectively for the two marking speeds, which we tested.

TABLE 1. EXPERIMENTAL RESULTS

№	n, бр.	h,mm	Sx,mm	σ,mm
1	2	3	4	5
V=0,300mm/s				
1	10	0,45	-0,05	-0,0158
2	20	0,51	+0,01	+0,0022
3	30	0,56	+0,06	+0,0110
4	40	0,42	-0,08	-0,0120
5	50	0,39	-0,11	-0,0156
6	60	0,38	-0,12	-0,0155
7	70	0,40	+0,10	+0,0119
8	80	0,42	-0,08	-0,0089
9	90	0.41	-0,09	-0,0095
10	100	0,48	-0,02	-0,0020
11	110	0,41	-0,09	-0,0086
12	120	0,52	+0,02	+0,0073
13	130	0,49	-0,01	-0,0009
14	140	0,38	-0,12	-0,0101
15	150	0,54	+0,04	+0,0033
16	160	0,49	-0,01	+0,0008
17	170	0,50	0,00	0
18	180	0,38	-0,12	-0,0089
19	190	0,31	-0,19	-0,0138
20	200	0,48	-0,02	-0,0014
21	210	0,52	+0,02	+0,0014
22	220	0,40	-0,10	-0,0067
23	230	0,68	+0,18	+0,0119
24	240	0,65	+0,15	+0,0097
25	250	0,55	+0,05	+0,0032
26	260	0,50	0,00	0
27	270	0,52	+0,02	+0,0012
28	280	0,42	-0,08	-0,0048
29	290	0,40	-0,10	-0,0059
30	300	0,51	+0,01	+0,0006
31	310	0,55	+0,05	+0,0028
32	320	0,57	+0,07	+0,0039
33	330	0,42	-0,08	-0,0044
34	340	0,44	-0,06	-0,0033
35	350	0,47	-0,03	-0,0016
36	360	0,58	+0,08	+0,0042
37	370	0,55	+0,05	+0,0026
38	380	0,65	+0,15	+0,0077
39	390	0,38	-0,12	-0,0061
40	400	0,55	+0,05	+0,0025
V=0,150mm/s				
1	10	0,55	+0,05	+0,0158
2	20	0,51	+0,01	+0,0022
3	30	0,58	+0,08	+0,0146
4	40	0,48	-0,02	-0,0032
5	50	0,54	+0,04	+0,0071
6	60	0,51	+0,01	+0,0013
7	70	0,49	-0,01	-0,0012
8	80	0,50	0,00	0
9	90	0,51	+0,01	+0,0011
10	100	0,46	-0,04	-0,0040
11	110	0,47	-0,03	-0,0029
12	120	0,51	+0,01	+0,0009
13	130	0,52	+0,02	+0,0018
14	140	0,50	0,00	0
15	150	0,49	-0,01	-0,0008
16	160	0,56	+0,06	+0,0047
17	170	0,51	+0,01	+0,0008
18	180	0,53	+0,03	+0,0022
19	190	0,55	+0,05	+0,0036
20	200	0,51	+0,01	+0,0007
21	210	0,50	0,00	0
22	220	0,50	0,00	0
23	230	0,50	0,00	0
24	240	0,49	-0,01	-0,0006
25	250	0,52	+0,02	+0,0013
26	260	0,53	+0,03	+0,0019

27	270	0,51	+0,01	+0,0006
28	280	0,52	+0,02	+0,0002
29	290	0,48	-0,02	-0,0012
30	300	0,49	-0,01	-0,0006
31	310	0,47	-0,03	-0,0017
32	320	0,48	-0,02	-0,0011
33	330	0,49	-0,01	-0,0005
34	340	0,50	0,00	0
35	350	0,52	+0,02	+0,0011
36	360	0,53	+0,03	+0,0016
37	370	0,51	+0,01	+0,0005
38	380	0,55	+0,05	+0,0026
39	390	0,50	0,00	0
40	400	0,49	-0,01	-0,005

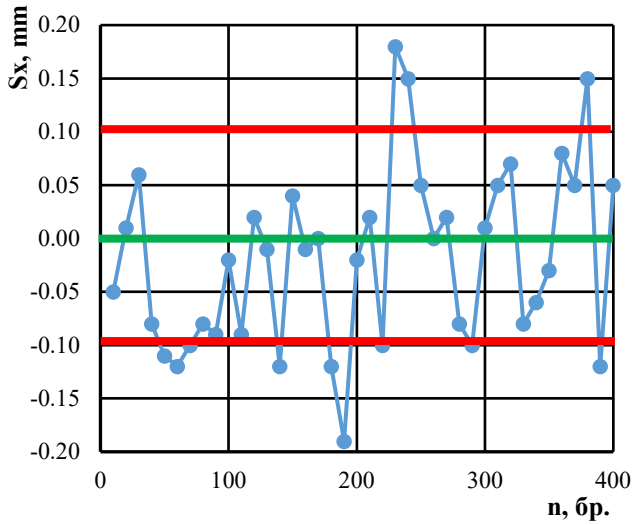

Figure 1. Deviation of the experimental results for the depth of the marking at speed of 0,300 mm/s

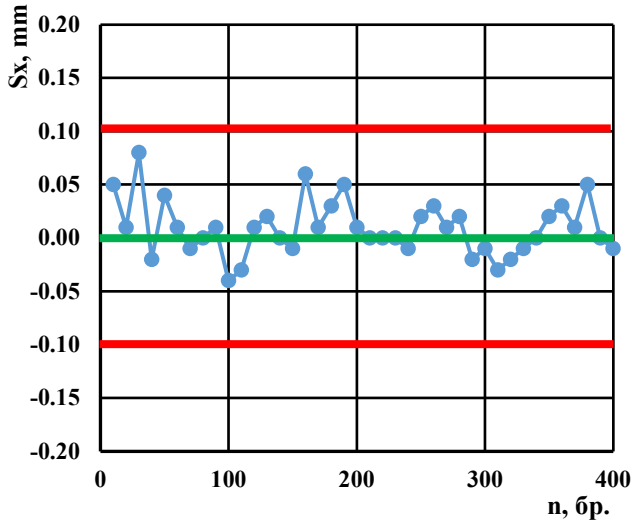

Figure 2. Deviation of experimental results for marking depth at marking speed of 0,150 mm/s

It can be seen from Fig. 1 that at a marking speed of 0.300 mm / s, in 25% of the cases the obtained results are outside the permissible range of 0,5±0,1mm, when only 5% from the experimental ones give the exact depth of penetration.

By reducing the marking speed to 0.150mm / s (Fig.2). it is found that there is a stabilization of the results around the baseline value - 0.5mm. and all values are within the tolerance of ± 0,1mm. In this case, the exact results are 17.5% of all measurements performed. The graphical interpretation of the results for the calculated statistical error according to formula 1 (column 5 of table 1) is shown in Figures 3 and 4.

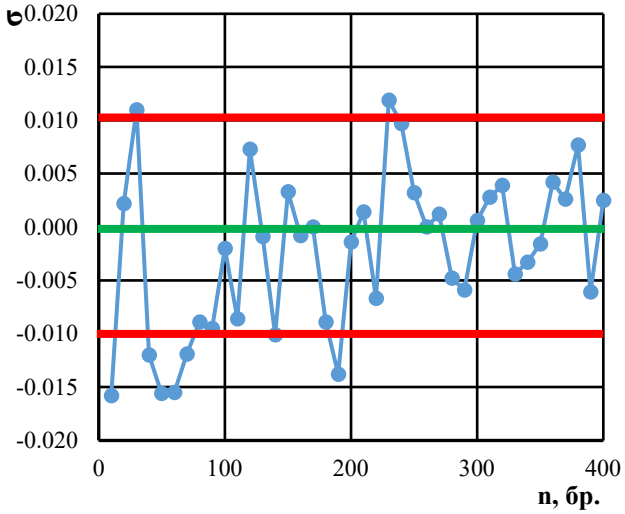

Figure 3. Deviation of the statistical error for the depth of the marking at a speed of 0.300 mm / s

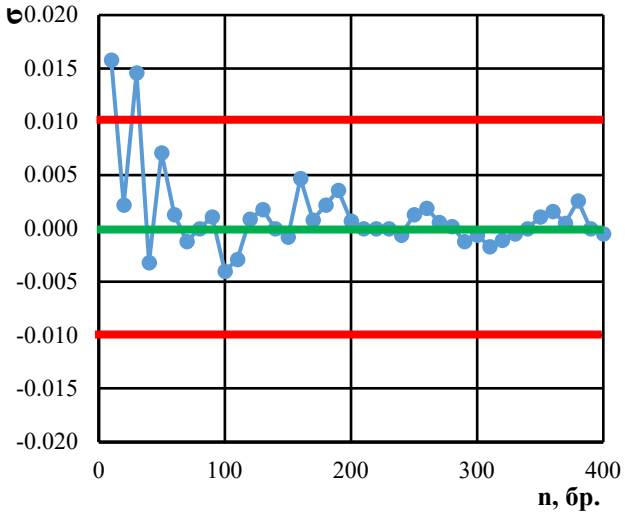

Figure 4. Deviation of the statistical error for the depth of the marking at a speed of 0,150 mm / s

It can be seen from the figures that regardless of the marking speed with increasing number of tested samples in the sample from 10 to 400, the statistical error decreases. As with fixed limit deviations ± 0,01, at a marking speed of 0,300 mm / s, 20% of the results are outside the limit deviations, and at a speed of 150 mm / s only 5%.

In both cases, the theory is confirmed that as the number of samples in the sample increases, the values of the statistical error decrease.

III. CONCLUSION

The scattering in the values when measuring the depth of penetration when laser marking of polyvinyl chloride samples with fiber laser with power 50W, at a marking speed of 0.150 ÷ 0.300 mm / s, set depth of 0.5 mm and a maximum deviation of ± 0.1 mm was studied.

It has been proved that at a marking speed of 0,300mm / s, 25% of the samples have values outside the tolerance of 0,5 ± 0,1mm, and at a speed of 0,150mm / s, all samples give values in the permissible zone, as in 17.5% of the samples accurate results were found. The experimental results in calculating the statistical error are similar.

It has been confirmed that as the sample size increases, the value of the statistical error decreases.

From the conducted tests and the obtained results, the conclusion can be formulated that for better marking of samples from polyvinylchloride it is recommended to use marking speed 0,150 mm / s.

IV. LITERATURE

[1] LATI Industria Termoplastici SpA, Italy, Laser Marking of Thermoplastics, 05.01.2016

[2] L. Lazov,, Hr. Deneva, P. Narica, Laser Marking Methods, ISSN 1691-5402 , © Rezekne Higher Education Institution (Rēzeknes Augstskola), Rezekne ,2015

[3] I.Mitev, Industrial Materials , ECS-PRESS, Gabrovo, 2017, ISBN 978-954-490-556.

[4] I. Mitev, Materials and blanks - part 1 (Materials), Credo - 3M, Gabrovo, 2021, ISBN 978-619-7100-44- 0

[5] I.Mitev, Materials and blanks - part 1II (Unconventional electrotechnological processes for obtaining blanks) , Credo - 3M, Gabrovo, 2021, ISBN 978-619-7100-46-4

[6] I.Mitev, I., Unconventional electrotechnological processes , EX-PRESS, Gabrovo, 2020, ISBN 978-954-490-698-7

[7] I.Mitev, Modern industrial technologies - part II / Electrophysical and electrochemical methods for forming / , EX-PRESS, Gabrovo, 2016, ISBN 978-954-490-413

[8] D.Schuőcker, Handbook of the Eurolaser Academy, Chapman & Hall, London, 1998

[9] M.Štěpánková et.al , Impact of laser thermal stress on cotton fabric. Fibers and Textiles in Eastern Europe , Vol.18, N3, p.70-73, 2010

[10] www.dapramarking.com/data-matrix.htm 2D Data Matrix Code Products

[11] D. Dichev, D. Diakov, R. Dicheva, I. Zhelezarov, O. Kupriyanov. Analysis of instrumental errors influence on the accuracy of instruments for measuring parameters of moving objects. XXXI International Scientific Symposium "Metrology and Metrology Assurance 2021", September, 2021, Sozopol, Bulgaria. DOI: 10.1109/MMA52675.2021.9610855

[12] D. Dichev, I. Zhelezarov, R. Dicheva, D. Diakov, H. Nikolova, G. Cvetanov. Algorithm for estimation and correction of dynamic errors. XXX International Scientific Symposium "Metrology and Metrology Assurance 2020", September, 2020, Sozopol, Bulgaria. DOI: 10.1109/MMA49863.2020.9254261

Improving the hard turning process when machining bearing steels

Georgi Karlovski
dept. Mechanical engineering and technology
Technical University of Gabrovo
Gabrovo, Bulgaria
g_karlovski@abv.bg

Kalin Krumov
dept. Mechanical engineering and technology
Technical University of Gabrovo
Gabrovo, Bulgaria
kalin_krasimirov_krumov@abv.bg

Irina Aleksandrova
dept. Mechanical engineering and technology
Technical University of Gabrovo
Gabrovo, Bulgaria
irina@tugab.bg

Simeon Tsenkulovski
dept. Mechanical engineering and instrument making
Technical University of Gabrovo
Gabrovo, Bulgaria
s.tsenkulovski@advanced-technology.eu

Ivan Mitev
dept. Management
Technical University of Gabrovo
Gabrovo, Bulgaria
imitev@tugab.bg

Abstract: Improving the efficiency of the hard turning process of bearing steels

Summary: The article presents experimental results obtained by hard turning of steel steels with different types of holders (standard and quick-change). A statistical analysis of the technological processes in a continuous cycle of bearing production on the territory of the company. It has been proven that when using a quick-change holder, the efficiency of the technological line increases 11 times.

Key words: hard turning, bearing steels, statistical analysis.

I. INTRODUCTION

In solving efficiency problems, it is important to ensure the accuracy and stability of technological processes, especially those parameters that have a significant functional impact on the performance of manufactured products [1,2,3]. For example, reducing the duration of the production process preserves the quality of the manufactured product, which is an important parameter that has a significant impact on the production cost.

In any production, the choice of technology is a complex task. Its solution is determined by satisfying the requirements for the processing of details with the quality specified by the users at the lowest possible production costs [5,7,8]. In order to reduce production costs, manufacturers strive for productions guaranteeing large volumes of the same type of production (mass and large series). This aspiration is at odds with consumer demand. With the development of technical progress, there is a tendency to increase the requirements for the quality of the details and to expand their nomenclature. In parallel with this, the terms for their moral obsolescence are constantly decreasing. Under these conditions, it is increasingly difficult and economically unprofitable to organize productions in compliance with the traditional principles of mass and large-scale production. Flexibility and adaptability to rapidly changing market conditions and consumer demand is required. To satisfy these mutually contradictory requirements in the production of bearings, it is necessary to make adequate decisions related to [5,7,8]:

• automation of structural and technological design;

• use of type and group technologies;

• introduction of universally assembled, reconfigurable and universal devices;

• construction of the machine park on an aggregate and modular basis;

• use of metal-cutting machines with digital program control (CPU), etc

When manufacturing parts for rolling bearings, turning is the main method of processing the surfaces. Depending on whether it is rough, clean or fine, it can reach 7÷14 degrees of accuracy, with roughness Rz 160÷1.6 μm and Ra 0.4÷1.25 μm [5]. When processing external rotary surfaces, the specified degrees of accuracy and surface roughness are achieved at a lower productivity due to the reduced stability of the technological system and, in particular, of the cutting tool.

For aggregate machines and those with CNC, the cutting tools are an integral part of the automated systems ensuring their efficient operation. The selection and preparation of the tools depend on the productivity and accuracy of processing, and to ensure the automatic processing cycle, high reliability of the cutting tool is required. Cutting tools operating in a continuous production cycle must satisfy requirements such as [7]:

• stable cutting properties;

• good chip formation and chip removal;

• versatility when used for typical processed surfaces of different details on different machine models;

• quick changeability when resetting another processed part or wear;

• provision of possibility to pre-adjust size outside the machine, etc.

• introduction of universally assembled, reconfigurable and universal devices;

978-1-6654-8569-2/22/$31.00 ©2022 IEEE

II. The aim of the present research is, based on accumulated information, to improve the efficiency of the production process in the production of bearing steel parts by stabilizing the cutting mode and using quick-changeable and adjustable cutting tools, thereby shortening the duration of the production process and the efficiency of an automatic line has improved.

III. EXPERIMENTAL RESEARCH

The production process of rolling bearings is carried out on an assembly line of seven aggregate machines, six of which carry out chip removal operations by hard turning.

TABLE I. In fig. 1 is a drawing of the initial blank for manufacturing bearing rings. According to construction documentation, it is assumed that the product will be made of bearing steel type SHX15 or 100Cr6, the chemical composition of which is presented in table 1 [4,6].

TABLE II. CHEMICAL COMPOSITION OF PROCESSED MATERIAL

Означение на материала	Химичен състав, %								
		C	Si	Mn	Ni	S	P	Cr	Cu
ШХ15, ГОСТ 801 (ISO 1.3505)	min	0.95	0.17	0.20	≤0.3	≤0.02	≤0.027	1.30	≤0.25
100Cr6, БДС EN 10027-1	max	1.05	0.37	0.40				1.65	

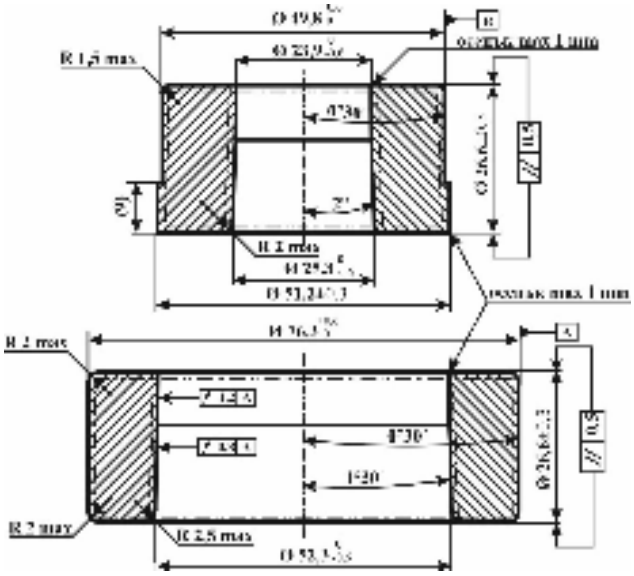

Fig. 1. Drawing of the part with the respective technical requirements to the product during its mechanical processing

In the state of delivery, the material has a hardness of 207HV after annealing at a temperature of 800±10ºC.

Parallel studies were carried out for processing the starting workpiece to the end, using monolithic holders in one case, and quick-change ones in the other - fig. 2.

Depending on the type of treated surfaces, five types of hard alloy mineral-ceramic plates with characteristics presented in table 2 were used.

TABLE III. TYPES OF CARBIDE PLATES [9,10]

Тип пластина	CNMG 1200408	SNMG 120408	RPHT 124MOT	Канална за фаски	Канална за „жлеб“
Марка	KYOCERA	KYOCERA	SECO		
Mineral-ceramic alloy	CA515	HB7010-1	MS2500		
Cutting depth ap, mm	1÷10	0.5÷6	0.5÷6,0	1÷8	1÷8
Submission f, mm/rev	0.25÷0.80	0.15÷0.50	0.15÷1,0	0.15÷0.20	0.15÷0.20
Cutting speed Vc, m/min	80÷450	120÷440	120÷440	80÷450	80÷450
Radius R, mm	0.8	0.8	0	-	-

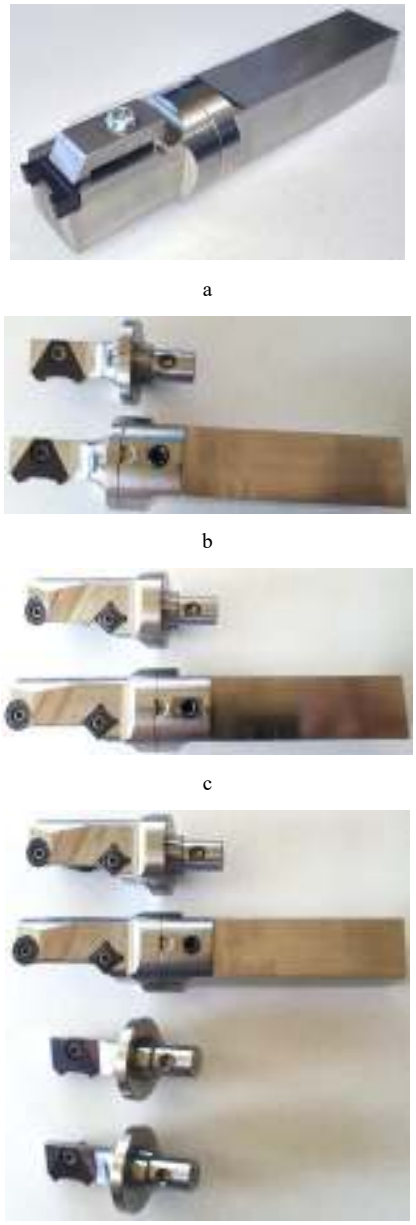

a

b

c

d

Fig. 2. Used metal-cutting tools in the implementation of the technological process with a quick-change holder: a - general type of quick-change holder; b - quick-change holder with a plate for turning the outer part of the bearing bracelet; c - combined holder for turning the forehead and scraping the

inner bracelet; d - quick-change holder with a set of interchangeable heads

The hard turning process is realized with the following elements of the cutting mode - cutting speed 130÷140 m/min, feed 0.15÷0.2 mm/rev and cutting depth 0.2 mm, selected based on the recommended values indicated in table 2.

It has been experimentally proven that with the selected cutting mode and processed material according to table 1, the average wear of carbide plates is after processing 650 workpieces. This cutting edge life is reached after observing the roughness class as well as linear dimension deviation. With a production cycle of 6÷7 s per operation and an eight-hour work shift – 28800 s, the theoretical productivity is of the order of 4100÷4800 bearing rings per change. Therefore, for one work shift, it is necessary to make 7 readjustments of the cutting tools.

Table 3 presents the time losses for work change and readjustment of the metal cutting tools and therefore the deviations from the theoretical (maximum) productivity of the assembly line.

TABLE IV. EXPERIMENTAL RESULTS

№	Characteristic	Standard holder	Quick change holder
1.	One time tool change and readjustment, s	1 380	53
2.	Tool changeover and readjustment time for a work shift – 8 h, s	9 660	371
3.	Unrealized output at a 6-second clock for a work shift, бр.	1 610	62
4.	Unrealized output at a 7-second clock for a work shift, бр.	1 380	53
5.	Productivity at a production cycle of 6s per work shift, бр.	3 190	4 738
6.	Productivity at production cycle 7s per work shift, pcs.	2 734	4 061
7.	Unrealized production compared to the theoretical one at 6 s clock, %	33.54	1.291
8.	Unrealized production compared to the theoretical one at 7 s clock, %	33.54	1.288

IV. CONCLUSION

It has been proven that for an eight-hour working day in a three-shift continuous mode of operation for seven days, the productivity of the line for bearing bracelets with a standard holder depending on the production cycle is 57414÷66990 parts, and when using a quick-change holder it is 85281÷99498 parts . This represents a deviation from the theoretical productivity of the assembly line - 86400÷100800 parts, respectively by 33.54% and by 1.29%.

From the obtained experimental results, it is found that when using a quick-change holder for turning workpieces from bearing steels, due to the improvement of the cutting process when turning and quick changeability when resetting another processed workpiece or wear, the productivity of the assembly line increases by 32.25%

.REFERENCES

[1] D. Dichev, I. Zhelezarov, N. Madzharov. Dynamic Error and Methods for its Elimination in Systems for Measuring Parameters of Moving Objects. Transactions of Famena, vol. 45, issue 4, 2021, pp 55-70.DOI: 10.21278/TOF.454029721.

[2] D. Dichev, D. Diakov, R. Dicheva, I. Zhelezarov, O. Kupriyanov. Analysis of instrumental errors influence on the accuracy of instruments for measuring parameters of moving objects. XXXI International Scientific Symposium "Metrology and Metrology Assurance 2021", September, 2021, Sozopol, Bulgaria, pp. 91-95. DOI: 10.1109/MMA52675.2021.9610855.

[3] D. Dichev, I. Zhelezarov, R. Dicheva, D. Diakov, H. Nikolova, G. Cvetanov. Algorithm for estimation and correction of dynamic errors. XXX International Scientific Symposium "Metrology and Metrology Assurance 2020", September, 2020, Sozopol, Bulgaria, pp. 91-95, DOI: 10.1109/MMA49863.2020.9254261.

[4] I. Mitev, Materials and preparations - part 1 (Materials), Credo - 3M, Gabrovo, 2021, ISBN 978-619-7100-44-0.

[5] I. Mitev, Materials and blanks - part 1I (Conventional technological processes for obtaining blanks), Credo - 3M, Gabrovo, 2021, ISBN 978-619-7100-45-7.

[6] I. Mitev, Industrial materials, EX-PRESS, Gabrovo, 2017, ISBN 978-954-490-556-9.

[7] T. Kuzmanov, K. Krumov, Technical preparation of production, EKS-PRESS, Gabrovo, 2013, ISBN 978-954-490-419-7.

[8] T. Kuzmanov et al., Processes and equipment for mechanical processing, UI "V. Aprilov", Gabrovo, ISBN 978-954-683-543-7.

[9] https://www.kyoceraprecisiontools.com

[10] https://www.iscar.com/eCatalog/Index.aspx

Digital transformation of activity management in a metrology laboratory through the implementation of a web-based system MET/ TEAM

1st Krasimir Bosilkov
Metrology Assurance Department
Kozloduy NPP EAD
Kozloduy, Bulgaria
kkbosilkov@npp.bg

2st Vladimir Lalev
Personnel and training centre
Directorate
Kozloduy NPP EAD
Kozloduy, Bulgaria
v_lalev@npp.bg

3st Kiril Banev
Metrology Assurance Department
Kozloduy NPP EAD
Kozloduy, Bulgaria
kbanev@npp.bg

4st Biser Borisov
Metrology Assurance Department
Kozloduy NPP EAD
Kozloduy, Bulgaria
biborisov@npp.bg

Abstract—In order to adopt the metrology assurance at NPP to the new challenges in the digital era (Industry 4.0), management of activities, transmission of units of physical quantities and calibration of working standards, web-based MET/TEAM metrology system and MET/CAL software for automated calibration have been implemented. The system enables management of measurement standards and coordination of all the activities related to their metrology assurance. MET/CAL software records and encrypts measurement data in its own centralised database with validated algorithms for estimation the uncertainty measurement results, and generates digitally readable calibration certificates; it is also used for analysis and monitoring the condition of measurement standards and instruments.

Keywords: **MET/TEAM, Fluke, metrology assurance, calibration, standards, analysis and monitoring.**

I. INTRODUCTION

In order to ensure the performance and safe operation of Kozloduy NPP, thousands of measurements are performed every minute. More than 50,000 measurement instruments and systems are used for these measurements, the metrology assurance of which is an obligation and responsibility of specialists from Kozloduy NPP Metrology Assurance Department.

The metrology assurance of these measurement instruments (assets) is related to implementation of activities that require collecting, processing and storage of a great amount of information that has to be easily accessible for use and processing by MA specialists.

A digital transformation of processes is performed for optimisation of activities related to metrological inspection and calibration of measurement instruments through implementation of web-based MET/TEAM Test Equipment Asset Management system with server-client interface and MET/CAL software for automated calibration with following advantages:

- Management of all metrology assurance aspects with a paperless solution;
- configuration and personalisation of business rules;
- web-based software – does not require installation at workstations, allows opening and editing multiple windows at the same time.

Fig. 1 User screen

II. ` CAPABILITIES OF MET/TEAM METROLOGY SYSTEM

The metrology system implemented at NPP enabled collecting great amount of information on used measurement instruments in one place and made coordination, monitoring and analysis of activities much easier due to the full use of its capabilities:

- work process management – tracking of assets movements, metrological activities planning by scheduling;
- ability to customise according to department needs – variety of additional fields and labels, quick links, maintaining templates for manual entry of calibration results, etc.;
- support for quality assurance process for a successful accreditation which complies with the

requirements of BDS ISO 17025 – all the changes are recorded and stored in a control log;

- automatic e-mail notifications of a forthcoming metrological inspection or calibration of measurement instruments;
- quick and easy creation of references, reports, records and certificates for metrological inspection and calibration using the Crystal Reports XI app, which enables both using ready made templates and creation of specific ones;
- automatic generation of stickers related to a specific order certifying the metrological control with a QR code integrated in them with a possibility provided by the system to read it by a reader and make reference by the information they contain;
- storage of metrological data as machine-readable documents;
- administrative data is maintained independently from the client in the form of user accounts, creation of data templates and storage procedures;
- improvement of productivity and reducing the operating costs;
- maintaining compliance with regulatory standards;
- management of shipping information, creation, tracking and completion of work orders;
- tracking customer and vendor information.

Automation of receiving and returning of mesurement instruments submitted for metrological control to Metrology Assurance Department laboratories at NPP.

Introducing a unified approach to work performance which is embedded in the web-based system and allows reducing the subjective error by eliminating the possibility of skipping steps of the process.

The flow-chart at fig. 2 shows the algorithm of receiving/submitting the assets.

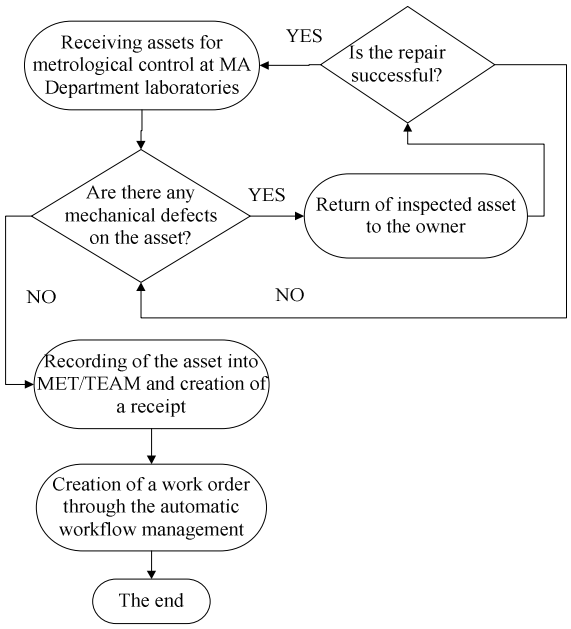

Fig. 2 Flow-chart presenting the algorithm of receiving the measurement instrument for metrological control.

When returning the asset after the metrological control, the work order and measurement data are automatically locked up by the system and archived.

III. Workflow Management

A system for metrological activities management supports a software – Workflow Management, which enables easy management of frequently performed tasks (Work Orders).

Fig. 3 Workflow Management interface

The software enables administration of requesting and receiving measurement instruments process by configuring assets, service types, status, priorities, require dates and other extended data. Created and configured this way data allows users do the following:

- receive/return assets: through the Find command or by scanning the bar-code the users can find and select an asset or a group of assets from the database and print receipt for customers;
- create a work order: assign technicians, schedule due date and next maintenance dates, select inspection or calibration procedure, set inspection or calibration intervals;
- complete work order information: record environmental conditions, record labour hours, possibility to add a record of the used spare parts and subcontractor information, etc.;
- monitor the stock of spare parts (mostly fuses) and automatically calculate the quantity to be ordered;
- enter a price for a metrological service as per the code from the MA Department price list and create a receipt for the activity performed;
- calculate the total time needed for a specific metrological activity and calculate the labour cost depending on the time spent and parts used for a specific measurement instrument.

IV. Calibration

Integrated into MET/TEAM MET/CAL software enables automatic calibration ensuring measurement data processing and interface compatibility with different measurement instruments. Specialists from the department use more than 2500 automated procedures in the course of their work including both procedures developed by the manufacturers and by the department specialists.

The specifics of high-level programming language impose high requirements to the competence and qualification of specialists for their development. The software for development of these procedures MET/CAL Editor is based on a SAP wide-range software package which operates on a server-customer base using a centralised database which administrates

and manages the compiled in a specific .pxe format (execution environment) procedures.

The use of MET/CAL software and standard high-precision instruments in the department laboratories has created automated workplaces for calibration of measurement instruments for different physical quantities applicable at NPP:

- level, flow rate and pressure measurement;
- ionizing radiation measurement;
- temperature measurements;
- mechanical, physical and chemical measurements.

The development of automated procedures and their validation in different measurement areas allows the specialist performing a measurement to follow a sequence of step-by-step procedures during the required switching and from the measurement diagrams displayed through the automated measurement procedure; standard values and measurement process values are set and data is processed by the specialised software. This allows the less-experienced specialists to perform metrological inspection while the control of activities and analysis of the results are performed by specialists of a higher hierarchical level within the structural unit in which the specific metrological activity takes place.

The measurement data from the reporting documents generated by the system can be saved in a digital format (.pdf) which provides opportunity to directly integrate them into SmartDoc digital infrastructure at NPP.

The data is integrated through scripts developed by specialists from the Computer and Information Systems Department.

The scripts are operationally compatible and more precisely the information transferred between integrated systems as specific data types preserves its original format and it is sure that all the software components in the system are compatible and can operate together as a unit. The security of transmitted data is ensured by checksums during the transfer.

V. References, reports and documents from the metrological activities

In order to optimise the activities performed at MA Department, multiple automatic references are made through the metrological software:

- scheduled activities;
- MA programme;
- list of technical measurement instruments;
- standard traceability;
- monthly report of MA Department by laboratories, etc.

The use of Crystal Reports 2013 software enabled creation of multiple templates for automatic user configurable references (Recall), creation of report documents from the metrological control and e-mail notification of responsible persons, owners of measurement instruments (users), about the following:

- measurement instrument is due for next periodic metrological control;

Fig. 4 Recall user screen

- decommissioned measurement instruments;
- business status of the measurement instrument (receiving/work/returning).

Fig. 5 Business Status user screen

- report on the metrology assurance of the measurement instruments at the NPP.

Fig. 6 Reports user screen

VI. MET/TEAM Customer Portal user platform

This is a web-based platform integrated with MET/TEAM, oriented to assets owners and ensuring the feedback between them and the MA department, enabling also the following:

- monitoring the metrological activities in a given laboratory by assets owners and metrology assurance responsible persons;
- recall reports and review the report documents and archived copies;
- management the assets status, control and change its physical location and definition a maintenance warranty interval.

Fig.7 MET/TEAM Customer Portal user platform

VII. CONCLUSION

The automated metrological control in the areas of measurement of different physical quantities within the NPP MA department requires use of a large number of software products such as Compass, Presscal, Comfort basic, Calegration, Vibration control software (VCS) issued by various manufacturers of measurement instruments and user databases their own development (access, sql, etc.) for measurement results storage. Modern digital metrology as a part of the global process in measurement data centralisation industry and subsequent data processing, visualisation and protection requires pooling of data of different format into a common database. The latter requirement places the need to implement MET/CONNECT software application to liaise to web-based system used at NPP for organisation of operating activity. Establishing the connections will allow a large number of users (more than 3,000) to use the obtained data.

The implementation of web-based system and MET/TEAM Test Equipment Asset Management Software for metrology assurance and automation of metrological control and calibrations enabled decrease of the subjective error factor when assessing and processing the measurement results, reduce the time for metrological control, and timely development of reporting documents following the activity.

Conditions were established for accumulation metrological activities data and flexible configuration and personalisation of criteria for assets metrological condition analysis.

A possibility was created for real-time on-line control of metrological activities performed in NPP MA Department through recall and reports valid at the time of their creation.

REFERENCES

[1] https://us.flukecal.com
[2] MET/TEAM user training

Automation of metrological control of measurement instruments at Kozloduy NPP Plc

1st Filip Filipov,
Metrology Assurance Department
Kozloduy NPP EAD
Kozloduy, Bulgaria
FGFilipov@no-mail.kz

2st Krasimit Bosilkov.,
Metrology Assurance Department
Kozloduy NPP EAD
Kozloduy, Bulgaria
kkbosilkov@npp.bg

3st Kiril Banev,
Metrology Assurance Department
Kozloduy NPP EAD
Kozloduy, Bulgaria
kbanev@npp.bg

4st Biser Borisov,
Metrology Assurance Department
Kozloduy NPP EAD
Kozloduy, Bulgaria
biborisov@npp.bg

Abstract: This report examines the commissioned automated workplaces for metrology control at Kozloduy NPP Metrology Assurance Department. There is a short description of the software platform, virtual instruments developed and implemented applications from manufacturers. It discusses their structure, hardware components, programme modes and working interfaces.

Key words: National Instruments, LabVIEW, metrology check, Fluke, automated workplace

I. Introduction

Accuracy and reliability of measurements of controlled technological parameters are an important factor for safe operation of nuclear facilities, protection of personnel health and environment. Thousands of measurements are performed every second at Kozloduy NPP. For this purpose, more than 50,000 measurement instruments and systems, approved for use by Kozloduy NPP metrologists, are used. The automation of activities is the solution to the problem of the large number of checks carried out during the limited period of the outage. Today, there are more than 12 automated workplaces in the laboratories of the department.

II. Automated workplaces

The automated workplaces have a number of advantages compared to the traditional ones, such as:

- decreased probability of error occurrence in the course of obtained results processing;
- absence of operator's errors;
- large volume of operations performed;
- high productivity;
- displays with friendly human-machine interface and possibilities for developing additional displays and modification of the present ones;
- reliable data archiving and its visualization on graphic displays;
- analysis of the data from the archive;
  - a possibility of modifying and supplementing both software and hardware without significant costs.

The automated workplaces used in the Metrology Assurance Department can be divided into two groups:

- developed by the equipment manufacturer;
- own development.

A. The first group includes:

- Automated workplace for check of БГР-Т-ДПИ (signal multiplicator with built-in range function) – of the Engineered Safety Features Actuation System (safety systems) - more than 1,000 pcs. Visual Studio Platform. Hardware БГРТ bench, manufacturer Radiy, Kirovgrad. Implemented in 2009.

Fig. *1 БГР-Т-ДПИ automated workplace*

Automated workplace for calibration of work standards and measurement instruments for electric, radiotechnical quantities and temperature - 500 pcs.

METTEAM/MetCal. Platform, manufacturer Fluke Inc., implemented in 2009

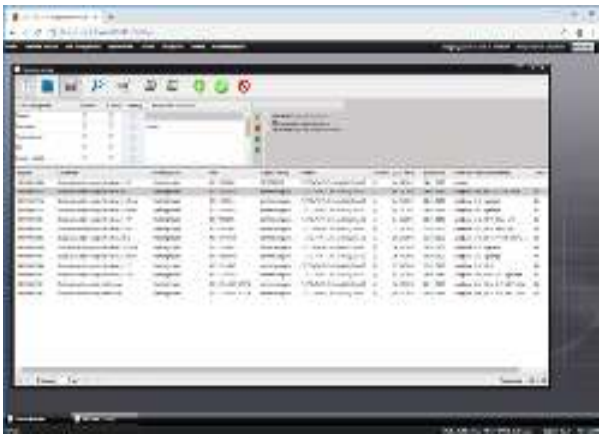

Fig. 2 METTEAM work display

Automated workplaces for check of more than 120 static energy meters – Calegration. Development of MTE, Switzerland, implemented in 2016.

Fig. 3 Check of energy meters

B. Automated workplaces - own development.

LabView-based – development environment, based on graphical programming language G, designed to communicate with hardware, such as GPIB, VXI, PXI, RS-232, RS-485, Field Point, and data collection devices. The software package uses terminology and icons, explaining programme actions mainly with graphical symbols called Virtual Instruments (VI). LabView contains wide libraries for data collection, analysis, presentation and storage, as well as the traditional software instruments.

*Automated workplace for check of measuring channels of Instrumentation for protection by process parameters - more than 220 pcs***.** Hardware CompaqDAQ, manufacturer National Instruments. Own development 2011, implemented for the Unit 6 Outage

The instrumentation for protection by process parameters А3ТП-06Р in the NPP is designed for control and measurement of the neutron power and the reactor period, control over the chain reaction and reactor trip. Until the introduction of the automated workplace, checks were performed manually by means of current sources and a frequency counter.

The CompactDAQ hardware platform was chosen for the implementation of the project.

Fig. 4. cDAQ chassis

Fig. 5. Block Diagram

The ППН (voltage transducer) to be checked connects to the CompactDAQ system. The NI 9265 module forms the set values of the current and after that they are passed to the input of the ППН. The NI9401 module and the counter/timers in the NI cDAQ-9172 chassis measure the output frequency. The programme saves all the results to a file, with the possibility of further processing, and creates reporting documents for the checks performed, enabling the selection of period, technological system, verifier, etc.

Automated workplaces for check of convertors for multiplication of current signals БР-Т from the УКТС(unified hardware complex)-normal operation systems – more than 2,400 pcs. **CompaqDAQ hardware, manufacturer National Instruments. Own development 2012, implemented for Unit 6 Outage**

Fig. 5 Check of current convertors

БР-Т units are designed for galvanic isolation and formation of six identical output signals out of the input current signal.

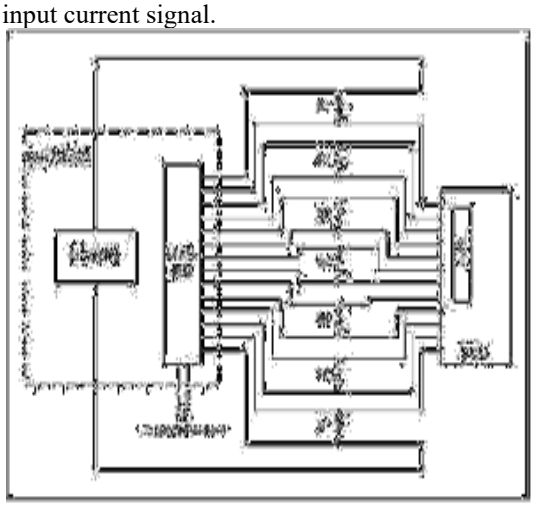

Fig. 6. Block diagram of an automated workplace

The NI-6704 module sets current which is passed in series through the resistors and the 6 channels of the convertor checked. The NI-4224 module measures the voltage drops over the seven standard resistors (6 for each channel of the БР-Т and one to compare the rest of them).

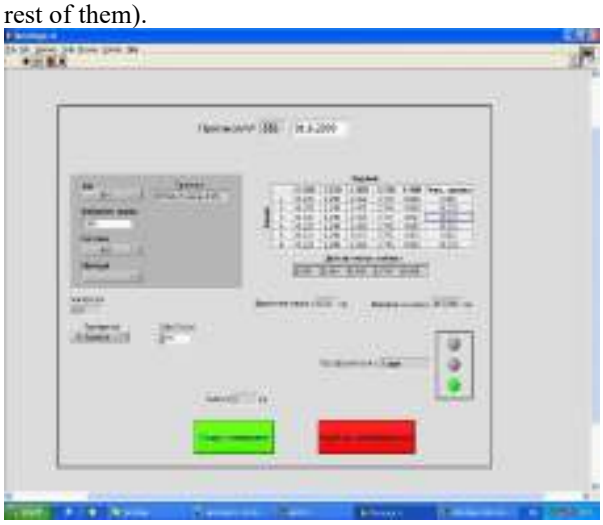

Fig.7 – Metrologic main display

Metrologic application performs the following:

- by means of the NI PXI-6704 module it detects sequentially the current value according to the set check points (e.g., 0,1-1,25-2,5-3,75-4,9 mA);
- using the NI PXI-4224 module, voltage drops are measured simultaneously on all channels of the unit at a rate of 1000 readings per second;
- it averages the readings for each channel separately;
- it calculates the measurement errors for each channel of the unit (by comparison with the measured value of the standard channel);
- it concludes on the suitability or unsuitability of the unit, depending on whether the maximum measurement error is within the permissible limits;
- it displays the results of the check, the errors and the conclusion (visually and in words);
- it saves all results to a file, with the possibility of further processing;
- it creates reporting documents for the check carried out, allowing the selection of period, technological system, verifier, etc.

The possibility of automatic entry of the data for the unit being checked by means of a barcode reader was introduced in the latest version of the programme which further reduced the check time.

Automated workplace for check of Triad T033 & Sineax P530 3-phase measuring transducers - more than 180 pcs. Own development 2015, implemented for Unit 5 Outage

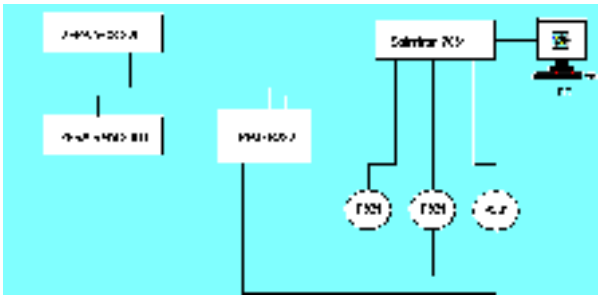

Fig. 8 Block diagram

The automated workplace for check of measuring transducers
includes:

- Solartron 7061 system voltmeter with 7½ digits.
- ZERA VCS 320 power source with a range from 1mA to 12A, from 30V to 500V, from 45Hz to 65Hz, power factor from 0 to ±1, and instability smaller than 0.1%.
- ZERA RMM 3000 reference multimeter with current and voltage ranges: from 1 to 200A, from 40 to 480V, and 0.05% uncertainty.
- LabView software package of National Instruments.
- Standard resistance coil P331 with nominal value 100Ω and 0.01% uncertainty – one per each channel of the measuring transducer checked.

Fig.9 – main display

MTransducer virtual instrument performs the following:

- it measures the voltage drops simultaneously on all channels by means of Solartron 7061 system voltmeter;
- it calculates the measurement errors for each channel of the measuring transducer;
- it concludes on the suitability or unsuitability of the measuring transducer, depending on whether the maximum measurement error is within the permissible limits;
- it displays the results of the check, the errors and the conclusion (visually and in words);
- it saves all results to a file, with the possibility of further processing;
- it creates reporting documents for the checks carried out.

Automated workplace for check of DMG700 and DMG800 3-phase analysers – more than 200 pcs. Lab View platform. Own development 2016, implemented for Unit 5 Outage (own development);

Fig. 10 Check of DMG700

The automated workplace for checking 3-phase analysers includes:

- PRS 600.3 power source (3-phase portable reference standard and power quality analyser) with a range from 1mA to 12A, 5V to 520V, 45Hz to 65Hz, power factor from 0 to ±1, and instability smaller than 0.02%.
- EXP1010 USB communication module;
- LabView software package of National Instruments.

The ***DMG700.vi*** virtual instrument performs the following:

- it sets parameters of the 3-phase grid – input voltage, current, power factor and harmonics by means of the PRS 600.3 power source, controlled via RS-232 channel;
- it reads the parameters measured by ***DMG700*** via UBS connection by means of the EXP1010 module;
- it calculates the measurement errors for each point of the check of the analyser;
- it concludes on the suitability or unsuitability of the analyser, depending on whether the maximum measurement error is within the permissible limits;
- it displays the results of the check, the errors and the conclusion (visually and in words);
- it saves all results to a file, with the possibility of further processing;
- it creates reporting documents for the checks carried out.

There are 11 measurements of active and reactive power with change of current, 8 measurements with change of voltage and phase angle, two measurements of THD by voltage and by current.

Automated workplace for the calibration of digital multimeters without communication interface, own development 2018

More than 100 digital multimeters (DMM) without communication interface are calibrated at NPP, and this process takes a lot of time and is related to the increased probability of mistakes by the operator entering the measured values. In order to optimize the calibration, an automated workplace has been developed that uses the possibilities of text optical recognition at LabView and automated calibration procedures at MET/CAL.

Fig. 11 LapView text optical recognition display

The automated workplace block diagram includes a personal computer with a GPIB controller, a multifunctional calibrator, a web camera and a digital multimeter.

Fig. 12 Block diagram of an automated workplace

The software is implemented by two individual sub-programmes:

- for the optical recognition of DMM values measured: LabView medium, which uses NI Vision Assistant and NI-IMAQ driver for USB Cameras.
- for the calibrator management, calculation of errors and recording of measurement results: MET/CAL software, Fluke company property.

Automated workplace for metrological check of WCM G01÷G08 (Westron Current Multiplicator)

Fig. 14 "Check WCM" Initial display

The technical protections at Kozloduy NPP are a part of the control system providing, in the event of an emergency, automatic implementation of discrete valve control operations. Metrological check of more than 4,500 cards is performed at Kozloduy NPP.

The card being checked is placed on the coupling of the bench. The current values set by the ***Check WCM*** application are formed by, then passed sequentially through the resistors and all channels of the card being checked. The NI-9239 module takes the values of the voltage drops across the resistors for each individual channel of the card checked, as well as the drop across the reference channel resistor.

Fig. 13 Record of results with "Check WCM"

Check WCM application performs the following:

- by means of a calibrator, the current value is sequentially detected according to the set check points;
- using the NI-9239 module, voltage drops are measured simultaneously on all channels of the unit at a rate of 1000 readings per second;
- it averages the readings for each channel separately;
- it calculates the measurement errors for each channel of the card (by comparison with the measured value of the standard channel);
- it concludes on the suitability or unsuitability of the card, depending on whether the maximum measurement error is within the permissible limits;
- it displays the results of the check, the errors and the conclusion (visually and in words);
- it saves all results to a file, with the possibility of further processing;
- it creates reporting documents for the checks performed, enabling the selection of period, technological system, verifier, etc.

III. CONCLUSION.

The implementation of automated workplaces enabled decrease of the subjective error factor when assessing and processing the measurement results, reduction of the time needed for the metrological control and timely development of the reporting documents following the activity. Conditions have been created for the accumulation of metrological checks data.

The examined developments ensure the quality performance of the metrological control activities, regardless of the reduced times for service and maintenance of the facilities.

REFERENCES

[1]http://www.ni.com;
[2]http://www.fluke.com;
[3]http://www.lovato.com

Reactor Coolant Pump Vibration Monitoring and Diagnostic System at Kozloduy NPP EAD (RCP VMDS - 195M)

Petio Simeonov
I&C Department
Kozloduy NPP EAD
Kozloduy, Bulgaria
ptsimeonov@npp.bg

Nadya Pagelska
Metrology Assurance Department
Kozloduy NPP EAD
Kozloduy, Bulgaria
nkpagelska@npp.bg

Vladimir Bashev
Metrology Assurance Department
Kozloduy NPP EAD
Kozloduy, Bulgaria
vtbashev@npp.bg

Ivaylo Cenov
I&C Department
Kozloduy NPP EAD
Kozloduy, Bulgaria
imcenov@npp.bg

Summary: *The report describes the implemented RCP vibration monitoring and diagnostic system and verification of measurement variables of the measurement channels for vibration velocity, vibration displacement and angular velocity (turnovers).*

- *It contains a short description of the vibration monitoring and diagnostic system (RCP VMDS - 195M).*
- *The structure of the vibration monitoring and diagnostic system (RCP VMDS - 195M), components, system operating modes, system graduation and calibration, and function of the main displays are considered are discussed.*

Key words: *The RCP VMDS – 195M, vibration monitoring and diagnostics, metrological verification, standards, graduation, calibration, and software for processing of the measurement results.*

I. INTRODUCTION

There are four 195 M type reactor coolant pumps in operation at Units 5&6 according to the design of Kozloduy NPP. In connection with the implementation of the approved design modification of the existing condition monitoring systems for the 195 M type reactor coolant pumps, there are 16 accelerometers and eddy current sensors (primary transducers) incorporated in the measurement channels for vibration velocity, vibration displacement and angular velocity, which are installed on each of the pumps. The installed primary transducers and related measurement transducers incorporated in the relevant measurement channel provide for the required input data based on which the system through the applicable software performs the vibration monitoring and diagnostics of the vibration parameters of the reactor coolant pumps. The systems were supplied and installed in 2021 under the WWER 1000 lifetime extension project.

II. VIBRATION MONITORING AND DIAGNOSTIC SYSTEM (RCP VMDS - 195M).

- The RCP VMDS - 195M is designed for both monitoring and diagnostics of vibration parameters of the 195M type reactor coolant pumps, and process parameters from the plant information and control system for early detection of the abnormal conditions of the mechanical and electric part of the reactor coolant pumps.

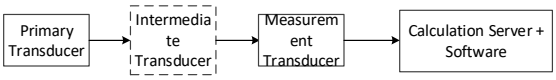

Fig. 1 Measurement channel configuration

- PT –Primary transducer
- IT - Intermediate transducer
- MT –Measurement transducer
- CS - Calculation server
- SW -Software
- Visualization of the data for recorded diagnostic events of the RCP VMDS - 195M;
- Operation of the RCP VMDS - 195M from a remote terminal;
- Interactive operation with the data base for the RCP VMDS - 195M;
- Providing the results from the functioning of the RCP VMDS - 195M;
- Recording, data processing, solution of diagnostic tasks, interaction with external systems, integrated processing and analysis of the data from the RCP VMDS - 195M; visualization and providing the information from the user of the RCP VMDS - 195M; documentation of the data from the operation of the RCP VMDS - 195M and reliable archiving of the all data;

III. MEASUREMENT VARIABLES OF THE VIBRATION MONITORING AND DIAGNOSTIC SYSTEM (RCP VMDS - 195M)

The implemented system consists of 64 measurement channels for the four reactor coolant pumps per unit. It provides for the metrological verification of the measurement variables of the measurement channels for monitoring and diagnostics of the vibration parameters of the 195M type RCP (Fig.2):
Measurement range of a measurement channel:

- Vibration velocity - ranging from 0 to 20 mm/s (from 2 to 3000 Hz) ± 3%;
- Vibration displacement of the rotor - ranging from 0.8 to 2.8 mm/s (from 1 to 5000 Hz) ± 3%;
- Angular velocity of the rotor rotation - from 0 to 1500 min^{-1} ± 3%;

Fig. 2 Vibration stand for verification of the measurement variables of accelerometers and eddy current sensors

IV. INSTRUMENTS FOR VERIFICATION OF THE MEASUREMENT VARIABLES

The description and characteristics of the instrumentation and equipment used for the verification of measurement variables are described in Table 1:

Table 1– Instruments for verification of the measurement variables

Description	Nominal values of the measurement limits	Tolerance
Signal generator Operating voltage, V Frequency, Hz	 5 10	 10 % ±0.05 %
Thermo hygrometer: Relative humidity, % Temperature, °C Atmospheric pressure, kPa	From 40 to 80 From 15 to 35 from 86 to 108	5 % ±2 °C ±1 kPa
Portable vibration stand: Root mean square of vibration velocity, mm/s Vibration displacement (peak-peak value), μm	from 0 to 20 From 0 to 1000	±3 %

V. METHODS FOR VERIFICATION OF THE MEASUREMENT VARIABLES

Before the beginning of every verification of measurement variables of a measurement channel of the RCP VMDS - 195M, a visual inspection to check for mechanical damage of the primary transducer body of the measurement channel and connection cable is carried out.

1. Verification of the measurement variables of the measurement channel for vibration velocity:

1.1 Graduation of the measurement channel for vibration velocity:

- placement of the primary transducer of the measurement channel for vibration velocity on the vibration stand platform;
- connection of the vibration stand;
- in the window of the software of the application software, the function for graduation of the measurement channel for vibration velocity of the relevant primary transducer is activated;
- calculation of the grading coefficients K_1 and K_2 is based on the measurement results with vibration parameters on the vibration stand: vibration velocity 1 and 18 mm/s at the frequency of 100 Hz:

$$K_1 = \frac{\bar{V}_{output2} - \bar{V}_{output1}}{V_{input2} - V_{input1}}, \qquad (1)$$

where:

$\bar{V}_{output1}, \bar{V}_{output2}$ - mean value of the results from 40 vibration velocity measurements of a measurement channel calculated by setting the first and second value of the vibration velocity on the vibration stand;

V_{input1}, V_{input2} - first and second values of the vibration velocity set on the vibration stand;

$$K_2 = \bar{V}_{output2} - V_{input2}.K_1, \qquad (2)$$

where:

$\bar{V}_{output2}$ - mean value of the results from 40 vibration velocity measurements of a measurement channelcalculated by setting the second value of the vibration velocity on the vibration stand;

V_{input2} - first and second values of the vibration velocity set on the vibration stand.

The grading coefficients are entered to the settings of the checked measurement channel for vibration velocity.

1.2 Definition of the measurement variables of the measurement channel for vibration velocity

In the window of the application software, the function for the definition of the measurement variables of the measurement channel for vibration velocity is activated:

- performance of the check within an amplitude range at the vibration frequency of 100 Hz and root mean square value of vibration velocity of 1, 5, 10, 15 and 20 mm/s;
- performance of the check within the frequency range for root mean square value of vibration velocity of 4 mm/s and vibration frequency of 30, 40, 80, 100, 160, 200,400 and 500 Hz.

2. Verification of the measurement variables of the measurement channel for vibration displacement

2.1. Graduation of the measurement channel for vibration displacement:

- it is performed as in Item 5.1.1
- grading coefficients K_1 and K_2 are calculated based on the results from the measurements at the vibration frequency of 100 Hz for two values of vibration displacement 50 and 350 μm according to the formulae (1) and (2).

The grading coefficients are entered to the settings of the checked vibration channels for vibration displacement.

2.2. Verification of the measurement variables of the measurement channel for rotor displacement

Identification of the signal generator parameters: signal shape - sinusoidal, frequency of generation 10 Hz, root mean square value of voltage 4 V.

The distance between the surface of the site of the vibration stand and the surface of the primary transducer of the measurement channel for rotor displacement should be 1.5±0.1 mm.

In the window of the application software, the function for the definition of the measurement variables of the measurement channel for vibration displacement is activated:

- performance of the check within an amplitude range at vibration frequency of 100 Hz and vibration displacement values of 50, 85, 175, 260 and 350 mm/s;

- performance of the check within the frequency range for vibration displacement velocity of 150 μm and vibration frequency of 30, 40, 80, 100, and 150 Hz.

3. Verification of the measurement variables of the measurement channel for angular velocity of the rotor rotation:

3.1. Verification of the measurement variables of the measurement channel for angular velocity of the rotor rotation

The distance between the surface of the site of the vibration stand and the surface of the primary transducer of the measurement channel for angular velocity of the rotor rotation should be 3.1±0.1 mm.

In the window of the application software, the function for the definition of the measurement variables of the measurement channel for angular velocity of the rotor rotation is activated.

- performance of the check at the vibration displacement value of 1000 μm and rotation frequency values of 480, 720, 1020, 1260, and 1500 1 Hz.

4. Processing of the measurement results

4.1. The relative percent error in the j^{th} point of the measuring range of the measurement channel for every i^{th} measurement is defined according to the formula:

$$\gamma_{ji} = \frac{X_{i\text{изм}} - X_{\text{д}}}{X_{\text{к}}} \cdot 100\ \%$$

4.2. The percent error of the n-measurement in the j^{th} point of the measurement span, γ_j, %, is defined according to the formula:

$$\gamma_j = \frac{1}{n}\sum_{j=1}^{n}\gamma_{ij}$$

where

n – the number of measurements of the signal in the j^{th}in the measurement span;

γ_{ij} – relative error in the i^{th} measurement of signal in the j^{th} point in the measurement units of the measured quantity.

4.3. The maximum of the actual values of the measurement channel error γ,%, obtained at all points in the measuring range are defined according to the formula:

$$\gamma = \max|\gamma_j|$$

where γ_j – relative percent error in the j^{th} point of the measuring range of the measurement channel.

The measurement channels are fit for operation if the maximum value of the obtained values does not exceed the value indicated in the technical documentation of the RCP VMDS - 195M.

After the completion of the operations for verification of measurement variables of the measurement channel, the data is recorded in the verification reports.

Upon a positive result of the verification of the measurement variables of the measurement channel of the RCP VMDS - 195M, a certificate for verification of the measurement variables of the RCP VMDS - 195M is issued.

VI. CONCLUSION

The implementation of the RCP VMDS - 195M provides for 100 % of metrological verification of a measurement channel. The system reduces the subjective error factor when assessing and processing the measurement results, reduction of the time required for the metrological control and prompt development of the final documentation following the activity. Conditions have been created for the accumulation of metrological verification data.

This development provides for qualitative and optimal performance of the metrological control activities.

Reference:

[1] 421412.120 И5 Metrology, Vibration Monitoring and Diagnostic System of Reactor Coolant Pumps at Units 5&6 of Kozloduy NPP (320 КАЭС RCP type VMDS). Procedure for verification of measurement variables. SRPA “Impulse”–Ukraine.

[2] 421412.120 ИЭ Vibration Monitoring and Diagnostic System of Reactor Coolant Pumps at Units 5&6 of Kozloduy NPP (320 КАЭС RCP type VMDS). Operating procedure. SRPA “Impulse”–Ukraine.

Calibration of pressure gauges, combined pressure gauges and vacuum gauges

1st Lyuboslav Hristov
Metrology Assurance Department
Kozloduy NPP EAD
Kozloduy, Bulgaria
LHHristov@npp.bg

2nd Petya Vassileva
Metrology Assurance Department
Kozloduy NPP EAD
Kozloduy, Bulgaria
PLVasileva@npp.bg

***Abstract*—The report discusses the requirements, methods and equipment to calibrate the pressure gauges, combined pressure gauges and vacuum gauges with scales in the measurement unit of the measured quantity or with scales with conventional intervals (further in after referred to as pressure gauges or calibrated instruments).**

The purpose is to find out the difference (deviation) between the pressure measured by the calibrated pressure gauge and reference pressure according to [1]. In the process of calibration, the real values of the pressure are identified in the measurement unit of the calibrated pressure gauge both in pascal, [Pa], or its multiple from the SI international system.

The technique is designed for the calibration of pressure gauges with a measuring range of minus 90 kPa to 60 MPa with an accuracy class higher or equal to 0.15 .

Key words—Pressure gauge, calibration, deviation, traceability

I. Introduction

The calibration is performed according to the method of direct comparison between the pressure measured by the reference pressure gauge and the calibrated pressure gauge.

The pressure created in the measuring system is measured by both the reference pressure gauge and the calibrated one.

The reference pressure gauge measures the pressure value set for the corresponding point of the measuring range of the calibrated pressure gauge.

The purpose is to find out the difference (deviation from) between the pressure measured by the calibrated pressure gauge and reference pressure according to [1]. In the process of calibration, the real values of the pressure are identified in the measurement unit of the calibrated pressure gauge both in pascal, [Pa], or its multiple from the SI international system.

Pressure gauges with a measuring range from minus 90 kPa to 60 MPa with an accuracy class higher or equal to 0.15 are subject to calibration.

II. Calibration conditions:

- Ambient temperature – 23 °C ± 5 °C, indicated in [1];
- Atmospheric pressure – from 950 hPa to 1050 hPa;
- The calibration is carried out in the absence of vibrations;
- The variation of temperature during calibration should be less than 1°C.

III. Applied reference equipment

Digital pressure gauges and vacuum gauges with uncertainty (from the latest calibration certificate) less than or equal to 1/4 of the permissible error of the calibrated pressure gauge for the relevant set value

The measuring range of the reference pressure gauge should correspond to the range of the calibrated pressure gauge.

The reference pressure gauge should be traceable to a national measurement standard.

IV. Sequence of the operations during calibration

The pressure gauge is reset if the design of the pressure gauge allows it. The set-up of zero is not allowed between the individual measurement series.

The pressure is gradually changed from the lower to the upper limit of the measuring range.

The readings for different values (points) of the set pressure, which, where possible, are uniformly distributed in the measuring range, are taken into consideration. The upper and lower limit values must be included.

Furthermore, the operations will be repeated when the pressure is decreased, from the upper to the lower limit of a measuring range.

TABLE 1

Calibration sequence		***Type A Figure No. 1***	***Type B Figure No. 2***
Accuracy class of the calibrated pressure gauge		0.1 to 0.6	Above 0.6
Number of measuring points with zero		9	5
Pre-set pressure increase to the maximum value, maximum value (number)		2	1
Pressure change + Response time (seconds)		> 30	> 30
Delay time to reach the final value of measuring series (minutes)		2	2
Number of measuring series	ascending order	2	1
	descending order	1	1

The measuring series are performed according to Table 1 depending on the accuracy class of the calibrated pressure gauge according to [1].

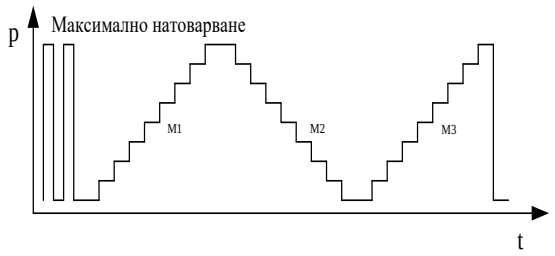

Fig. 1

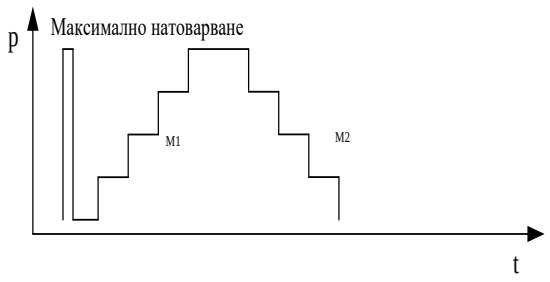

Fig. 2

V. PROCESSING OF CALIBRATION RESULTS

A. Mathematical model

The mathematical model specified in [1] of the relation between the pressure measured by the calibrated pressure gauge, the pressure measured by the reference pressure gauge, and the input quantities is as follows:

$$\Delta P = P_{изм.} - \overline{P}_{em.} + \delta P_{хист.} + \delta P_{повт.} + \delta P_{нула} \quad (1)$$

where:

ΔP - deviation of the pressure measured by the calibrated pressure gauge from the actual pressure (measured by the reference pressure gauge);

P_{change} – value measured by the calibrated pressure gauge;

$\overline{P}_{standard}$ – root mean square value of the set (real) value of the reference pressure gauge with the correction from the calibration certificate;

$\delta P_{hysteresis}$ - evaluation of the correction for hysteresis of the readings of the calibrated pressure gauge;

$\delta P_{repeatability.}$ - evaluation of the correction for repeatability of the readings of the calibrated pressure gauge;

δP_{zero} - evaluation of the zero-point correction.

B. Evaluation of the input quantities, Xi

Evaluation of the quantity measured by the calibrated pressure gauge is defined as arithmetic mean value $\bar{P}_{em}$

$$\overline{P}_{em,j} = \frac{1}{n}\sum_{i=1}^{n} x_{i,j} \quad (2)$$

where:

$x_{3,j}$ – readings of the reference pressure gauge for the *i*-series of measurements for the j[th] point;

n – number of series.

$P_{изм}$ is the reading of the calibrated pressure gauge for the relevant rated value.

The evaluation of the correction of the hysteresis of readings $\delta P_{hysteresis}$ is a rectangular distributed quantity with zero value and dissipation area with a value calculated according to the formula:

$$h_j = |(x_{2,j} - x_{1,0}) - (x_{1,j} - x_{1,0})| \quad (3)$$

where:

h_j – hysteresis of the j[th] point;

$x_{1,0}$ – readings of the calibrated pressure gauge for pressure equal to zero for the first series of measurements;

$x_{2,,j}$ – readings of the calibrated pressure gauge for the j^{th} point for the second series of measurement;

$x_{1,,j}$ –readings of the calibrated pressure gauge for the j^{th} point for the first series of measurement.

The evaluation of the correction of the hysteresis of the readings δP_{hyst} is a rectangular distributed quantity with zero value and dissipation area with a value calculated according to the formula:

$$b_{repeatability\ ,j} = |(x_{3,j} - x_{3,0}) - (x_{1,j} - x_{1,0})| \quad (4)$$

$$b = max\{b_{repeatability,j}\} \quad (5)$$

where:

$x_{3,0}$ – readings of the calibrated pressure gauge for pressure equal to zero for the third series of measurements;

$x_{1,0}$ – readings of the calibrated pressure gauge for pressure equal to zero for the first series of measurements;

$x_{3,,j}$ – readings of the calibrated pressure gauge for the *j*-th point for the third series of measurements;

$x_{1,,j}$ –readings of the calibrated pressure gauge for the j^{th} point for the first series of measurements.

The evaluation of the zero-point correction $\delta P_{hysteresis}$ is a uniformly distributed quantity with zero value and dissipation area with a value calculated according to the formula (5).

The zero point is set up before the first measuring cycle and should be recorded before and after the measuring cycle. The deviation from the zero point is calculated according to the formula:

$$f_o = \{x_{2,0} - x_{1,0}\} \quad (6)$$

where:

$x_{1,0}$ – readings of the calibrated pressure gauge for pressure equal to zero for the first series of measurements;

$x_{2,0}$ – readings of the calibrated pressure gauge for pressure equal to zero after the second series of measurements;

C. Root mean square uncertainty of the inputs, u(xi)

- Root square uncertainty of the input estimates of the quantities characterized by rectangular distribution are calculated according to the formulae:

› The contribution to the uncertainty of $P_{изм}$ is evaluated by the end resolution of the calibrated pressure gauge *r* and is a rectangular distributed quantity with value of zero and limits equal to 1/10 of the value of one of the scale intervals of the relevant pressure gauge:

$$u(r) = \frac{r}{\sqrt{3}} \quad (7)$$

› for the hysteresis correction of the readings:

$$u(\delta P_{hysteresis}) = \frac{h}{2.\sqrt{3}} \quad (8)$$

› for the correction of the repeatability of the indications:

$$u(\delta P_{repeatability}) = \frac{b}{2.\sqrt{3}} \quad (9)$$

› of the correction of the deviation from the zero point of the readings:

$$u(\delta) = \frac{f_0}{2.\sqrt{3}} \quad (10)$$

- Root square uncertainty of the contribution to the uncertainty of the measurement imported from the reference pressure gauge is calculated according to the formula:

$$u(P_{em.}) \quad (11)$$

where:

U_{ref} – expanded uncertainty of the reference pressure gauge from the calibration certificate for the relevant value;

k - coverage factor, from the calibration certificate of the reference pressure gauge;

In the event the value of U_{em} is unknown from the certificate, the highest value for the relevant range is accepted.

In the event U_{em} is significantly lower (up to 5 times the contribution, which is usually that from the resolution of the calibrated pressure gauge), the determination of the total combined uncertainty is neglected.

D. Sensitivity factors

When evaluating the measured pressure values and contribution of the inputs, the functional dependence $P = f(x_i)$ is linear and the sensitivity factors are $|c_i| = 1$.

I. Contributions to the measurement uncertainties, ui(p).

The contributions to the inputs $u(x_i)$ for the uncertainties of the measured pressure are calculated as:

$$u_i(p) = c_i.u(x_i) \quad (12)$$

F. Combined root square uncertainty, uc(P)

When all inputs are non-correlated or the correlation between them is negligibly low, the combined root square uncertainty of the measured pressure is calculated as a square root of the sum of the contributions of the inputs:

$$u_c(P) = \sqrt{\sum_{i=1}^{n} u_i^2}\,(p) \quad (13)$$

G. Expanded uncertainty, U

The expanded uncertainty *U* of the measured pressure is calculated according to the formula:

$$U = k.u_c(P) \quad (14)$$

where:

The value of *k* is defined according to the selected coverage factor. For a coverage factor of 95 %, *k* is accepted to be equal to 2.

VI. Conclusion

The presented methods for calibration of pressure gauges, combined pressure gauges and vacuum gauges with a digital pressure gauge are developed in compliance

with the requirements of the company and international regulations.

It is designed to comply with the requirements for providing traceability of the measurement results when calibrating the pressure gauges, combined pressure gauges and vacuum gauges.

When the pressure gauge complies with the requirements of the current methodology, a calibration certificate is issued.

It is assumed that the maximum value of all obtained values is indicated as the uncertainty of the performed calibration.

There are three electronic procedures developed for calibration of pressure gauges Mechanical gauge kgf/cm2, Mechanical gauge bar, Mechanical gauge Pa in software METCAL Runtime to MET/TEAM. Working conditions, access to the relevant software necessary for the implementation of the procedures and qualified personnel to work with them are provided.

When starting the procedure in METCAL Runtime we have the option to enter environmental parameters (temperature, humidity), enter input data for the calibrated manometer such as range, accuracy class, resolution, number of scale divisions, then proceed to enter the reported values during the calibration of the corresponding pressure gauge for the corresponding number of calibrated points according to the current methodology.

METCAL Runtime software performs the necessary calculations to process the entered data and then generates an electronic document with the calibration results (calibration certificate).

Developed procedures provide an opportunity:

-limits the possibility of errors during data entry and processing by the specialist who performed the calibration,

-significantly reduces calibration time,

-ensures the storage of information in a single database,

-ensures traceability over time of the metrological characteristics of each means.

REFERENCE

[1] German Calibration Service (former DKD). Calibration of pressure measuring devices DKD-R 6-1

[2] Radev, R., Metrology and measurement equipment, Sofia, 1986

Metrology Assessment Frame of the Production of Power Transformers and Tap Changers

Iliyana Bogdanova
Department of Electrical Measurements
Technical University of Sofia
Sofia, Bulgaria
ibogdanova@tu-sofia.bg

George Milushev
Department of Electrical Measurements
Technical University of Sofia
Sofia, Bulgaria
gm@tu-sofia.bg

***Abstract*— The paper presents a frame of the structure of the metrology assessment of the production of power transformers and tap changers based on the experience of the authors. The main processes in the production are described with the relevant measurement tools for each operation. Metrological characteristics of the proposed measurement devices are considered. (*Abstract*)**

Keywords— Metrology, Metrology Assessment, Measurement Tool, Power Transformer, Tap Changer, Measurement Process, Metrological Characteristics

I. Introduction

The production of power transformers and tap changers is a key element of building electrical infrastructure. The establishment of such production requires a significant long-term investment in metrological assets as laboratories with corresponding management systems, qualified personnel, measurement tools and measurement systems. The decisions about the selection of the proper metrology assets determine the quality level of the production of power transformers and tap changers. The production specifics define the production processes. Metrology assessment is consequently defined by the typical metrology processes corresponding to the production ones. The paper aims to specify the typical measurement tools with the relevant metrology characteristics based on the metrology processes in the production of power transformers and tap changers.

II. Production Processes and Relevant Control

Significant importance from metrological the point of view have the different types of control and inspections before, during and after the production processes.

A. Final Control

The final control includes inspections during the preparation for shipment /packing, marking/, including a check for compliance with the technical documentation and the contract.

B. Incoming Control

The incoming control of the products has the goal to establish compliance with technical documentation, product identification and document control results. It includes organoleptic inspection, samples taking, measuring and testing.

Measurement tools and instruments necessary for these important inspections are:

- Gas Chromatograph for transformer oil;
- Spectral Analyzer for chemical composition of materials;
- Closed crucible flame temperature instrument with a range of 0 to 150 °C and a resolution of 0,1 °C;
- Titration system;
- Device for the breakdown strength of liquid dielectrics with a range up to 100 kV and accuracy class 5;
- Tan δ of liquid dielectrics measuring instrument;
- Testing machine from 0 to 100 kN and accuracy class 1; resolution 0,01 N, U – 0,5 %
- Testing machine with a range up to 2500 N and a resolution of 0,001 N;
- Microohmmeter with a range 0,001 mΩ to 200 Ω;
- Hipots with ranges 10 kV and 50 kV, accuracy class 5;
- Analytical Balance with a range of 220 g and resolution of 0,001 g.

C. Production and After Sales Service Operations

The production technical processes directly related to the quality in the creation of the products are: preparation, mechanical processing /turning, milling, grinding/, welding, assembly, drying, oiling, varnishing, packaging, storage and shipping. Each process requires operational control using the respective measurement tools and systems.

III. Operational Control of the Production of Power Transformers

Specific processes and the required operational control of the production of power transformers are listed here:

A. Control of Isolation Parts

The control of isolation parts is a dimensional control with measuring devices:

- Type measure with a range of 3 m and resolution 1 mm;
- Calipers (Fig. 1.) with ranges 150 mm, 320 mm and 500 mm with resolution respectively 0,05 mm, 0,02 mm and 0,01 mm;

The authors would like to thank the Research and Development Sector at the Technical University of Sofia for the financial support.

978-1-6654-8569-2/22/$31.00 ©2022 IEEE

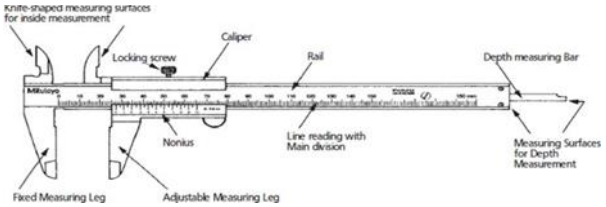

Fig. 1. Caliper for dimensional control

B. Control of cross cutting of electrical steel

The indicators of control are: dimensions, hems, deviation from the shape and appearance.

- The control of the dimensions is carried out on a measuring table with dimensions X 3 m, Y 1,5 m;
- The size of the hems is measured with a micrometer (Fig. 2.) with a range of 25 mm and resolution 0,01 mm;

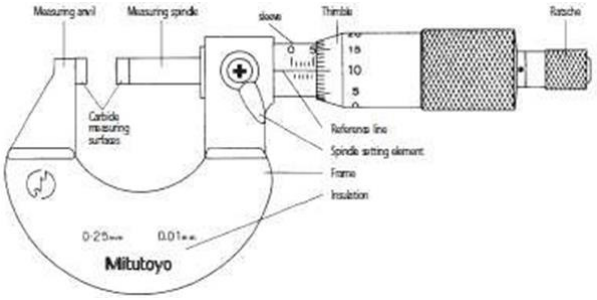

Fig. 2. Micrometer for dimensional control

- The control of shape deviations is carried out with plates with a width of 150 mm.

C. Control of the Corps

The indicators are: dimensions of the core, appearance, quality of the mounting, inspection of the isolation with applied voltage.

The appropriate measuring tools are:

- Calipers (Fig. 1.) with ranges150 mm, 500 mm and 1000 mm with with resolution respectively 0,05 mm, 0,02 mm and 0,01 mm;
- Type measures with ranges of 3 m, 5 m and 10 m and resolution 1 mm;
- Diametral tape measure with range of 10 m and resolution 1 mm;
- A set of gauge plates;
- Torque wrench with a range 5-40 Nm and uncertainty 3.5 %;
- Insulation dielectric strength meter with ranges from 500 to 2500 V AC, 50 Hz, accuracy class 0,5.

D. Coil Control

The control indicators are: appearance, dimensions and checking for continuity and short circuit between parallel wires.

- A tape measure with a range of 3 m and resolution 1 mm is the tool for control indirectly the outside and inside diameter of the coil;
- A voltage tester 36 V DC is appropriate to check the continuity and short circuit between parallel wires.

E. Control during and pressing of coils

Control indicators are crimp force, coil height, continuity check and short circuit between parallel leads.

- A press with a range of up to 190 tf with
- A digital pressure gauge display device class 0.5 with a range of 600 bar, a resolution of 1 bar to control the press force;
- A tape measure with ranges of 3 m, 5 m and 10 m and resolution 1 mm to control the height;
- A voltage tester 36 V DC to test the continuity.

F. Control during the installation of the active part of power transformers

The control has three stages 1) after charging, 2) before drying and 3) after drying. The appropriate measuring tools are:

- A tape measure with range 3 m and resolution 1 mm for dimensional measurements;
- A transformer ratio meter with ranges 5/5 A and 50/5 A, uncertainty 0,0006 to 0,001 to measure the transformer ratio between parts of HV coil and LV coil for all the positions of the tap changer.
- System for measurement of idle losses for phase by phase measurement of idle current and idle losses described below (Fig. 3.)
- Microohmeter with ranges 2 Ω and 20 Ω, uncertainty 0,004 mΩ to 0,0008 Ω to measure the coils resistance with DC current
- Insulation dielectric strength meter with 2000 V AC, 50 Hz, for control of the isolation

G. Control during the installation of built-in air reactors

- Torque wrench to control stud tightening torques;
- Caliper for dimensional measurements;
- Plumb line and tape measure to control reactor vertical deviations;
- Insulation dielectric strength meter with 2500 V AC, 50 Hz, for control of the isolation;
- R-L meter to control the resistance and inductance of the coils.

H. Measurement and testing of transformers in the production process

- System for measurement of idle losses (Fig.3.) consists:

1 Generator

2 Additional transformer

3 Current transformer (Table I.)

4 Voltage transformer (Table I.)

5 Transformer under test

6 AC-Power Analyzer with ranges 0,1÷1000 $V_{AC/DC}$; 0,03÷10 A $_{AC/DC}$; uncertainty from 0.006 to 0.011 range

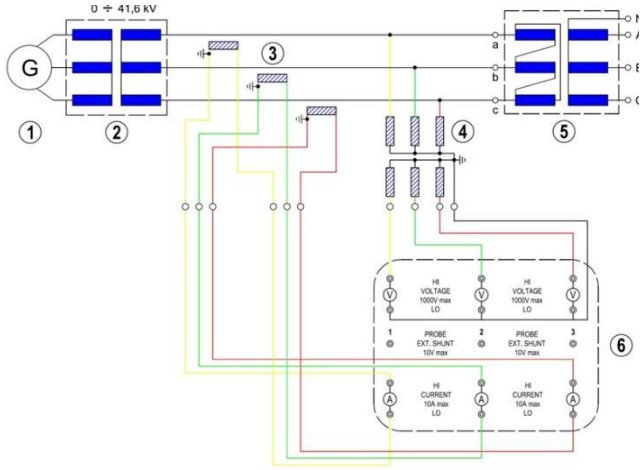

Fig. 3. Idle losses measurement system

TABLE I. TRANSFORMERS USED WITH IDLE LOSSES MEASUREMENT SYSTEM

№	Transformer Specification		
	Transformer type	***Rates***	***Uncertainty***
1	Instrument current transformer	5, 10,20 / 5 A	0.003 %; 0.13 min
2	Instrument current transformer	50, 100, 200 / 5 A	0.004 %; 0.16 min
3	Instrument current transformer	500, 1000, 2000 / 5 A	0.005 %; 0.18 min
4	Instrument current transformer	6000/5 A	0.005 %; 0.16 min
5	Instrument voltage transformer	6-10-15-20-30/0.1 kV	0.009 %; 0.30 min

- A megaohmmeter with applied voltages of 1000V, 2500V, 5000 V and uncertainty form 1,2 MΩ to 2,3 MΩ is used for control of the insulation of the magnet core. It tests the isolation between the coils and the tank (Fig. 4.);

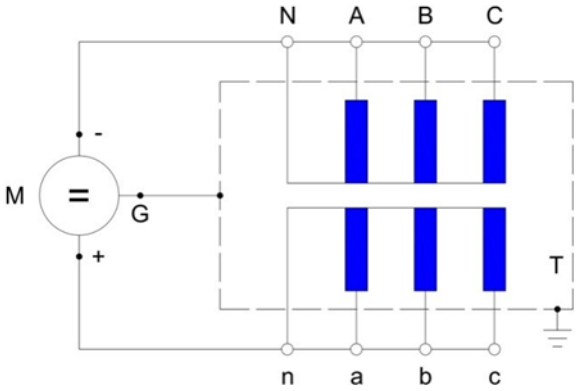

Fig. 4. Insulation Measurement of the transformer

- A digital thermometer with a range from 0 ºC and 300 ºC with a resolution of 0,1 ºC is used during the insulation test;
- A Transformer Ratio Meter with range 1 ÷ 9999, uncertainty 0,3 %, class 1 is used for transformers ratio control.

IV. OPERATIONAL CONTROL OF THE PRODUCTION OF TAP CHANGERS

The measurements and tests of tap changers and switches without excitation, carried out in the production process, are control measurements and type measurements. Specific processes and the necessary operational control of the production of tap changers follow:

A. Control of the mounting of the auger mechanism with a pointer

- Caliper or air gauge for control of worm axial clearance
- Air gauge to control of the clearance between shaft with sleeve and flywheel (Maltese wheel)

B. Control of the installation of switches without excitation

- Contact pressure measuring device (for 200 A and 400 A from 45 N to 55 N, for 630 A and 1000 A from 55 N to 70 N) with a range 20 N, resolution 1 N and uncertainty form 0,8 to 1,8 N
- Torque wrench to control the tightening of bolted joints

C. Testing the manual operation of a switch without excitation

- Continuity tester;
- Multimeter;
- Insulation dielectric strength meter with 2000 V AC, 50 Hz, for control of the isolation;

D. Dielectric type test of tap changers and switches without excitation

The technical provision meets the requirements of IEC 60060-2:2010 and consists of:

- Impulse system for impulse voltage including: Control unit, voltage regulator, compensating reactor LV, control cables, fail-safe circuit breaker, control and measurement system, high-voltage generator /cascade/, voltage divider, partial discharge interference filter for high voltage, connected capacitor;
- tg δ measurement system with range 100 pF (50 Hz), 300 pF (50 Hz), 1000pF (50 Hz), 10000pF (50Hz), 7000pF (50 Hz) with uncertainty from 1,2 to 1,6 %;
- Partial discharge measurement system LI and SI consisting: HV divider type 3600/400, two LV parts, 75 Ω cable, digital registration type HIAS 743. Uncertainty for the ranges 200 kV - 700 kV LI from 1.9 % to 4.3 %, 400 kV LIC from 1.9 % to 5.4 %, 30 kV - 400 kV-LI from 2.5 % to 5.4 %, 200 kV LIC from 2.2 % to 4.2 %, 200 kV - 500 kV SI from 1.6 % to 2.6 %;
- Digital pulse recording system with ± 3% accuracy;
- High voltage pulse voltage divider 700 kV, uncertainty from 0,86% to 4,08 % in a set with amplitude voltmeter class 0,5;
- AC voltage divider kit;
- Amplitude voltmeter with a range of 8,48 V to 141,42 V and an uncertainty of 0,0047 V to 0,06 V;
- Set of apparatus for measuring partial discharges with range 1-100000 pC and uncertainty from 1,22 to 0,65 %.

E. Type test of mechanical wear resistance of tap changers and switches without excitation.

- A test bath in which the tested tap changers and switches without excitation can be completely immersed;
- Motor drive;
- Low temperature chamber that can reach a temperature of minus 25 ºC;
- Device for creating pressure with a value of 0.6 bar;
- Source with a voltage of 15 V and a current of up to 5 A;
- Four channels oscilloscope with ranges from 0,005 to 0,048 V;
- Two channels oscilloscope with ranges from 1 mV to 5V/div; time base from 0,2 s to 2 s/div, uncertainty from 0,01 mV to 0,1 V
- Pressure gauge with an accuracy class at least 1;
- Contact thermometer with a range from 0 ºC to 100 ºC.

F. Type test of electrical wear resistance of tap changers with reduced step voltage

- Power Transformer;
- Loading Resistors;
- Complex switchgear with a breaker Un ⩾ 1300 V, In ⩾ 400 A;
- Current transformers 2000/5 A, class 1;
- Voltage transformers 10000/100 V;
- Amplitude limiter for the arc voltage registration with measurement system;
- Ammeter with accuracy class 1.

G. Type test of overheating of current-limiting resistors of tap changers

- Electrical power source 400 V; 515 V; 1300 V;
- Thermocouples type T;
- Motor drive or contactor;
- Time relays;
- Oscilloscope;
- Current transformer class 0,5;
- Reference resistor 1%;
- Ammeter with accuracy 0,5%.

H. Type test of overheating of the contact points of a current-carrying loop of tap changers and switches without excitation

- Adjustable voltage source;
- Current injector;
- Bath clean insulating liquid;
- Thermocouples type T;
- Reference thermometer with a range of 0 to 300 ºC;
- Current transformer class 0,5;
- Ammeter with accuracy 0,5%.

I. Type test of tap changers with short-circuit currents

- Primary current injector 4000 A, 8KVA, 0.5% accuracy
- Circuit break timer test set

J. Type test of electrical wear resistance of tap changers with nominal step voltage and switching off abilities

Same equipment as the type test of electrical wear resistance of tap changers with reduced step voltage is used.

V. CONCLUSION

An overview of the measurement instrumental set necessary for the production of Power Transformers and Tap Changers is done in the form of specification. The specification bases on the typical test and measurement processes for such production. For most items the general metrology parameters are specified. The processes are well separated. Some of the instruments are used in several processes.

The presented specification is appropriate for general planning of the metrology assurance of the production, planning a calibration schedule, planning metrology investments etc.

REFERENCES

[1] T. Grozdanov and I. Yachev, High Voltage Electrical Apparatuses, Ist. Ed., ICON, 1994

[2] T. Grozdanov, Tap Changers for High Voltge, Hyundai Heavy Industries Co – Bulgaria – 2011

[3] Elprom Heavy Industries – A Company Materials for Power Transformers and Tap Changers

[4] P. Penchev, Electrical Apparatuses, Technica, Sofia 1976

[5] A Dachev, Special Power Transformers, Technica, Sofia, 1967

SECTION X
QUALITY MANAEMENT AND CONTROL

Quality Management and Control Training Within the ICT-TEX Project

Velizar Vassilev
Faculty of Mechanical Engineering
Technical University of Sofia
Sofia, Bulgaria
vassilev_v@tu-sofia.bg

Sanja Ercegovic Razic
Faculty of Textile Technology
University of Zagreb
Zagreb, Croatia
sanja.ercegovic.razic@ttf.hr

Angel Terziev
Faculty of Power Engineering and Power Machines
Technical University of Sofia
Sofia, Bulgaria
aterziev@tu-sofia.bg

***Abstract*— This paper gives a brief presentation of the ICT-TEX project, as well as discusses the main points of the developed module Industrial Engineering, Quality Control, and Management and its courses "Information Technologies for Statistical Analysis and Quality Control" and "QMS/EMS implementation and control".**

Keywords*— *textile industry, Erasmus+, ICT-TEX, training course, quality control, quality management systems.

I. Introduction

The European textile industry is a traditional but leading sector, with around 160.000 small and medium-sized companies. They are renowned for their innovative and high-quality products and focus on creativity and an outstanding customer service. It is important that the next generation textile industry workforce is well educated and has the required competencies and skills. The ICT-TEX project (ICT in Textile and Clothing Higher Education and Business) responds to this need by elaborating a number of on-line courses. It is an EU funded project that aims to improve the competencies in Information and Communication Technology (ICT) for people working in the Textile and Clothing Industry (TCI) field. The project is an Erasmus+ Knowledge Alliance, which are transnational result - driven projects with partners from higher education and business aiming to strengthen Europe's innovation capacity and foster innovation in higher education [1].

II. About the Project

To capture the real needs in the Textile and Clothing Industry in terms of the digital skills of its employees, desk research, field research and a gap analysis whereas performed. The full report with detailed results of the findings of this study is available on the project website (https://ict-tex.eu/). The study resulted in defining the specific topics of the courses to be developed within the project. They are structured into eight modules, covering all textile subareas (Knitwear; Woven fabrics; Apparel, Technical and smart textiles; Industrial engineering, quality control and management; Finishing, printing, and functionalization), completed with a module on Digital Skills and one on Entrepreneurial Skills (Fig. 1). For each of the courses within these modules, clear course objectives and learning outcomes (in terms of knowledge, skills, and responsibilities) are defined. The learner is also informed on the required time investment.

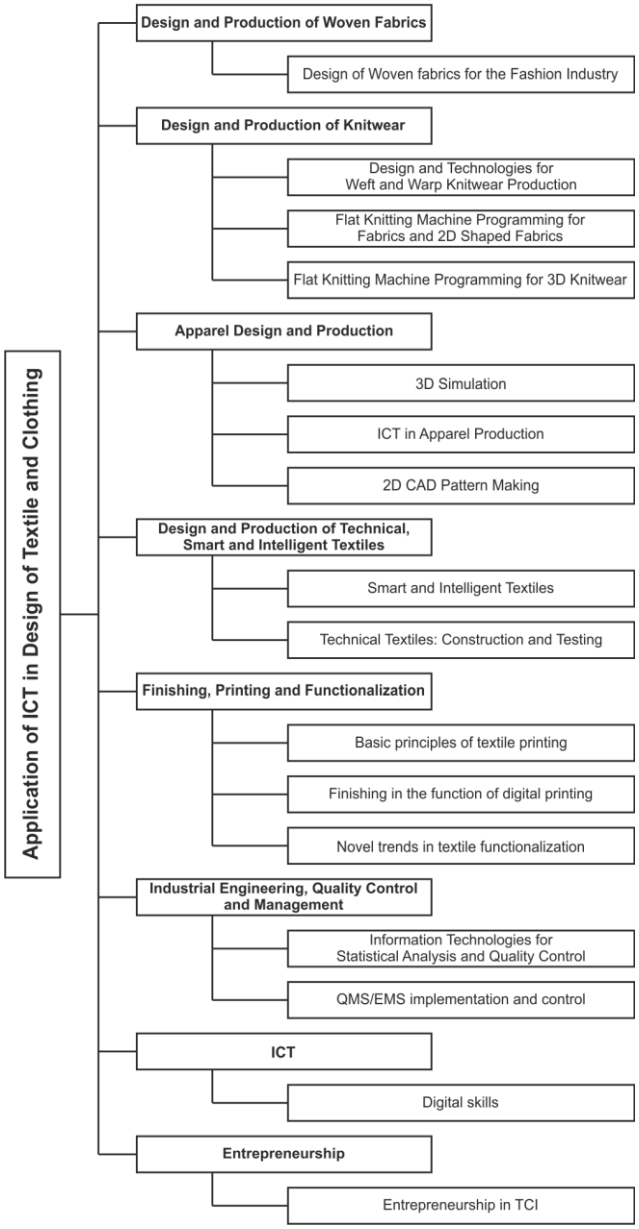

Fig. 1. Curriculum of the Application of ICT in Design of Textile and Clothing

978-1-6654-8569-2/22/$31.00 ©2022 IEEE

The courses are made available on the ICT-TEX web platform, that which has been developed on top of the well-known MOODLE open-source management platform. The platform is very user-friendly and flexible in use. The course target three groups of learners: students with a bachelor's degree, Staff, and University teachers/researchers.

Last year, five pilot courses have been made available on the platform: 2D CAD Pattern Making, 3D CAD Simulations, Apparel Production (part of the module on Apparel Design and Production), Entrepreneurship in TCI and Digital Skills. This year (2022), all other courses are publicly available[1].

III. About the Information Technologies for Statistical Analysis and Quality Control Course

A. *Course objectives*

Information technology systems can improve quality and increase productivity. In addition to software different statistical methods can be used to evaluate critical processes in order to control production procedures and performances. The course in Information Technologies for Statistical Analysis and Quality Control includes basic issues of mathematical statistics and its application for the needs of the textile and clothing industry. The training is carried out with both universal and specialized software products.

B. *Course Topics*

The course consists of the following 12 topics:

- The Seven Basic Quality Control Tools
- The Seven Management and Planning Tools
- Quality function deployment (QFD)
- Failure modes and effects analysis (FMEA)
- Probability distributions with application in textile practice
- Statistical estimates of random variables
- Testing of non-parametric statistical hypothesis
- Testing of parametric statistical hypothesis
- Application of statistical hypothesis tests in Statistical Process Control (SPC) and Acceptance Sampling (AS)
- Analysis of variance (ANOVA)
- Regression analysis
- Design of experiments

Every topic includes theory, step-by-step calculations and examples. These examples are separated in three sections:

- for students;
- for staff
- for university teachers/researchers.

The examples for the students are developed with MS Excel, the examples for the staff are developed with Minitab and the examples for university teachers/researchers are developed with the data science programming language "Python".

Screenshots of some of the examples for Analysis of variance (ANOVA) lesson are given in fig. 2, fig. 3 and fig. 4.

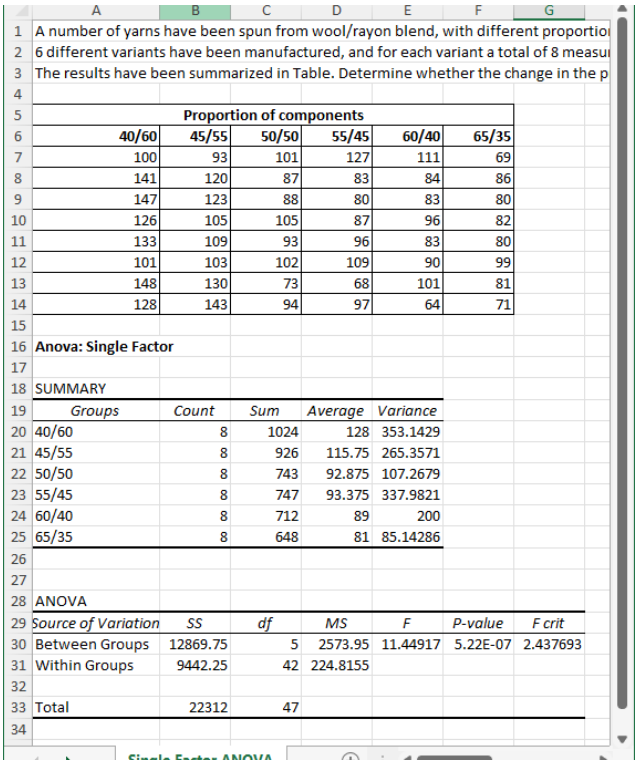

	A	B	C	D	E	F	G
1	A number of yarns have been spun from wool/rayon blend, with different proportio						
2	6 different variants have been manufactured, and for each variant a total of 8 measu						
3	The results have been summarized in Table. Determine whether the change in the p						
4							
5		Proportion of components					
6		40/60	45/55	50/50	55/45	60/40	65/35
7		100	93	101	127	111	69
8		141	120	87	83	84	86
9		147	123	88	80	83	80
10		126	105	105	87	96	82
11		133	109	93	96	83	80
12		101	103	102	109	90	99
13		148	130	73	68	101	81
14		128	143	94	97	64	71
15							
16	Anova: Single Factor						
17							
18	SUMMARY						
19	*Groups*	*Count*	*Sum*	*Average*	*Variance*		
20	40/60	8	1024	128	353.1429		
21	45/55	8	926	115.75	265.3571		
22	50/50	8	743	92.875	107.2679		
23	55/45	8	747	93.375	337.9821		
24	60/40	8	712	89	200		
25	65/35	8	648	81	85.14286		
26							
27							
28	ANOVA						
29	*Source of Variation*	*SS*	*df*	*MS*	*F*	*P-value*	*F crit*
30	Between Groups	12869.75	5	2573.95	11.44917	5.22E-07	2.437693
31	Within Groups	9442.25	42	224.8155			
32							
33	Total	22312	47				
34							

Fig. 2. Example of solving a texitle industry problem with Single Factor ANOVA and MS Excel

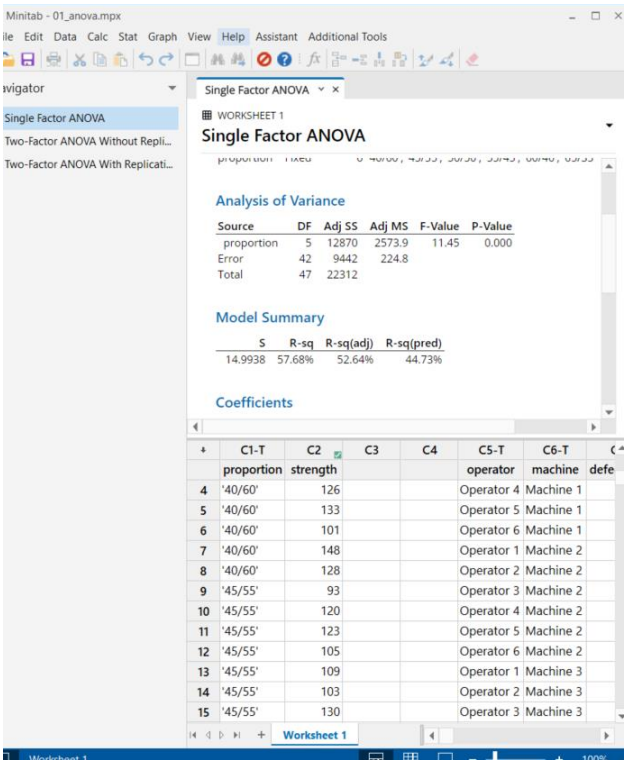

Fig. 3. Example of solving a texitle industry problem with Single Factor ANOVA and Minitab

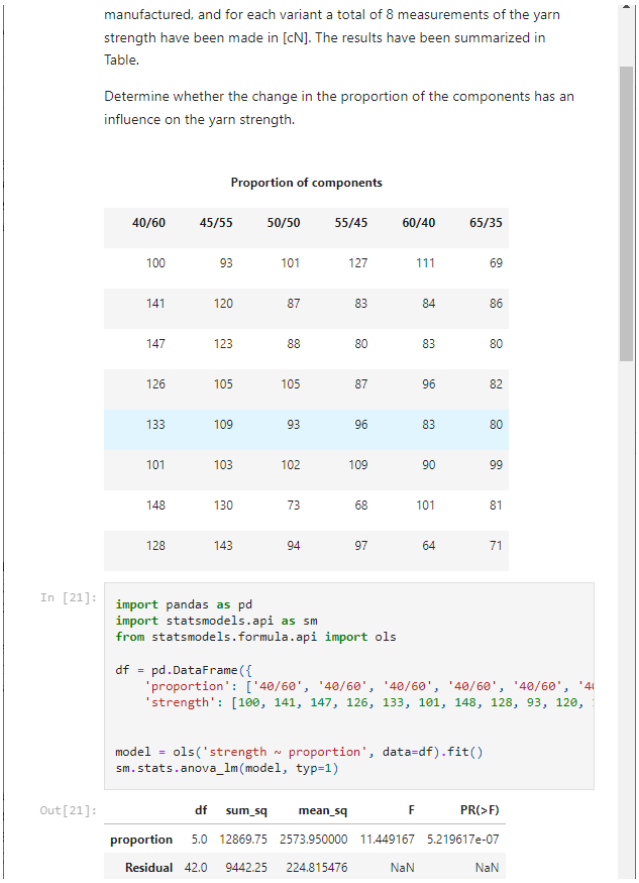
manufactured, and for each variant a total of 8 measurements of the yarn strength have been made in [cN]. The results have been summarized in Table.

Determine whether the change in the proportion of the components has an influence on the yarn strength.

Proportion of components

40/60	45/55	50/50	55/45	60/40	65/35
100	93	101	127	111	69
141	120	87	83	84	86
147	123	88	80	83	80
126	105	105	87	96	82
133	109	93	96	83	80
101	103	102	109	90	99
148	130	73	68	101	81
128	143	94	97	64	71

In [21]:
```
import pandas as pd
import statsmodels.api as sm
from statsmodels.formula.api import ols

df = pd.DataFrame({
    'proportion': ['40/60', '40/60', '40/60', '40/60', '40/60', '4
    'strength': [100, 141, 147, 126, 133, 101, 148, 128, 93, 120,

model = ols('strength ~ proportion', data=df).fit()
sm.stats.anova_lm(model, typ=1)
```

Out[21]:

	df	sum_sq	mean_sq	F	PR(>F)
proportion	5.0	12869.75	2573.950000	11.449167	5.219617e-07
Residual	42.0	9442.25	224.815476	NaN	NaN

Fig. 4. Example of solving a texitle industry problem with Single Factor ANOVA and Python

C. *Learning outcomes*

The Learning outcomes of the course are grouped in three sections: Knowledge, Skills, and Responsibilities/autonomy. They are given in Table 1.

TABLE I. LEARNING OUTCOMES

Learning Outcomes of the Information Technologies for Statistical Analysis and Quality Control Course
Knowledge
• To understand the basics of the quality control tools • To aware and understand the essentials of QFD • To comprehend the elements of FMEA method • To understand different probability distribution, parameters and properties related to textile variables • To apprehend how to treat random variables in order to consider them in the quality control process • To adopt different kind of hypothesis testing to support your decisions • To comprehend variance and regression analysis principles
Skills
• To solve problems using the quality control tools • To respond to the needs and expectations of the customers using QFD • To take actions to eliminate or reduce failures using FMEA • To represent test results using different methods • To use specialized software for data analysis to support quality control • To apply statistical hypothesis tests in Statistical Process Control (SPC) and Acceptance Sampling (AS) • To apply variance and regression analysis to concrete cases both for forecasting and control purposes
Responsibilities/autonomy
• To assure and manage the quality control process by usingthe quality control tools • To bring new and improved products to market whilereducing development time. • To documents current knowledge and actions about the risksof failures • To optimise the regression model in order to get to the bestpossible hypothesis considering data variables • To support the quality control process by applying relevantstatistical models

IV. ABOUT THE QMS/EMS IMPLEMENTATION AND CONTROL COURSE

A. *Course objectives*

The quality of textile products needs to be assured in accordance with modern production and environmental requirements.

Quality specification, conformity and environmental assessment of textile products are integral part of the production process and can contribute to an enterprise differentiation strategy.

Students will be introduced in the definition of systematic approach in quality assurance and quality management with the support of the latest ICT systems. They will learn how to set an organization effective management system (QMS) and environmental management system (EMS) in accordance with the standard requirements with the support of the latest technologies.

B. *Course Topics*

The course topics of this course are separated in three categories: for students, for staff, and for university teachers/researchers.

The topics related to the training of students are as it follows:

- Lecture I: Quality as strategic category in business
- Lecture II: Quality management system implementation according to ISO standard
- Lecture III: Certification of the Quality Management System
- Lecture IV: Auditing management system according to standard ISO 19011:2018
- Lecture V: The environmental management system (EMS)
- Lecture VI: Certification process for confirmation of compliance with requirements of ISO 14001
- Lecture VII: Eco-Management and Audit Scheme (EMAS)

The topics related to the university teachers/researchers are:

- Lecture I: Introduction to the Quality as strategic category in business
- Lecture II: Quality management system according to ISO standards

- Lecture III: Certification of the Quality Management System
- Lecture IV: Auditing management system according to standard ISO 19011:2018
- Lecture V: The environmental management system (EMS)
- Lecture VI: Certification process for confirmation of compliance with requirements of ISO 14001
- Lecture VII: Eco-Management and Audit Scheme (EMAS)File 1.2MB PDF document

The topics related to the staff are:

- Topic 1: Introduction to the Quality as strategic category in business
- Topic 2: Quality management system according to ISO standards
- Topic 3: Certification of the Quality Management
- Topic 4: Auditing management system according to standard ISO 19011:2018
- Topic 5: The environmental management system (EMS)
- Topic 6: Certification process for confirmation of compliance with requirements of ISO 14001

C. Learning outcomes

Like the previous course the learning outcomes of the course are grouped in three sections: Knowledge, Skills, and Responsibilities/autonomy and they are given in Table II.

TABLE II. LEARNING OUTCOMES

Learning Outcomes of the QMS / EMS Implementation and Control Course
Knowledge
• To understand the systematic approach to quality assurance and quality management of textile and clothing products • To apprehend the standardized model of environmental management system (EMS) according to ISO 14000 • To understand the concept of Life Cycle Assessment (LCA), identify the elements of LCA, their relationship and impact on the environment • To adopt the principles of assessing and labelling the ecological characteristics of processes and products • To recognize product quality as a strategic category essential for business success
Skills
• To apply the general quality management system ISO 9000 • To support the introduction of systematic quality management in the organization • To use statistical tools for product quality management • To use the PDCA quality loop to improve business quality and product development • To use the methodology for the implementation of EMS in the company according to ISO 14001 • To use the concept of LCA as relevant tool in sustainable development
Responsibilities/autonomy
• To contribute to the definition of systematic approach in quality assurance and quality management, setting specific goals and key factors that need to be monitored, measured and harmonized with legislation at the level of the organization • To interpret the data and adjust the variables according to the defined goals in the different segments of work and production phases

REFERENCES

[1] Hertleer., C.; Razic, S., Terziev, A., Malengier, B., Saeed, H., Dimov A., ICT-TEX Courses - New Opportunities for E-Learning Digital Skills for the Textile and Clothing Industry, 14th Scientific-Professional Symposium Textile Science and Economy, 26 January, 2022, Zagreb, Croatia

[2] https://ict-tex.eu/

[3] https://platform.ict-tex.eu/

TECHNICAL UNIVERSITY OF SOFIA

RESEARCH AND DEVELOPMENT SECTOR OF TECHNICAL UNIVERSITY OF SOFIA

The Technical University of Sofia is a modern educational and research institution, with highly qualified lecturers, researchers, engineers and technicians. The laboratory facilities with advanced equipment and qualified research staff provide high-quality scientific and experimental research.

The main goal of the Technical University of Sofia is its establishment as the leading European scientific and research center. Through its infrastructure, research potential and network of contacts, the University supports the solution of many scientific and engineering problems related to the needs of society.

Technical University of Sofia conducts a variety of applied research activities and provides opportunities for technology transfer at national and international level through the following units:

- Research and development sector
- "Technical University of Sofia – Technologies" Ltd.
- Small enterprises
- Educational-experimental enterprise
- The publishing house of the Technical University of Sofia

An important role for the establishment of TU-Sofia as a leading educational and research engineer center in the country and the region has the numerous annual scientific forums, united in the unique format "Science Days of TU-Sofia".

The strong international character, the high scientific level of the presented research findings and papers, included in proceedings, referenced and indexed in leading international science databases, and the significant support of the industrial partners make this forum an efficient environment for the transfer of knowledge, ideas and technologies from science to industry and business.

The introduced e-learning system E-SCIENCE provides the opportunity to obtain unified, complete and comprehensive information on scientific activities, projects and the scientists' career development. The system provides ways and methods for finding optimal management decisions and improves the effectiveness of research and applied work. Thanks to the publications module, updated daily, bibliographic data and summaries of scientific papers, publications, and posters are available on the web.

Training and Sport Wellness base "LAZUR" is the host of the annual international scientific conferences "Science Days of TU-Sofia" in the town of Sozopol, where the scientific elite of Bulgaria and the world is held.

The forums organized by the TU-Sofia are a meeting place for scientists from different research fields, challenged to transform innovative ideas into products and services that create sustainable partnerships between science and business, build high-skilled human potential, giving new skills that provides prepared researchers and specialists.

Technical University of Sofia
8 Blvd. Kl. Ohridski, 1797, Sofia, Bulgaria
Phone: (+359) 2 96 25 72, (+359) 2 868 51 83, Fax: (+359) 2 96 25 72
www. tu-sofia.bg

СЪЮЗ НА МЕТРОЛОЗИТЕ В БЪЛГАРИЯ

UNION OF THE METROLOGISTS IN BULGARIA